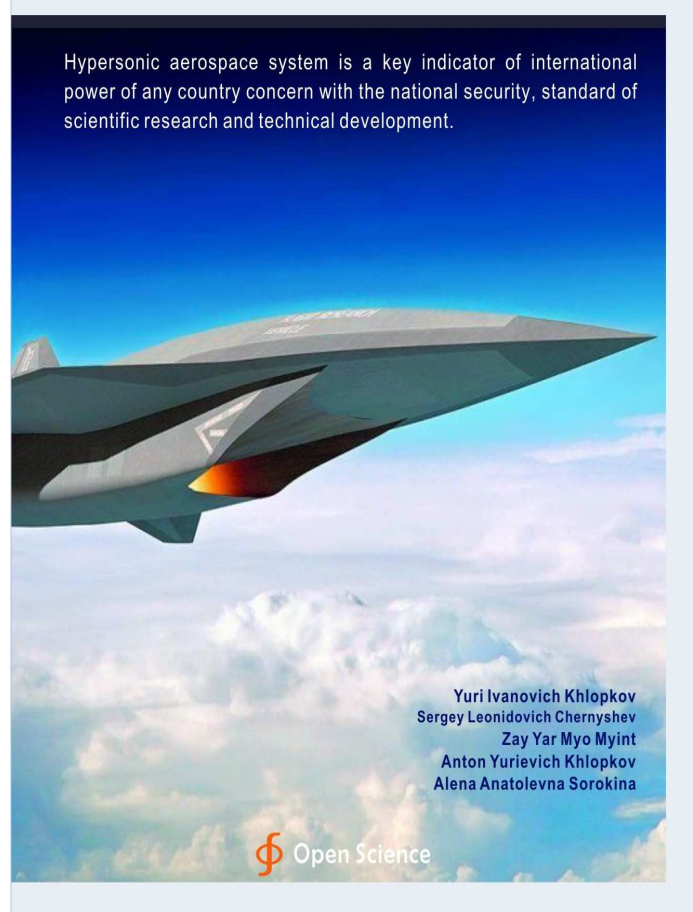
NOTABLE ACHIEVEMENTS IN AVIATION AND AEROSPACE TECHNOLOGY



Author(s)



Yuri Ivanovich Khlopkov

Doctor of Physical and Mathematical Sciences, Leading Researcher, Central Aerohydrodynamic Institute named after professor N.E. Zhukovsky, Russia; Professor, Moscow Institute of Physics and Technology (State University), Russia; Academician of the Russian Academy of Natural History.



Sergey Leonidovich Chernyshev

Doctor of Physical and Mathematical Sciences, Executive Chief, Central Aerohydrodynamic Institute named after professor N.E. Zhukovsky, Russia; Professor, Moscow Institute of Physics and Technology (State University), Russia; Corresponding Member of Russian Academy of Sciences.



Zay Yar Myo Myint

Candidate of Physical and Mathematical Sciences, Assistant Lecturer, Military Computer and Technological Institute, Myanmar; Doctoral Candidate, Moscow Institute of Physics and Technology (State University), Russia; Professor of Russian Academy of Natural History.

NOTABLE ACHIEVEMENTS IN AVIATION AND AEROSPACE TECHNOLOGY

Yuri Ivanovich Khlopkov^{1, 2}, Sergey Leonidovich Chernyshev^{1, 2}, Zay Yar Myo Myint², Anton Khlopkov², Alyona Sorokina²

¹Central Aerohydrodynamic Institute named after Professor N.E. Zhukovsky ²Moscow Institute of Physics and Technology (State University)

This book is dedicated to the 50th anniversary of the Department of Aeromechanics and Flight Engineering of Moscow Institute of Physics and Technology and same age of the department of Vasiliev S.A.

PREFACE

The cost of a launch the payload into orbit at the present time is still extremely high. This is due to the high cost of the rocket engine, complex control system, expensive materials used in the construction of rocket and their engine, and mainly by their single use.

At the end of XX and beginning of the XXI centuries, the unit cost of a deliver the payload into low earth orbit for non-reusable and reusable carrier of U.S. and Western Europe is approximately 10 000 to 25 000 \$/kg. Since 1981, NASA's dream of a reusable spacecraft "Space Shuttle" was realized and has launched more than 100 missions, but the price tag of space shuttle missions has changed not much. For space transportation system "Space Shuttle", the cost of deliver payloads into low earth orbit is 10 416 \$/kg (in 2011). Using the new generation expendable launch systems type of "Atlas V", "Delta IV" and "Ariane 5" should lead to some reduction in the unit cost of launch, but, as expected, are not too significant. Due to the peculiarities of the development of space technology in the USSR, the unit cost to deliver payload into orbit by expendable launch

system of Russian are noticeably smaller. For example, the cost of a launch by "Soyuz" and "Proton" actually is 2400 and 2100 \$/kg, respectively. Nevertheless, further reducing the cost of a launch the payload into orbit associated with reusable hypersonic aircraft.

A new space transportation system being developed could make travel to geostationary earth orbit a daily event and transform the global economy. Theoretically, the most beneficial from an economic point of view, the delivery of payloads and passengers into space is the Russian idea "Space Elevator".

In 1895, the father of astronautics Konstantin Eduardovich Tsiolkovsky in one of his articles described the gigantic structure with a rope stretched to the "Heavenly Palace" where had to climb the elevator, then to fly further into space.

The future "Space Elevator" would be made of a carbon nanotubes composite ribbon anchored to an offshore sea platform would stretch to a small counterweight approximately 100 000 km (62 000 miles) into space. Mechanical lifters attached to the ribbon would then climb the ribbon, carrying cargo and humans into space, at a price of only about 220 to 880 \$/kg (100 to 400 \$/lb).

At the Department of Aeromechanics and Flight Engineering (DAFE) of Moscow Institute of Physics and Technology (MIPT) was developed the information technology projects "ADANAT" (Aerodynamic Analysis of Ensuring the Establishment of Aviation and Space Techniques) and "TURBO SEARCH" by Professor Yuri Ivanovich Khlopkov. Many research grants from the Russian Foundation for Basic Research (RFBR) and Russian Science Foundation (RSF) supported these projects. The parallel calculation center of DAFE MIPT is equipped with the modern CFD software. DAFE with the famous organizations of Russia "Central Aerohydrodynamic Institute (TsAGI), Central Institute of Aviation Motor Development (TsIAM), Dorodnicyn Computing Centre of the Russian Academy of Sciences, Institute for Problems in Mechanics

of the Russian Academy of Sciences, Sukhoi Aviation Holding Company, engineering company "TESIS", etc" was defined many fundamental problems in the field of creation of new generation of aviation and space techniques. Development of the center allowed promoting in the solution of the most complex challenges of computing in aerothermodynamics problems. Some of these are the problems of hypersonic aerothermodynamics, rarefied gas dynamics and task about flows in turbojets, etc.

Under the projects the following books were published:

- 1. Khlopkov Yu.I., Zharov V.A., Gorelov S.L. Guidelines for Computer Analytics. Moscow, MIPT, 2000. 118 p. (in Russian)
- 2. Khlopkov Yu.I., Zharov V.A., Gorelov S.L. Coherent Structures in Turbulent Boundary Layer. Moscow, MIPT, 2002. 268 p. (in Russian)
- 3. Khlopkov Yu.I. Statistical Modelling in Computational Aerodynamics. Moscow, MIPT, 2006. 158 p. (in Russian)
- 4. Belotserkovskii O.M., Khlopkov Yu.I. Monte-Carlo Methods in Mechanics of Fluid and Gas. Moscow, Azbuka-2000, 2008. 330 p. (in Russian)
- 5. Khlopkov Yu.I., Zharov V.A., Gorelov S.L. Renormalization Group Methods for Describing Turbulent Flow of Incompressible Fluid. Moscow, MIPT, 2006. 492 p. (in Russian)
- 6. Khlopkov Yu.I., Zharov V.A., Gorelov S.L. Lectures on Theoretical Methods for Studying Turbulence. Moscow, MIPT, 2005. 178 p. (in Russian)
- 7. Belotserkovskii O.M., Khlopkov Yu.I., Zharov V.A., Gorelov S.L., Khlopkov A.Yu. Organize Structures in Turbulent Flows. Moscow, MIPT, 2009. 303 p. (in Russian)

- 8. Belotserkovskii O.M., Khlopkov Yu.I. Monte-Carlo Methods in Mechanics of Fluids and Gas, World Scientific publication, Singapore, New Jersey, London, Hong Kong, Beijing, 2010. 268 p.
- 9. Afanasyeva L.A., Khlopkov Yu.I., Chernyshev S.L. Introduction to Speciality. The Aerodynamics Aspects of Flight Safety. Moscow, MIPT, 2011. 184 p. (in Russian)
- 10. Khlopkov Yu.I., Cernyshev S.L., Zay Yar Myo Myint, Khlopkov A.Yu. Introduction to Speciality II. High-speed Aircrafts. Moscow, MIPT, 2013. 192 p. (in Russian)

Historical overview of development of hypersonic and aerospace vehicles, perspective programs in aerospace programs of developed countries are presented in this book. Analysis of methods to predict aerothermodynamics characteristics of hypersonic and aerospace vehicles from orbital flight to continuum flow regime are also described. Application of cognitive approach in computational aerodynamics, in particularly, in hypersonic vehicle design technology is introduced. The basic principle of hypersonic propulsion systems: rocket engine, turbojets, ramjets, scramjets, and the dual-combustion ramjet are explained. The most beneficial system to deliver payloads and crews into space "Space Elevator", the project plans and concepts are highlighted. In the last chapter, also highlighted that we need to consider medico-bilogical effect and to improve system for the medical support of human in space due to future space exploration plans of delivery manned spacecrafts with crews to the Moon and Mars.

The authors would like to thank professors Tsipenko Vladimir Grigorevich, Lipatov Igor Ivanovich, associate professors Zharov Vladimir Alekseevich, Gorelov Sergey Lvovich, Voronich Ivan Viktorovich, Yumashev Vladimir Lvovich, Dorofeev Evgeny Aleksandrovich for useful discussions. Thanks to Kira Gusarova, who supported and encouraged. The support from the Russian Foundation for Basic Research and the Russian Science Foundation are appreciated by the authors.

CHAPTER 1 INTRODUCTION

1.1. Historical overview

The earliest practical work on rocket engines designed for spaceflight occurred simultaneously during the early 20th century in three countries by three fathers of rocket scientists: Konstantin Eduardovich Tsiolkovsky (in Russia), Robert Hutchings Goddard (in the United States) and Hermann Julius Oberth (in Germany).







Tsiolkovsky K.E.

Goddard R.H.

Oberth H.J.

After World War II, the Soviet Union and the United States created their own missile programs. On October 4, 1957 the Soviets launched the first artificial satellite "Sputnik 1" into space. Four years later on April 12, of 1961, Russian cosmonaut Yuri Alekseyevich Gagarin became the first human to orbit Earth in Vostok 1. His flight completed a single orbit of Earth in approximately 108 minutes, and Gagarin reached an altitude of 327 km (about 202 miles) [1].

On January 31, 1958, the first U.S. satellite "Explorer 1" went into orbit. In 1961 Alan Shepard became the first American to fly into space. On February 20, 1962, John Glenn's historic flight made the first American to orbit Earth. During the 1960s unmanned spacecrafts photographed and probed the moon before astronauts ever landed. On July 20, 1969, astronaut Neil Armstrong stepped onto the moon and became first man to walk on the moon.

Hypersonic technologies also became important as policy makers looked ahead to an era in which the speed and performance of fighters and bombers might increase without limit [2].

In accordance to the plan of the Soviet Union air forces, the project of a 2 stage launcher plane began in 1965 and was entrusted to OKB-155 Mikoyan A.I. whose chief of the engineering and design department was Gleb Evgeniyevich Lozino-Lozinskiy. The project received the name of "Spiral" (in Russian: Спираль) and was to prepare the Soviet Union to the war in space. The project "Spiral" have been competition between two construction bureaus of Pavel Osipovich Sukhoi and Artem Ivanovich Mikoyan [3].



Yuri A. Gagarin



Neil Armstrong

In 1966, the project "Spiral" connected with TsAGI (Tsentralniy Aerogidrodinamicheskiy Institut, the Central Aerohydrodynamic Institute), which at that time the chief was Vladimir Myasischev and widely conducted the Exploration aerodynamics of hypersonic speeds. It was proposed to use the "Spiral" space plane to do three main jobs: the reconnaissance version of the Spiral would carry a photo camera with a resolution of 0.75-1 meter and radar payloads to conduct on-demand spy missions over the Earth's surface; the bomber version would be equipped with orbit-to-surface missiles, capable of

hitting targets on Earth; the interceptor version would be capable of inspecting and destroying targets in space. For all three applications, the "Spiral" would have to compete in performance with unmanned military satellites. At the time the Spiral was conceived, the jury was still out on which type of vehicle would be better suited for the job. Due to the claimed cost efficiency of the "Spiral" system, the replacement of unmanned payloads with the manned spacecraft formed an ideal flexible, fast response launch vehicle system.

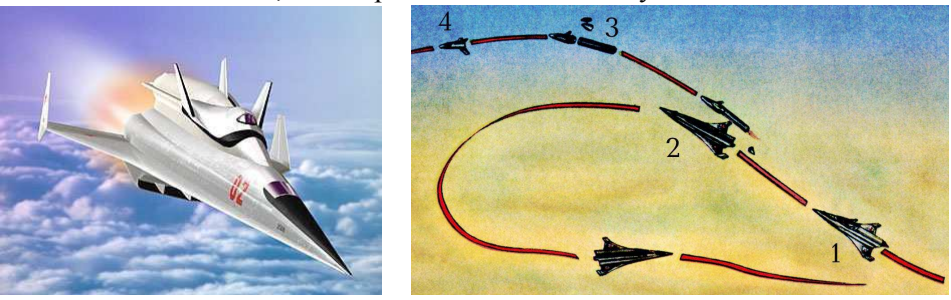


Figure 1.1 Reusable aerospace system "Spiral" and the scheme of its launch

In accordance with the requirements of the customer the system included a supersonic horizontal launcher, an orbital space plane, and an auxiliary rocket. The departure was envisaged into horizontal position like a plane (1), at an altitude of 28-30 km the orbital space-plane and its rocket were detached from the launcher (2), the plane launcher then return to its base. When the fighter arrive at an altitude of 120-130 km it separated from its auxiliary rocket (3) and could make up to 2 revolutions to reach (a satellite) or to fly over its objective (to shoot photographs) (4), when the mission was accomplished it started its re-entry in the atmosphere, protected by an abrasive heat shield, moreover the cold part of the fuselage was assembled on special fixings to enable him to become deformed under heat. When the atmosphere was rather dense the wings of the plane were spread, then towards the end of the flight the pilot lit his turbojet to facilitate the landing and the final approach. An important advantage of the Spiral launcher was its great payload capacity, 2 or 3 times higher than a traditional system of the

same mass. The cost of the put into orbit per kilogram was 3 to 3.5 times inferior. Moreover, by using the principle of a plane launcher the Spiral could reach any orbit, make operations in space and turn back to the ground even under difficult climatic conditions. In 1976 the project was stopped (the Buran project had just started) except for the tests of model 105.11. The Spiral system was finally abandoned at the end of the 70's to the profit of the Energia-Buran system.





Figure 1.2 Manned reusable aerospace system "Dyna-Soar"

The Boeing X-20 "Dyna-Soar" (Dynamic Soarer) was a United States Air Force program to develop a space plane that could be used for a variety of military missions, including reconnaissance, bombing, space rescue, satellite maintenance, and as a space interceptor to sabotage enemy satellites [4]. The program ran from 24 October 1957 to 10 December 1963, and was cancelled just after spacecraft construction had begun. The proposed project would develop a manned, winged vehicle that would be rocket-boosted to hypersonic speed at an altitude above 30 km.

The objective of shuttles construction is intended to tasks of defense, maintenance of various space objects and for their return onto earth, the delivery of modules and cosmonauts. The structure of "Buran" were used various materials such as aluminium alloys and steel. To resist heating during the reentry in the dense layers of the atmosphere, the external surface of the shuttle was covered by a special heat shield. The most intense stage of the heating is accompanied by the formation of a characteristic of plasma. However, the

temperature of the structure of the shuttle does not exceed 160 °C at the end of the flight. Each 38 600 tile has a specific place which made the external shape of the body of the shuttle. Lastly, the structure was made to support 100 flights.



Figure 1.3 Automatic landing the orbiter "Buran" with the accompaniment of the Mig-25

The engine system includes 2 engines for the orbital operations functioning with liquid oxygen and kerosene, and 46 engines (orbital maneuvering system) with gas for the control of trajectory, gathered in 3 blocks (1 in the nose and 2 in the tail). The length of "Buran" is 35.4 m, the height is 16.5 m, the span of the wings is 24 m, wing surface is 250 m², the width of the fuselage of 5.6 m, the height is 6.2 m, and the payload bay has a diameter of 4.6 m and a length of 18 m. The starting mass reaches 105 tons, the mass of payload that can be put into orbit is 30 tons and return value is 15 tons. Propellant total mass is 14 tons. For its first flight, the Buran shuttle had an orbit altitude of 250.7/260.2 km (slope of 51.6°) and a period of revolution of 89.5 minutes. With a loading of propellant of 14 ton and a payload of 27 ton, the altitude of 450 km can be reached.

The first trial flight of "Buran" was completed after the execution of 2 revolutions around the Earth, then by the successful landing in automatic mode on the aerodrome in the area of Baikonur. The breaking impulse was started at an altitude of 250 km, at a distance of almost 20 000 km from the aerodrome.

The development of "Buran" went on 10 years. Ten years during which important research tasks and experiments were carried out in various technical fields: acoustics, thermodynamics, systems design, dynamics of flight on simulator, design of the control panel, making of new materials, developing of methods and equipment for the landing in automatic mode (flying laboratories), atmospheric flight tests of the similar shuttle (another model of "Buran" with turbines), outsides tests of the heat shield and aerodynamic tests on "BOR" (in Russian – Беспилотный Орбитальный Ракетоплан, Orbital Plane without Pilot) models. The numerous studies in laboratory and wind tunnels have made it possible to define the new design of "BOR" lifting bodies. They became at their turns the models for the various orbital systems of the USSR.



Figure 1.4 The BORs at International Aviation and Space Salon

The National Aeronautics and Space Administration's (NASA) space shuttle "Columbia" fleet began setting records with its first launch on April 12, 1981 and continued to set high marks of achievement and endurance through 30 years of missions. Starting with Columbia and continuing with Challenger, Discovery, Atlantis and Endeavour, the spacecraft has carried people into orbit repeatedly, launched, recovered and repaired satellites, conducted cutting-edge research and built the largest structure in space, the International Space Station. Twenty-four successful shuttle launches fulfilled many scientific and military requirements

until January 1986, when the shuttle Challenger exploded after launch, killing its crew of seven. The Challenger tragedy led to a reevaluation of America's space program [5].

The final space shuttle mission, STS-135, ended July 21, 2011 when Atlantis rolled to a stop at its home port, NASA's Kennedy Space Center in Florida. As humanity's first reusable spacecraft, the space shuttle pushed the bounds of discovery ever farther, requiring not only advanced technologies but the tremendous effort of a vast workforce. Thousands of civil servants and contractors throughout NASA's field centers and across the nation have demonstrated an unwavering commitment to mission success and the greater goal of space exploration.



Figure 1.5 Reusable spacecraft system "Space shuttle"

NASA will continue architecture planning for a Multi-Purpose Crew Vehicle (MPCV) capable of taking human explorers to distant locations throughout the inner solar system. The Space Launch System (SLS) Program will develop the heavy lift vehicle that will launch the MPCV, other modules, and cargo for these missions [6].

The new goal was to make certain a suitable launch system was available when satellites were scheduled to fly. Today this is accomplished by having more

than one launch method and launch facility available and by designing satellite systems to be compatible with more than one launch system.

Space systems will continue to become more and more integral to homeland defense, weather surveillance, communication, navigation, imaging, and remote sensing for chemicals, fires and other disasters. The International Space Station is a research laboratory in low Earth orbit. With many different partners contributing to its design and construction, this high-flying laboratory has become a symbol of cooperation in space exploration, with former competitors now working together.

1.2. Russia's aerospace programs The Clipper

"Clipper" (in Russian: Клипер) is a proposed partly reusable manned spacecraft by S.P. Korolev Rocket and Space Corporation "ENERGIA". Due to lack of funding from the European Space Agency (ESA) and Russian Federal Space Agency (RSA), the project has been indefinitely postponed as of 2006 [7]. Designed primarily to replace the Soyuz spacecraft, Clipper was proposed in two versions: as a pure lifting body design and as space plane with small wings. In either case, the craft would have been able to glide into the atmosphere at an angle that produces much less stress on the human occupants than the current Soyuz. It was intended to be designed to be able to carry up to six people and to perform ferry services between Earth and the International Space Station (ISS).

In February 2004 RSA announced that the Clipper project for 2005-15. It had been developed since 2000 and reportedly relied heavily on research studies as well as proposals for a small Russian lifting body spacecraft from the 1990s. Externally its design was comparable to the cancelled European mini-shuttle Hermes or the NASA's X-38. It was planned to be the successor to the veteran spacecraft Soyuz, which has been built in various modifications since 1961. The

Clipper program was proposed to go beyond Earth orbit to the Moon and even Mars.



Figure 1.6 Manned spacecraft "Clipper" and very fast sailing ship of the middle third of the 19th century "Clipper"

At the end of 2005, It design was changed again and the most likely solution for a carrier rocket became the Soyuz 2-3, an upgraded Soyuz 2 rocket. This enhanced Soyuz should have been able to launch Clipper into space because of weight reduction resulting in the use of the Parom as a space tug [7].

The Rus

Russia's next generation manned spacecraft "Rus" (in Russian: Русь) which is called the Advanced Crew Vehicle (ACV) will launch atop a different rocket than planned, one originally designed for only robotic spacecraft. Its first test flight in 2018, using a launcher named Angara A5 developed for unmanned missions



Figure 1.7 Manned spacecraft "Rus"

The Angara A5 rocket is the new version of Angara (family of four rockets based on common core architecture that uses liquid oxygen and kerosene). The ACV will carry six cosmonauts, 500 kg (1100 pounds) of cargo and could travel to the moon. Like the Soyuz capsule, which Russia currently uses to launch humans to orbit, the ACV will use rockets to land [8].

The Baikal

The "Baikal" booster (in Russian: Байкал) is a reusable flyback booster for the Angara rocket family. It was designed by the Molniya Research and Industrial Corporation for the Khrunichev Space centre, reusing the flyback and control system for the reusable Buran orbiter.

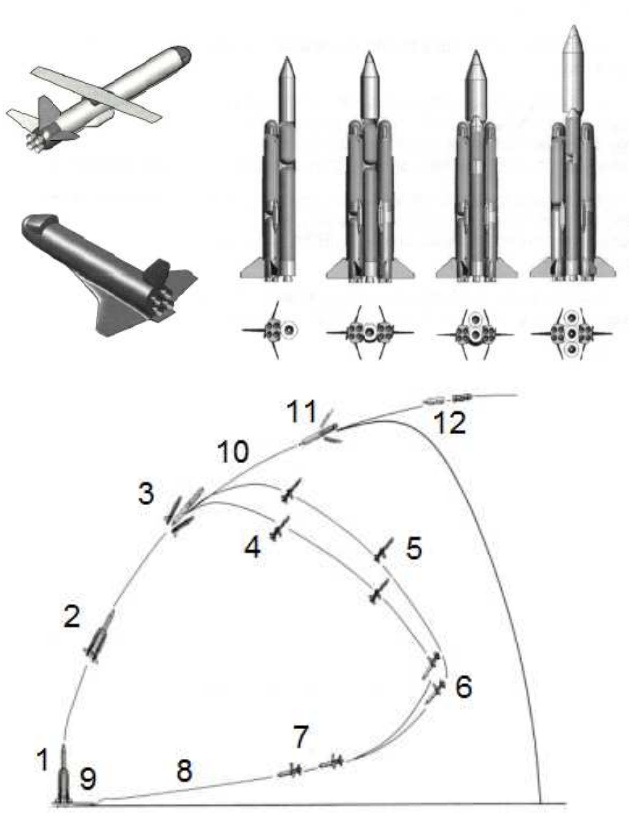


Figure 1.8 General view of reusable space-rocket system "Baikal-Angara" and its scheme of flight

The booster would be equipped with an RD-191 rocket engine burning kerosene and liquid oxygen to provide approximately 200 tons of thrust. It would be equipped with a folding wing stored parallel to the fuselage of the vehicle during the booster stage of the flight. After separation from the Angara launcher's second stage at an altitude of about 75 km and a speed of Mach 5.6 (5800 km/h, 3600 mph), the Baikal's wing would rotate 90 degrees and the booster glides in upside down position reducing speed. Once the booster reaches subsonic speeds a U-turn is performed and an air-breathing jet engine in its nose section is started to fly back to its launching site and make a powered horizontal landing on a runway [9].

Apart from economic advantages, this procedure greatly reduces the risk of falling space debris. Currently the project for creating reusable space-rocket system remains relevant and promising, but its full implementation is possible not earlier than 2020.

1.3. The United States hypersonic aircraft programs The X-51

The Boeing "X-51A" (X-51 WaveRider) is an unmanned scramjet demonstration aircraft for hypersonic flight testing (Mach 6, approximately 6400 km/h at altitude). Its first powered hypersonic flight completed on 26 May 2010. After two unsuccessful test flights, the X-51 completed a flight of over six minutes and reached speeds of over Mach 5 for 210 seconds on 1 May 2013 for the longest duration hypersonic flight.

The X-51 received the name "WaveRider" because it uses its shock waves to add lift. The program was a cooperative effort of the United States Air Force, DARPA, NASA, Boeing, and Pratt & Whitney Rocketdyne. The program was managed by the Aerospace Systems Directorate within the U.S. Air Force Research Laboratory (AFRL) [10].



Figure 1.9 Artist's concept of X-51A during flight

X-51 technology will be used in the High Speed Strike Weapon (HSSW), a Mach 5+ missile planned to enter service in the mid 2020.

The FALCON project

The DARPA's "FALCON" project (Force Application and Launch from CONtinental United States) is a two-part joint project between the Defense Advanced Research Projects Agency (DARPA) and the United States Air Force (USAF) and is part of Prompt Global Strike. The Falcon Hypersonic Technology Vehicle 2 (HTV-2) is a multiyear research and development effort to increase the technical knowledge base and advance critical technologies to make long-duration hypersonic flight a reality. The DARPA had two HTV-2 built for two flight tests in 2010 and 2011. DARPA planned the flights to demonstrate thermal protection systems and aerodynamic control features. Test flights were supported by NASA, the Space and Missile Systems Center, Lockheed Martin, Sandia National Laboratories and the Air Force Research Laboratory's (AFRL) Air Vehicles and Space Vehicles Directorates [11].

The first HTV-2 flight was launched on 22 April 2010. The HTV-2 glider was to fly 7700 km (4800 miles) across the Pacific to Kwajalein at Mach 20. The launch was successful, but the first mission was not completed as planned. Reports stated that contact had been lost with the vehicle nine minutes into the mission.

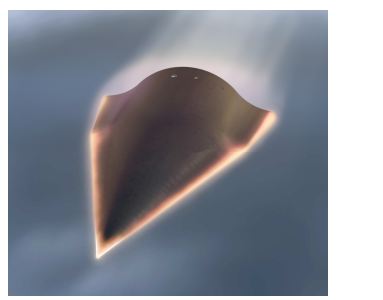




Figure 1.10 DARPA's "Falcon HTV-2" and a "Falcon"

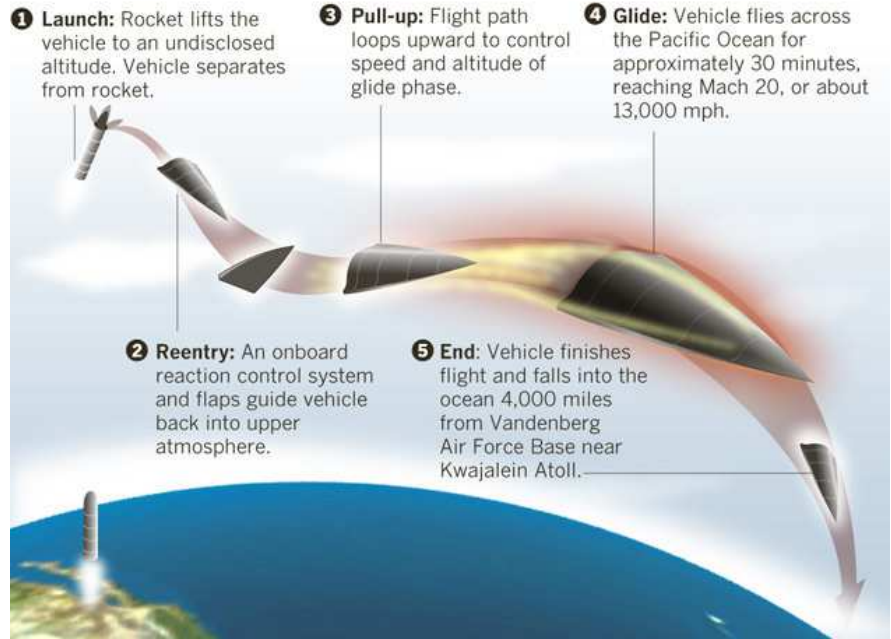


Figure 1.11 The scheme of HTV-2 flight

A second flight was launched on 11 August 2011. The unmanned Falcon HTV-2 successfully separated from the booster and entered the mission's glide phase, but again lost contact with control about nine minutes into its planned 30 minute Mach 20 glide flight. Initial reports indicated it purposely impacted the Pacific Ocean along its planned flight path as a safety precaution. Some analysts thought that the second failure would result in an overhaul of the Falcon program.

The US government's vision of an ultimate prompt global reach capability (circa 2025 and beyond) is engendered in a reusable Hypersonic Cruise Vehicle (HCV). The HCV is designed and constructed under DARPA's Force Application and Launch from the Continental United States (FALCON) program. This autonomous aircraft would be capable of taking off from a conventional military runway and striking targets 9000 nautical miles distant in less than two hours.



Figure 1.12 The scheme of HCV flight

It could carry over 5400 kg (12000 lbs) payload consisting of Common Aero Vehicles (CAV), cruise missiles, small diameter bombs or other munitions. The HCV innovative concepts could enable effective global reach missions and potentially provide the first stage of a two-stage access to space vehicle [12].

The XS-1

The DARPA have also other plans for the vehicle program that also aims to launch payloads into orbit on the cheap - known as Experimental Spaceplane, or XS-1. It follows in the footsteps of previous DARPA hypersonic projects, such as the HTV-2 aircraft. Officials want the reusable, unmanned XS-1 to take advantage of capabilities to be showcased under another

The United States military is making progress toward developing a new unmanned spaceplane, which it aims to begin flight-testing in 2017. DARPA has

high expectations for the XS-1 program, which it hopes can eventually launch 1361 to 2268 kg (3000 to 5000 lb) payloads to orbit for less than \$5 million per flight – and to do it at least 10 times per year [13].



Figure 1.13 Artist's concept of Experimental Spaceplane (XS-1) [11]



Figure 1.14 Artist's concept of ALASA and XS-1 [11]

DARPA announced that the Airborne Launch Assist Space Access (ALASA) program, which aims to launch satellites (up to 100 lb, or 45 kg) to orbit for less than 1 million dollars apiece using traditional airplanes outfitted with expendable upper stages in the 2016.

The SR-72

In 1976, U.S. Air Force SR-71 (Blackbird) crews flew from New York to London in less than two hours, reaching speeds exceeding Mach 3 and setting world records that have held up for nearly four decades. In 2014, Lockheed Martin's engineers are developing an unmanned hypersonic aircraft SR-72 (speeds up to Mach 6) that will go twice the speed of the SR-71. In fact, an SR-72 could be operational by 2030 [14].



Figure 1.15 The SR-71



Figure 1.16 The SR-72

For the past several years, Lockheed Martin has been working with Aerojet Rocketdyne to develop a method to integrate an off-the-shelf turbine with a supersonic combustion ramjet air breathing jet engine to power the aircraft from standstill to Mach 6. The SR-72's design incorporates lessons learned from the Falcon HTV-2, which flew to a top speed of Mach 20, or 20 921 km/h (13 000 mph), with a surface temperature of 1927°C (3500°F).

1.4. Europe's spacecraft mission

Europe's ambition for spacecraft is a cornerstone for a wide range of space application such space transportation, robotic servicing of space infrastructure and exploration. To achieve this goal, the International eXperimental Vehicle (IXV) program was realized. The spaceplane IXV launched on a Vega rocket on 11 February 2015. The mission of 100 minutes was flawless and ended with a safe splashdown in the Pacific Ocean.



Figure 1.17 Intermediate eXperimental Vehicle (IXV) on Vega rocket

General mission is to launch into a suborbital trajectory on ESA's small Vega rocket from Europe's Spaceport in French Guiana, IXV will return to Earth from a low-orbit mission, to test and qualify new European critical reentry technologies such as advanced ceramic and ablative thermal protection [15].

1.5. Aerospace programs of other developed nations

Since the 1980s, in every developed country have their aerospace programs (some of them are not realized until now) as described below.



Figure 1.18 Germany's aerospace plane "Sänger"

Germany's aerospace plane "Sänger" (Silver bird) is horizontal takeoff ship performs and at height of 25 km above it will make cruising at speeds of up to 4.5 Mach. Followed by a ramp area to climb up to 30 km and the speed increases

up to 6-8 Mach. After the separation of the second stage goes into orbit, and the first returned to the starting place [16].



Figure 1.19 France's manned spacecraft "Hermes"

France's project "Hermes" developed under the auspices of the ESA. Hermes was to have been part of a manned space flight program. It would have been launched using an Ariane 5. The project was approved in November 1987, with an initial pre-development phase from 1988 to 1990. The project suffered numerous delays and funding issues [17].



Figure 1.20 British's aerospace plane "HOTOL"

The British unmanned air-breathing spaceplane "HOTOL" (Horizontal Take-Off and Landing) was intended to put a payload of around 7 to 8 tons in orbit, at 300 km altitude. It was intended to take off from a runway, mounted on the back of a large rocket-boosted trolley that would help get the craft up to 'working speed'. The engine was intended to switch from jet propulsion to pure rocket propulsion at 26–32 km high, by which time the craft would be travelling at Mach 5 to 7. After reaching orbit, HOTOL was intended to re-enter the atmosphere and glide down to land on a conventional runway (approx 1500 meters minimum) [18].



Figure 1.21 Japan's aerospace plane "HOPE"

Japan's HOPE-X (H-II Orbiting Plane-Experiment) was to be launched by an H-II rocket and is expected to transportation between the Earth and orbit, the vehicle is designed to be able to carry out experiments and to make observations on orbit. HOPE was initially to be an unmanned spacecraft with a one-metric-ton payload capacity which could service the International Space Station (ISS). A 20-metric-ton version of HOPE, possibly manned with a 3-3.5 metric ton payload capacity, was also considered. To support the larger HOPE, the H-II launch vehicle would require additional strap-on boosters (up to six solid boosters or a combination of solids and liquids) [19].

The "Shenlong" (Divine Dragon) spaceplane project is headed by China's People's Liberation Army (PLA). The vehicle benefits heavily from Northwestern Polytechnic University (NPU) development programs, but was manufactured by the Chengdu Aircraft Plant and the Chinese Academy of Launcher Technology.



Figure 1.22 China's spaceplane "Shenlong"

Shenlong models dropped from the belly of Chinese H-6 bombers. The Shenlong is broadly similar to U.S. and other unmanned space planes designed to

test new technologies. These would include the U.S. Orbital Sciences X-34, Boeing X-37 and Japan's HOPE-X. One Chinese study has outlined the results of modeling and simulation of a scramjet-powered vehicle with a range of between 1000-2000 km, flying toward its target at an altitude of between 25-30 km and speed of Mach 6 [20]. China had more than 100 teams from leading research institutes and universities involved in the hypersonic glide vehicle "WU-14".

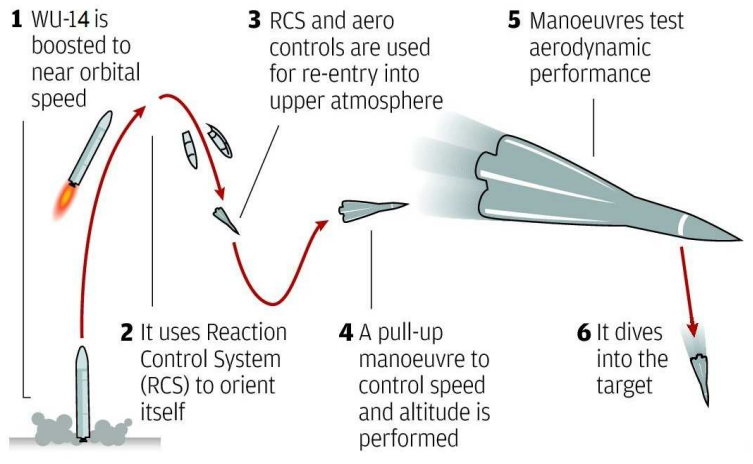


Figure 1.23 The scheme of hypersonic glide vehicle flight [Credit: scmp]



Figure 1.24 India's spaceplane "AVATAR"

AVATAR (Aerobic Vehicle for Hypersonic Aerospace TrAnspoRtation) is a concept for a manned single-stage reusable space plane capable of horizontal takeoff and landing by India's Defense Research and Development Organization with Indian Space Research Organization and other research institutions. The mission concept is for low cost military and commercial satellite space launches, as well as for space tourism [21].

CHAPTER 2 MONTE-CARLO METHODS IN HIGH-ALTITUDE AERODYNAMICS

2.1. Basic principle of Monte-Carlo methods

The appearance of statistical simulation (Monte Carlo) methods in various fields of applied mathematics is usually caused by the appearance of qualitatively new practical problems. The examples include the creation of nuclear weapons, space development, the study of atmospheric optics phenomena, and the study of physicochemical and turbulence processes. One good definition is as follows: The Monte Carlo methods are the methods designed for solving mathematical problems (e.g., systems of algebraic, differential, or integral equations) based on the direct statistical simulation of physical, chemical, biological, economic, social, and other processes using the generation and transformation of random variables.

The first paper devoted to the Monte Carlo method was published as early as in 1873 [22]. It described the experimental determination of π by a realization of the stochastic process of tossing a needle on a sheet of ruled paper. A striking example is the use of von Neumann's idea to simulate the neutron trajectories in the Los Alamos laboratory in 1940. Although the Monte Carlo methods require a large amount of computations, the absence of computers at that time did not discourage the researchers. The name of these methods comes from the capital of the Principality of Monaco, which is famous for its Casino; indeed, the roulettes used in the casino are perfect tools for generating random numbers. The first paper [23] that systematically expanded this method was published in 1949. In that paper, the Monte Carlo method was used to solve linear integral equations. It could easily be guessed that these equations were related to the problem of the passage of neutrons through matter. In Russia, studies concerning the Monte Carlo methods appeared after the Geneva International Conference on the Peaceful Uses of Atomic Energy. One of the first Russian studies is [24].

The revelation of the methods of statistical modeling (Monte-Carlo) in various areas of the applied mathematics is connected as a rule with the necessity of

solution of the qualitatively new problems, arising from the needs of practice. Such a situation appeared by the creation of the atomic weapon, at the initial stage of a mastering of space, by the investigation of the phenomena of atmospheric optics, the physical chemistry, and the modeling of turbulence flow (John von Neumann, Nicholas Constantine Metropolis, Stanislaw Marcin Ulam, Vasilii Sergeevich Vladimirov, Ilya Meerovitch Sobol, Gury Ivanovich Marchuk, Sergey Mikhailovich Ermakov, Gennady Alekseyevich Mikhailov, G.A. Bird, John Kenneth Haviland, Graeme A. Bird, Iain D. Boyd, Mikhail Naumovich Vladimir Alexandrovich Kogan, Perepukhov, Oleg Mikhaylovich Beloserkovskii, Yuri Ivanovich Khlopkov, Vitaliy Yevgenyevich Yanitskii, Mikhail Samuilovich Ivanov, Aleksandr Ivanovich Eropheev and et al.).



Metropolis N.C.



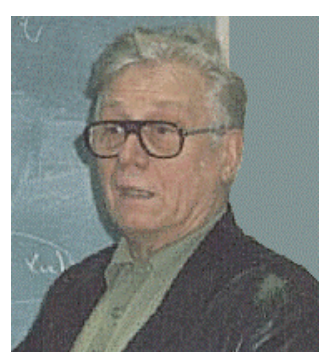
Ulam S.M.



V.S. Vladimirov



O.M. Beloserkovskii



S.M. Ermakov



Mikhailov G.A.

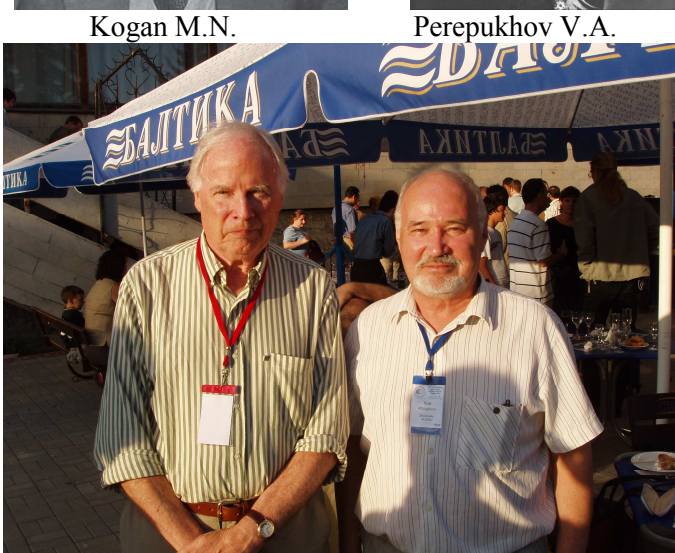


Marchuk G.I.



Kogan M.N.





Bird G.A. and Khlopkov Yu.I.

The general scheme of the Monte Carlo method is based on the central limit theorem, which states that random variable

$$Y = \sum_{i=1}^{N} X_i$$

is equal to the sum of a large number of random variables with the same expectation m and the same variance σ^2 has the normal distribution with the expectation N and the variance N σ^2 . Assume that we want to solve an equation or find the result of a certain process I. If we can construct the random variable ξ with the probability density p(x) such that the expectation of this variable is equal to the unknown solution $M(\xi) = I$, then we obtain a simple method for estimating the solution and its error [25]:

$$I = \mathbf{M}(\xi) \approx \frac{1}{N} \sum_{i=1}^{N} \xi_i \pm \frac{3\sigma}{\sqrt{N}}$$

This implies the following general properties of the Monte Carlo methods:

- (1) The absolute convergence to the solution with the rate 1/N.
- (2) An unfavorable dependence of the error ε on the number of trials: $\varepsilon \approx 1/\sqrt{N}$ (to reduce the error by an order of magnitude, the number of trials must by increased by two orders of magnitude).
- (3) The main method of reducing the error is the variance reduction; in other words, this is a good choice of the probability density p(x) of the random variable ξ in accordance with the physical and mathematical formulation of the problem.
 - (4) The error is independent of the dimensionality of the problem.
- (5) A simple structure of the computation algorithm (the computations needed to realize a proper random variable are repeated *N* times).

(6) The structure of the random variable ξ can be generally based on a physical model of the process that does not require a formulation of the controlling equations as in regular methods; this fact is increasingly important for modern problems.

We illustrate the main features of the Monte Carlo methods and the conditions under which these methods outperform the conventional finite difference methods or are inferior to them using the following example. Suppose that we want to evaluate the definite integral of a continuous function over the interval [a, b]:

To evaluate this integral using the Monte Carlo method, we construct a random variable with the probability density p(x) such that its expectation

$$M(\xi) = \int_{-\infty}^{\infty} \xi p(x) dx$$

is equal to *I*. Now, if we set $\xi = f(\mathbf{x})/p(\mathbf{x})$ within the integration limits, then we have, by the central limit theorem,

$$I = \frac{1}{N} \sum_{i=1}^{N} \xi_i \pm \frac{3\sigma}{\sqrt{N}}$$

On the one hand, the evaluation of I by formula described above can be interpreted as the solution of a mathematically stated problem; on the other hand, it can be interpreted as a direct simulation of the area under the plot of $f(\mathbf{x})$. The evaluation of the one-dimensional integral I_1 by the Monte Carlo method corresponds to the computation of I using the rectangular rule with the step $\Delta x \approx 1/\sqrt{N}$ and an error $O(\Delta \mathbf{x})$. If f(x) is sufficiently "good", the integral I_1 in the one-dimensional case can be calculated accurate to $O(\Delta x^2)$ using the trapezoid rule, accurate to $O(\Delta x^3)$ using the parabolic rule, and to any desired accuracy without a considerable increase in the computational effort. In the multidimensional case, the difficulties in using schemes of a high order of accuracy increase; for this

reason, they are rarely used for the calculation of *n*-dimensional integrals I_n for $n \ge 3$.

Let us compare the efficiency of the regular and statistical methods for the problem described above. Let n be the dimensionality of the problem, Y be the number of nodes on an axis, $R = Y^n$ be the total number of nodes for the regular methods, q be the order of accuracy, N be the number of statistical trials, and v be the number of operations needed to process one node (to perform one statistical trial). Then, $\varepsilon_L = Y^{-q}$ is the error of the regular methods, $\varepsilon_K = N^{-1/2}$ is the error of the statistical methods, $L(\varepsilon) = vR = v\varepsilon_L^{-n/q}$ is the number of operations when the problem is solved by a regular method, and $K(\varepsilon) = vN = v\varepsilon_K^2$ is the number of operations when the problem is solved by the Monte Carlo method. Then, in the case of an equal number of operations needed to obtain a solution with the same accuracy using each of the methods, we have n = 2q. Therefore, for $n \ge 3$ and q = 1 (first-order schemes), the Monte Carlo methods are preferable. For other classes of problems, the relation between the efficiency of the methods can be different.

2.2. The Monte Carlo methods in computational aerodynamics

The Boltzmann integro-differential kinetic equation for the single-particle distribution density is

$$\frac{\partial f}{\partial t} + \xi \nabla f = \int (f' f_1' - f f_1) \mathbf{g} b db d\varepsilon d\xi_1 = J(f)$$
 (2.1)

here, $f = f(t, x, y, z, \xi_x, \xi_y, \xi_z)$ is the distribution density. f, f_1, f', f_1' , correspond to the molecules with the velocities ξ , $\xi 1$ and ξ' , before and after the collision, g is the relative velocity of the molecules in binary collisions $\mathbf{g} = |\mathbf{g}| = |\xi_1 - \xi|$, and b and ε are the impact parameter and the azimuth angle for the collision.

The complex nonlinear structure of the collision integral and the large number of variables (seven in the general case) present severe difficulties for the analysis including the numerical analysis. The high dimension, the probabilistic nature of the kinetic processes, and complex molecular interaction models are the natural prerequisites for the application of the Monte Carlo methods. Historically, the numerical statistical methods in rarefied gas dynamics developed in three directions:

- (1) The use of the Monte Carlo methods to evaluate the collision integrals in the regular finite difference schemes for solving the kinetic equations.
- (2) The direct statistical simulation of physical phenomena, which is subdivided into two approaches: the simulation of trajectories of test particles by the Haviland method [26] and the simulation of the evolution of the ensemble of particles by the Bird method [27].
- (3) The construction of a stochastic process using the Ulam–Neumann procedure [28] corresponding to the solution of the kinetic equation.

The hierarchy of levels of the description of large molecular systems includes a wide range of approaches, and various descriptions of the molecular dynamics at different levels can be used for constructing efficient statistical simulation methods.

The most detailed level of description is a dynamical system. To describe a system consisting of a large number N of particles (a molecular gas is a system of this kind), one must specify the initial coordinates and velocity of each molecule \mathbf{r}_{j} , \mathbf{x}_{j} and the evolution equations of this system

$$m\frac{d^2\mathbf{r}_j}{dt^2} = \sum_{i \neq j}^N R_{ij} \tag{2.2}$$

The solution of such a system is an unrealizable (cannot be solved in practice) problem even for a very rarefied gas. Indeed, at a height of 400 km (the most

popular satellite orbits), one cubic centimeter contains 10⁹ molecules. For this reason, a less detailed statistical description is used.

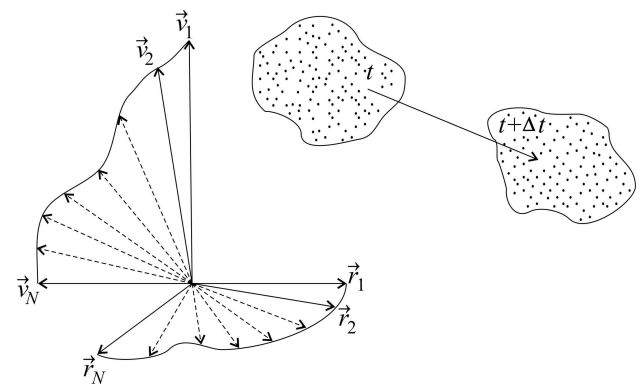


Figure 2.1 Dynamical system of molecules

Following the Gibbs formalism, rather than consider a single system, an ensemble of systems in the 6*N*-dimensional Γ -space distributed according to the *N*-particle distribution function $f(t, \mathbf{r}_1, ..., \mathbf{r}_N, \xi_1, ..., \xi_N) = f_N$ is considered. This function is interpreted as the probability of finding the system in the neighborhood $d\mathbf{r}_1 ... d\mathbf{r}_N d\xi_1 ... d\xi_N$ of the point $\mathbf{r}_1, ..., \mathbf{r}_N, \xi_1, ..., \xi_N$ at the moment t:

$$dW = f_N d\mathbf{r}_1 ... d\mathbf{r}_N d\mathbf{\xi}_1 ... d\mathbf{\xi}_N$$

Such an ensemble is described by the Liouville equation

$$\frac{\partial f_N}{\partial t} + \sum_{i=1}^N \xi_i \frac{\partial f_N}{\partial \mathbf{r}_i} + \sum_{i\neq j}^N \sum_{i=1}^N \frac{F_{ij}}{m} \frac{\partial f_N}{\partial \xi_i} = 0$$
 (2.3)

From now on, the Liouville equation and all the subsequent kinetic equations following from the Bogolyubov chain including the last Boltzmann equation have a probabilistic nature. Although Eq. (2.3) is simpler than system (2.2), it takes into account the collisions of N molecules and is very difficult to analyze. A less detailed description is achieved by roughening the description using s-particle distribution function $f_s = \int f_N d\mathbf{r}_{s+1}...d\mathbf{r}_N d\mathbf{x}_{s+1}...d\mathbf{x}_N$, which determine the

probability to simultaneously find s particles independently of the state of the remaining (N-s) particles.

Following Bogolyubov's ideas, we obtain the chain of linked equations

$$\frac{\partial f_s}{\partial t} + \sum_{i=1}^s \xi_i \frac{\partial f_s}{\partial \mathbf{r}_i} + \sum_{i=1}^s \sum_{j=1}^s \frac{F_{ij}}{m} \frac{\partial f_s}{\partial \xi_i} = -\sum_{i=1}^s (N-s) \frac{\partial}{\partial \xi_i} \int \frac{F_{ij}}{m} f_{s+1} d\mathbf{r}_{s+1} d\xi_{s+1}$$
(2.4)

up to the single-particle distribution function $F_1 = f(t, r, \xi)$ corresponding to the Boltzmann gas, which only takes into account the binary collisions:

$$\frac{\partial f_2}{\partial t} + \sum_{i=1}^2 \xi_i \frac{\partial f_2}{\partial \mathbf{r}_i} + \sum_{i=1}^2 \sum_{j=1}^2 \frac{F_{ij}}{m} \frac{\partial f_2}{\partial \xi_i} = -\sum_{i=1}^2 (N-2) \frac{\partial}{\partial \xi_i} \int \frac{F_{ij}}{m} f_{2+1} d\mathbf{r}_{2+1} d\xi_{2+1}$$

For triple collisions:

$$\frac{\partial f_3}{\partial t} + \sum_{i=1}^3 \xi_i \frac{\partial f_3}{\partial \mathbf{r}_i} + \sum_{i=1}^3 \sum_{j=1}^3 \frac{F_{ij}}{m} \frac{\partial f_3}{\partial \xi_i} = -\sum_{i=1}^3 (N-3) \frac{\partial}{\partial \xi_i} \int \frac{F_{ij}}{m} f_{3+1} d\mathbf{r}_{2+1} d\xi_{3+1}$$

Following Boltzmann, we assume that the molecules are spherically symmetric and accept the molecular chaos hypothesis $F_2(t, r_1, r_2, \xi_1, \xi_2) = F_1(t, r_1, \xi_1)F_1(t, r_2, \xi_2)$ to obtain Eq. (2.1).

It is very interesting to consider a particular case of Liouville's equation (2.3) and of Bogolyubov's chain (2.4) that describe a spatially homogeneous gas consisting of a bounded number of particles and corresponding to two-particle collisions; in this case, on the final link of the chain, we obtain the Kac master equation [29]

$$\frac{\partial \varphi_1(t, \xi_1)}{\partial t} = \frac{N-1}{N} \int [\varphi_2(t, \xi_1', \xi_2') - \varphi_2(t, \xi_1, \xi_2)] \mathbf{g}_{12} d\sigma_{12} d\xi_2 \quad (2.5)$$

where φ_1 and φ_2 are the one- and two-particle distribution functions. In contrast to the Boltzmann equation, Eq. (2.5) is linear, which will be used in the development and justification of efficient numerical direct statistical simulation schemes.

Returning to the Boltzmann equation, we easily obtain all the macroscopic parameters from the definition of the function f. For example, the number of molecules n in a unit volume of the gas is

$$n(t,\mathbf{r}) = \int f(t,\mathbf{r},\boldsymbol{\xi})d\boldsymbol{\xi}$$

The mean velocity of the molecules, the strain tensor, and the energy flux are determined by the relations

$$\mathbf{v}(t,\mathbf{r}) = \frac{1}{n} \int \xi f(t,\mathbf{r},\xi) d\xi,$$

$$P_{ij} = m \int c_i c_j f(t,\mathbf{r},\xi) d\xi,$$

$$q_i = \frac{m}{2} \int c^2 c_i f(t,\mathbf{r},\xi) d\xi,$$

where $c = \xi - V$ is the thermal velocity of the molecules. The mean energy of the heat motion of molecules is usually described in terms of the temperature

$$\frac{3}{2}kT = \frac{1}{n}\int \frac{mc^2}{2}f(t,\mathbf{r},\xi)d\xi$$

Applying the Chapman–Enskog procedure to the Boltzmann equation, we obtain the hydrodynamical level of description. This sequentially yields the Euler, Navier–Stokes, Barnett, etc., equations:

$$\begin{split} \frac{\partial \rho}{\partial t} + \frac{\partial \rho V_i}{\partial x_i} &= 0 \\ \left(\frac{\partial}{\partial t} + V_j \frac{\partial}{\partial x_j} \right) V_i &= -\frac{1}{\rho} \frac{\partial P_{ij}}{\partial x_j} \\ \frac{3}{2} R \rho \left(\frac{\partial}{\partial t} + V_j \frac{\partial}{\partial x_j} \right) T &= -\frac{\partial p_j}{\partial x_j} - P_{ij} \frac{\partial V_j}{\partial x_j} \\ p_{ij} &= \mu \left(\frac{\partial V_i}{\partial x_j} + \frac{\partial V_j}{\partial x_i} - \frac{2}{3} \delta_{ij} \frac{\partial V_r}{\partial x_r} \right) \\ q_i &= -\lambda \frac{\partial T}{\partial x_i}. \\ p &= \rho R T \end{split}$$

The expressions for the components of the thermal velocity can be obtained by simulating the normally distributed random variable

$$\xi_x = \sqrt{\frac{2k_B T}{m}} \sqrt{-\ln \alpha_1} \cos(2\pi\alpha_2)$$

$$\xi_y = \sqrt{\frac{2k_B T}{m}} \sqrt{-\ln \alpha_1} \sin(2\pi\alpha_2)$$

$$\xi_z = \sqrt{\frac{2k_B T}{m}} \sqrt{-\ln \alpha_3} \cos(2\pi\alpha_4)$$

here, α_k is independent random numbers that are uniformly distributed on the interval (0, 1). In order to reproduce the mean velocity more accurately, it is reasonable to use the following symmetrized algorithm: the thermal velocities of the particles with the odd indexes are calculated, and the thermal velocities of the particles with the even indexes are set equal to the velocities of the corresponding odd particles with the opposite sign.

The complex nonlinear structure of the collision integral and the large number of variables (seven in the general case) present severe difficulties for the analysis including numerical analysis. The high dimension, the probabilistic nature of the kinetic processes, and complex molecular interaction models are the natural prerequisites for the application of the Monte Carlo methods [25, 30].

Let's see the kinetic equations for triple molecular collisions. The statistical independence of particles before collision, solution of equation is [31] $f_3(t, \tau_1, \tau_2, \tau_3) = f_1(t_0, \tau_{10}) f_1(t_0, \tau_{20}) f_1(t_0, \tau_{30}).$

where $\tau_{a0} = \tau_{a0}$ (t, t_0 , τ_1 , τ_2 , τ_3) – coordinate and impulse values which particles at the moment t_0 for that at the time t get into given points τ_1 , τ_2 , τ_3 of the phase space.

Now, let's move from f_1 to $f = Nf_1$, and find kinetic equation in the form of

$$\frac{\partial f}{\partial t} + \overline{\xi} \nabla f = St_2 f + St_3 f ,$$

$$St_2 f(t, \tau_1) = \int \frac{\partial F_{12}}{m} \frac{\partial}{\partial \xi} \{S_{12} f(t, \tau_1) f(t, \tau_2)\} d\tau_2$$
 - Integral for pair collisions

$$St_3f(t,\tau_1) = \frac{1}{N} \int \frac{F_{12}}{m} \frac{\partial}{\partial \xi} \left\{ R_{123}f(t,\tau_1)f(t,\tau_2)f(t,\tau_3) \right\} d\tau_2 d\tau_3 \quad \text{- Integral for triple collision}$$

here S_{12} and R_{123} – some operators. Let's consider a few of collision processes taking into account integral. First of all, the operator R_{123} is zero, if at least one of the particles does not interact with the others. The process $R_{123} \neq 0$ is not only the triple collisions, but also combination of several pair of molecules. We consider several types of collisions (Fig. 2.2 (a, b, c)) [31].

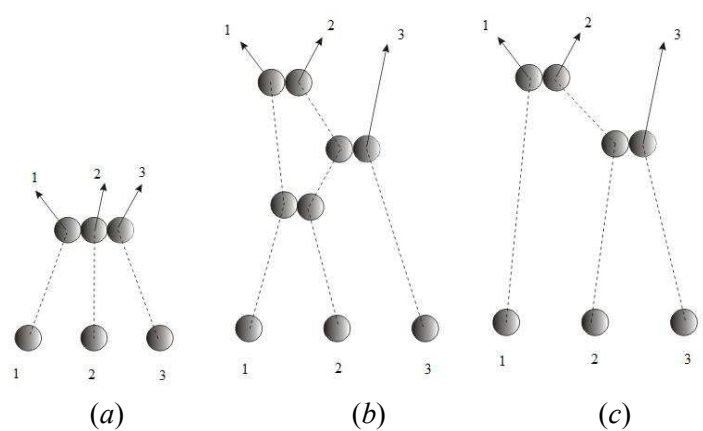


Figure 2.2 The basic trajectories of triple collisions of molecules

Figs. 2.3 show the distribution of the velocity of the molecules before and after collisions (total number of particles $N = 9 \times 10^5$). From the graphs, it is clear that the velocity distribution of the molecules before and after collision is the same. Elastic collision is defined as collision in which there is no exchange between the translational and internal energies. Triple collisions will occur, after colliding as pair molecular collisions. Although the Lennard-Jones potential and is used in simulations of liquid and solids, strictly speaking, the molecular interaction at high densities is no longer a pair collision [32].

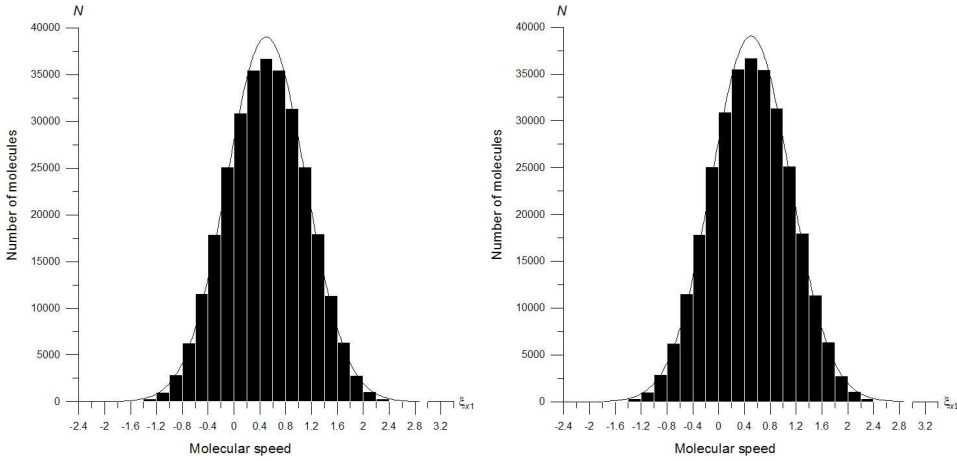


Figure 2.3 Velocity distribution function before and after collisions

In condensed mediums, to consider the collisions of molecules, the environment affects on the molecules. So, the solid argon contribution to the energy of the triple collisions can reach 10 % [33]. However, taking into account the triple collisions of molecules computationally too expensive to simulate in rarefied gas dynamics approach [34-36].

2.3. Method for surface description of the complex vehicle design

One of the basic technology questions of aerodynamic characteristics calculation of the arbitrary apparatus shape is the rational choice of way to describe of surface geometry. Methods for describing of complex surfaces can be divided into two main groups: mathematical approximation of a surface and space distribution of large number surface points which restored the system of surface element. The main disadvantage of the first group of methods are usually related to approximation of complex mathematical problems, essentially nonlinear surfaces on small number of control points, and the second - difficulty preparation of initial data. In the given work, these both methods are used: due to comparative simplicity and universality of the task of control points, and finally restore surface on the control points, the modeled body is divided into number of

specific parts (wing, fore part, bottom-most part of fuselage, etc.), for each of those is conducted square-law interpolation on control points [37].

For each part introduces the axis (x, y', z'), which are the axes of the symmetric coordinate system. Axis divided into a finite number of characteristic points defined by the parameters x_i , y_i , z_i . These points in a cylindrical coordinate system are given by section: φ_j , R_{ij} ; φ_{yi} , R_{yij} ; φ_{zi} , R_{zij} . Depending on the shape of the cross section, it can be defined as a discrete and in analytical form.

For qualification the surface of the passing points provides an interpolation procedure. Intermediate points on the axes and the angles are according to the formulas of the linear interpolation,

$$x_{i} = \frac{1}{2} \left(x_{\frac{i-1}{2}} + x_{\frac{i+1}{2}} \right),$$

$$\varphi_{j} = \frac{1}{2} \left(\varphi_{\frac{j-1}{2}} + \varphi_{\frac{j+1}{2}} \right)$$

Radius value by use of Lagrange polynomial interpolation is interpolated twice – by φ и x:

$$R(a) = \sum_{i=1}^{3} R(a_i) \prod_{j \neq 1} \frac{a - a_j}{a_i - a_j}$$

where $a_{i,j}$ - correspond to the values of $\varphi u x$ in the interpolation points.

Thus, with the required accuracy are given by the initial points on the surface. The question remains, how is spanned by the available core surface of the streamlined apparatus. As already noted, the aim is suitable linear approximation, so in the capacity of basic will consider the linear element, correspond triangle, which was build by nearest three points. Vertices of triangles in rectangular coordinates for the different parts are defined by formula.

For fuselage

$$r = \begin{pmatrix} x \\ y \\ z \end{pmatrix} = \begin{pmatrix} x_i \\ R_{ij} \cos \varphi_j \\ R_{ij} \sin \varphi_j \end{pmatrix}$$

For wing

$$\begin{pmatrix} x \\ y \\ z \end{pmatrix} = \begin{pmatrix} x_0 + z_i \cos \alpha_z - R_{zij} \cos \gamma_{zi} \\ y_0 + z_i \sin \alpha_z + R_{zij} \sin \varphi_{zj} \\ z_0 + z_i \cos \alpha_z \cos \beta_z - R_{zij} \cos \varphi_{zj} \sin \gamma_{zi} \end{pmatrix}$$

Where (x_0, y_0, z_0) - initial coordinates of the axis of the wing z', α_z - angle of slope of axis of the wing to the surface y = 0, β_{zi} - angle of slope of the axis of the wing to the axis z, γ_{zi} - the angle of slope defined by sections on the axis z'. For full definition of elements it is necessary to determine its orientation and surface area.

Let $\mathbf{a} = r_2 - r_1$, $\mathbf{b} = r_3 - r_1$, generating elements of the vector. Then element of the area and normal to the surface

$$S = \frac{1}{2} (\mathbf{a} \times \mathbf{b}),$$

$$\mathbf{n} = (\mathbf{a} \times \mathbf{b}) / (|\mathbf{a} \times \mathbf{b}|)$$

An estimate error for approximation by linear elements in the process for free molecular flow regime gives good results. So, for the approximation in calculation the resistance of cone accurate within 5% (average error of statistical methods) should be about 10 elements, and for approximation of the sphere – 100, single application of the interpolation procedure reduces the error by an order [37].

2.4. The Mathematical description of gas-surface interaction models

The collision process between gas molecule and solid surface is termed gassurface interaction. In kinetic theory, the gas-surface interaction forms a boundary condition between the gas molecules and solid surface. For scales relevant to kinetic theory, the gas-surface interactions are usually modeled with parameters having macroscopic character, in order to have manageable and efficient calculations. Although various gas-surface interaction models have been proposed over the past century and a half, the validity of these models remains tenuous for rarefied gas flow condition. In particularly, intended to analyze gas-surface interaction models on aerodynamic effects (Maxwell model, Cercignani-Lampis-Lord (CLL) model and Lennard-Jones potential).

The majority of gas dynamic problems include the interaction of gas particles with the body surface. Diffusion reflection with complete momentum and energy accommodation is most frequently used in DSMC method. In a diffuse reflection, the molecules are reflected equally in all directions usually with a complete thermal accommodation. The problem of gas-surface interaction takes an essential place in aerodynamics. The role of laws of molecular interaction with surfaces is shown more strongly, than more gas is rarefied [32]. Boundary conditions for Boltzmann equation are the conditions relating the distribution function of incident and reflected molecules.

Maxwell model

The most popular gas-surface interaction model for kinetic theory is specular and diffuse reflection model developed by Maxwell (1879). This model is based on the assumption that the portion $(1 - \sigma_{\tau})$ of molecules reflected specularly from the surface, and the rest part σ_{τ} of the molecule diffusely. The density of distribution of reflected molecules is set as follows:

$$f_r(\mathbf{x}_w, \boldsymbol{\xi}_r) = (1 - \sigma_{\tau}) f_i(\mathbf{x}_w, \boldsymbol{\xi}_r - 2(\boldsymbol{\xi}_r \cdot \mathbf{n})\mathbf{n}) + \sigma_{\tau} n_r \pi^{-3/2} h_r^{3/2} \exp(-h_r \boldsymbol{\xi}_r^2), \ (\boldsymbol{\xi}_r \cdot \mathbf{n}) > 0$$

and the scattering kernel has form

$$K(\boldsymbol{\xi}_{i} \to \boldsymbol{\xi}_{r}) = (1 - \sigma_{\tau})\delta\left[\boldsymbol{\xi}_{i} - 2(\boldsymbol{\xi}_{r} \cdot \mathbf{n})\mathbf{n}\right] - \sigma_{\tau} \frac{2h_{r}^{2}}{\pi} \exp\left[-h_{r}\boldsymbol{\xi}_{r}^{2}\right] \cdot (\boldsymbol{\xi}_{i} \cdot \mathbf{n}), h_{r} = \frac{m}{2kT_{r}}$$

Here, ξ_r -velocity vector of the reflected molecules, δ - Dirac delta-function, n -outward unit normal to the surface x_w , h_r - most probable velocity of molecules at temperature T_w . Indexes i and r denote the quantities for the incident and reflected fluxes, and an index w - the value corresponding to diffuse reflection at temperature of wall T_w . Parameter $0 \le \sigma_\tau \le 1$ in Maxwell model defines accommodation coefficient for the tangential momentum.

$$\sigma_{\tau} = \frac{p_{i\tau} - p_{r\tau}}{p_{i\tau}}$$

For complete specular reflection $\sigma_{\tau} = 0$, for complete diffuse reflections $\sigma_{\tau} = 1$. Popularity of Maxwell model is due to its simplicity and with the fact that it satisfies the principle of detailed balance. Maxwell's model proved suitable for low speed experiments and low rarefaction environments.

The velocity vector components at diffuse reflection are modelled in local spherical coordinate system which axis is directed along outward unit normal to the surface, by means of expressions [30]

$$|\xi_r| = h_r^{-1/2} \sqrt{-\ln(\alpha_1 \alpha_2)}$$
, $\cos \theta = \sqrt{\alpha_3}$, $\phi = 2\pi \alpha_4$

Where α_1 , α_2 , α_3 , α_4 - the independent random numbers uniformly distributed between 0 and 1. θ , ϕ - polar and azimuthal angles. The Accommodation coefficient of kinetic energy is defined in terms of incident and reflected fluxes as follows

$$\sigma_E = \frac{E_i - E_r}{E_i - E_w} = \frac{\xi_i^2 - \xi_r^2}{\xi_i^2 - h_w^{-1}}$$

Here E_w - energy which would be carried out the reflected molecules if gas is in equilibrium with wall, i.e., when $T_r = T_w$. Expression for velocity of the reflected molecule corresponding to not full accommodation of kinetic energy looks like

$$\mid \xi_r \mid = k h_r^{-1/2} \sqrt{-\ln(\alpha_1 \alpha_2)} \;, \qquad \qquad k = \sqrt{(1 - \sigma_E) \xi_i^2 h_r + \sigma_E}$$

Cercignani-Lampis-Lord model

In work [38] is proposed phenomenological model of Cercignani-Lampis (CL) which also satisfies to principle of reciprocity and is reported improvement of the Maxwell models [32]. The model is based on introduction of two parameters which represent accommodation coefficient of kinetic energy connected with coefficients of normal momentum $\sigma_n = \sigma_{En}$, and tangential momentum accommodation σ_{τ} , respectively.

Model CL well corresponds to results of laboratory researches with high-speed molecular beams. Although comparison is limited by laboratory conditions, CL model is theoretically justify and relatively simple. Later, there were modification of scattering kernel of CL model; however, they give slight improvement at comparison with laboratory experiments. Generally the interaction model has some arbitrary physical parameters that allow to achieve the reasonable agreement with results of laboratory researches in range of conditions. In this sense, original model CL is enough physical and suitable for theoretical research. The universal model should use the scattering kernel received on the basis of physical experiment in a wide range of Knudsen numbers and velocity of stream.

In CL model, the diffusion kernel of velocity for surface normal has the following form

$$K(\xi_{ni} \to \xi_{nr}) = \frac{2\xi_{nr}}{\sigma_n} I_0 \left(2\sqrt{1 - \sigma_n} \frac{\left| \xi_{ni} \right| \xi_{nr}}{\sigma_n} \right) \exp \left[-\frac{\xi_{nr}^2 + (1 - \sigma_n) \xi_{ni}^2}{\sigma_n} \right]$$
$$I_0(x) = \frac{1}{2\pi} \int_0^{2\pi} \exp(x \cos \phi) d\phi$$

Here I_0 -first type Bessel function, ξ_{ni} , ξ_{nr} - molecular velocities of surface normal for the incident and reflected molecules, rating as $h_w^{-1/2}$. A scattering kernel is written as follow

$$K(\xi_{\tau i} \to \xi_{\tau r}) = \frac{1}{\sqrt{\pi \sigma_{\tau}(2 - \sigma_{\tau})}} \exp \left[-\frac{\left(\xi_{\tau r} - (1 - \sigma_{\tau})\xi_{\tau i}\right)^{2}}{\sigma_{\tau}(2 - \sigma_{\tau})} \right]$$

Here $\xi_{\tau i}$, $\xi_{\tau r}$ – molecular velocities of tangent to surface for the incident and reflected molecules, rating as $h_w^{-1/2}$.

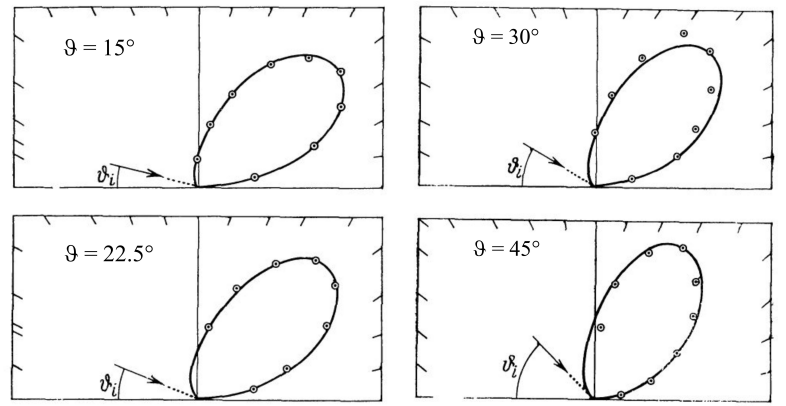


Figure 2.4 Comparison of the experimental data of [39] with the calculated results by using the kernel [38] $(\sigma_n = 0.3, \sigma_\tau = 0.1, \theta = 15^\circ, 22.5^\circ, 30^\circ \text{ and } 45^\circ)$

Twenty years after creation CL model have been published the algorithm of its realization based on some transformation with the limits of direct statistic simulation method [40]. The model in this form is called as Cercignani-Lampis-Lord model (CLL). Usage of CL model transformation expands to account for rotational energy exchange between gas and surface. Then, updating CLL model in the form of [41] is to account for vibrational energy exchange and extend rang of states of the scatted molecule. CLL model is widely recognized examples of its application are presented in multiple works [42-55].

In order to simulate the partial surface accommodation, the CLL model was implemented into this DSMC calculation [56]. The CLL model is derived assuming momentum components. The two adjustable parameters appearing in the CLL model are the normal component of translational energy α_n and the

tangential component of momentum σ_{τ} . However, in the implementation of the CLL model in the DSMC method, Bird has shown that it is equivalent to specify the normal α_n and tangential α_{τ} components of translational energy, since $\alpha_{\tau} = \sigma_{\tau}(2 - \sigma_{\tau})$, and thus $\sigma_{\tau} < \alpha_{\tau}$, assuming that σ_{τ} lies between 0 and 1.

Nocilla model

The model (Nocilla, 1963) [57] was for the first time applied to the calculation of aerodynamic coefficients of drag and lift for simple figures in a free-molecular flow. The model is more general as compared to the Maxwell model; but at the same time, it is also simple in application. We can see more about explanation about Nocilla model in the work [58-63].

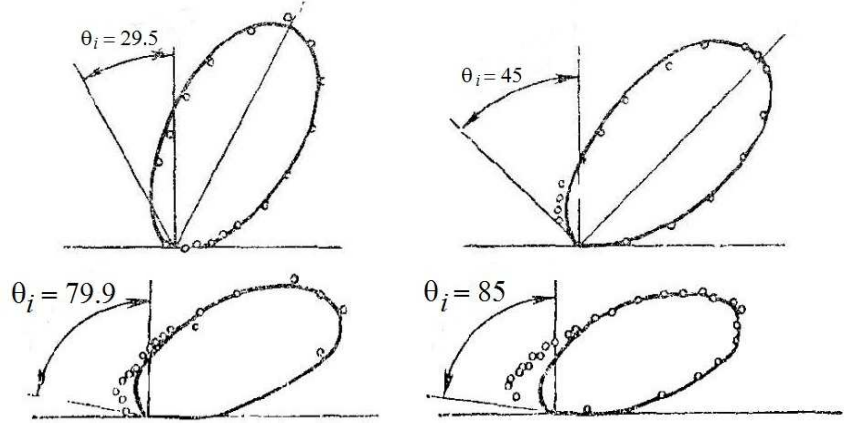


Figure 2.5 Comparison of the experimental data [32]

The distribution functions of the particles reflected from the surface are presented in the following form:

$$f_r = n_r \left(\frac{\pi}{h_r}\right)^{3/2} \exp\left\{-\left[\left(h_r\right)^{1/2} \xi_y - S_{nr}\right]^2 - \left[\left(h_r\right)^{1/2} \xi_x - S_{\tau r, x}\right]^2 - \left[\left(h_r\right)^{1/2} \xi_z - S_{\tau r, z}\right]^2\right\}$$

here ξ , n_r are the velocity and density of reflected molecules, and S_{nr} , $S_{\tau r}$ are the velocity vector components of incident molecules. Parameters of the function f_r are selected depending on available experimental data and the law of mass conservation.

$$S_{nr} = 0.1 - 0.65 \frac{2\theta}{\pi},$$

$$S_{\tau r,x} = \frac{\tau_{r,x}}{p_r} \cdot \frac{J_2(S_{nr})}{J_1(S_{nr})}, \quad 2\frac{k}{m} T_r = \left(\frac{p_r}{q_{mr}}\right) 2 \left[\frac{J_1(S_{nr})}{J_2(S_{nr})}\right]^2,$$

$$n_r = q_{mr} \left(2\frac{k}{m} T_r\right)^{-1/2} J_1^{-1}(S_{nr}),$$

$$\tau_{r,x} = -\left(a_{\tau} + b_{\tau} \frac{4\theta - \pi}{2\pi}\right) q_{mi} \xi \sin\theta,$$

$$p_r = \left\{\left(a_n + b_n \frac{2\theta}{\pi}\right) \xi + \left(\frac{\pi}{2} \frac{kT_w}{m}\right)^{1/2} \right\} q_{mi},$$

$$J_1(t) = \frac{1}{\sqrt{\pi}} \int_0^{\infty} q \exp\left[-(q - t)2\right] dq = \frac{1}{\sqrt{2\pi}} \left[e^{-t^2} + \sqrt{\pi} t(1 + erf(t))\right],$$

$$J_2(t) = \frac{1}{\sqrt{\pi}} \int_0^{\infty} q^2 \exp\left[-(q - t)2\right] dq = \frac{1}{\sqrt{2\pi}} \left[te^{-t^2} + \sqrt{\pi} \left(\frac{1}{2} + t^2\right)(1 + erf(t))\right],$$

$$erf(t) = \frac{2}{\sqrt{\pi}} \int_0^t e^{-s^2} ds, \quad q_{mr} = q_{mi} = mq_1; \quad q_1 = 1 \left[m^{-2} s^{-1}\right].$$

here, θ – angle between velocity vector of incident and internal normal to the surface, T_r – wall temperature, q_{mr} , q_{mi} – incident and reflected flux, which are used by normal distribution function f_r in Monte-Carlo method. The parameters a_n , b_n , a_τ and b_τ depends on material of surface which obtained from experimental work. The Nocilla model is use in the complex program "SMILE" [64] and "MONACO" for spacecraft aerodynamics investigation [65].

Lennard-Jones potential

Generally speaking, at molecular level it is necessary to consider interaction potentials, using electron-nuclear representations. Empirical potential dependences reflect the fact, that attractive forces at large distance and repulsive forces at short distances. This feature is reflected most simply with Lennard-

Jones potential. The sixth power is decrease of potential simulate electrostatistical dipole-dipole and dispersive attraction. The twelfth-power repulsive potential is decrease from reasons of mathematical convenience. At the same time, it models rigid enough repulsion.

$$U(r) = 4\varepsilon \left[\left(\frac{\sigma}{r} \right)^{12} - \left(\frac{\sigma}{r} \right)^{6} \right]$$

when $r = \sigma$ the potential is equal to zero.

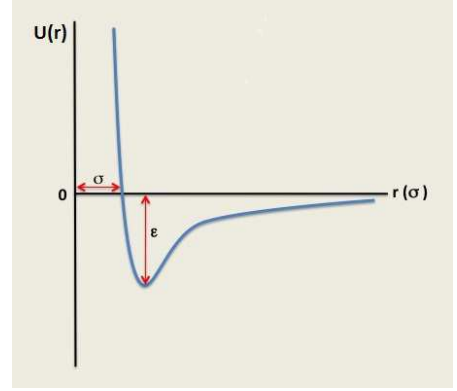


Figure 2.6

The value ε characterizes depth of a potential hole of the one electron volt. This feature is most simply reflects Lennard-Jones potential. It's shown that this model qualitatively correctly described the behavior of aerodynamic characteristics [32].

2.5. Modelling of the aerodynamic characteristics of aerospace vehicles in free molecular flow

The calculation has been carried out through the method described in the previous section within the range of angles of attack α from – 90 deg to +90 deg with a step of 5 deg. The parameters of the problem are the following: ratio of heat capacities $\gamma = 1.4$; temperature factor $t_w = T_w/T_0 = 0.04$; velocity ratio $M_\infty = 20$, energy accommodation coefficient $\sigma_n = 0.5$, 0.9, 1, momentum

accommodation coefficient $\sigma_{\tau} = 0.5, 0.9, 1$. The coefficients of drag force C_D , lift force C_L and pitching moment M_Z which are calculated according to equations as below

$$C_{i} = \frac{F_{i}}{\frac{1}{2}\rho_{\infty}V_{\infty}^{2}S_{ref}}, \quad m_{Z} = \frac{M_{i}}{\frac{1}{2}\rho_{\infty}V_{\infty}^{2}L_{ref}S_{ref}}, \qquad i = x, y, z$$

 L_{ref} , S_{ref} – references length and surface; F_i M_i – resultant force acting on the vehicle and moment, respectively.

In the figure 2.8 presented the results of the calculation of the coefficients of drag force C_x , lift force C_y with value of angle of attack α from 0 deg to 30 deg for reentry vehicle (fig. 2.7) by using DSMC method with the use of three gassurface interaction models (Maxwell, Cercignani-Lampic-Lord).

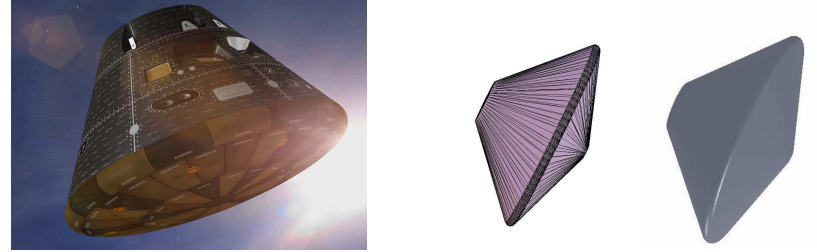


Figure 2.7 General view and schematic view of reentry vehicle

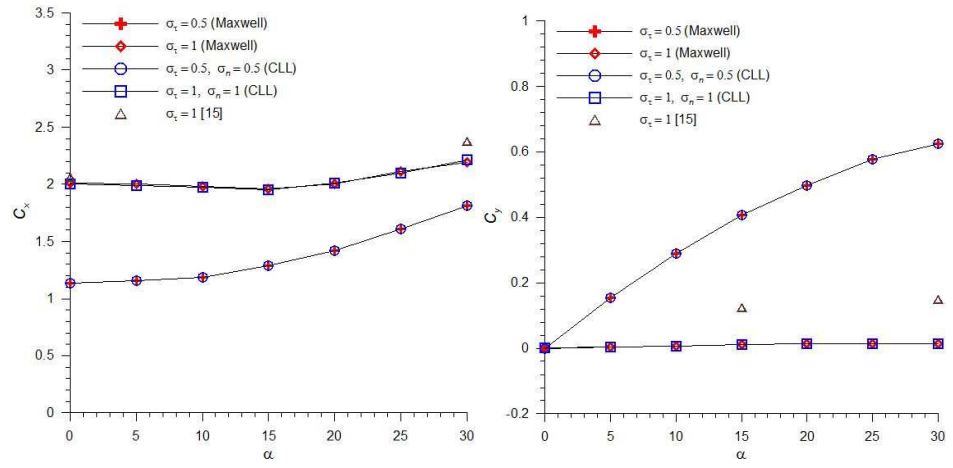


Figure 2.8 Dependencies of $C_x(\alpha)$ and $C_y(\alpha)$ for reentry vehicle

In the fig. 2.10 presented the results of the calculation of the coefficients of drag force C_x , lift force C_y with value of angle of attack α from – 90 deg to +90 deg for aerospace vehicles (fig 2.9) by using DSMC method with the use of three gas-surface interaction models. In several works (Vaganov A.V., Drozdov S., Kosykh A.P., Nersesov G.G., Chelysheva I.F., Yumashev V.L., Khlopkov Yu.I., Voronich I.V., Zay Yar Myo Myint, Khlopkov A.Yu.) investigated the aerodynamics characteristics of aerospace vehicle "Clipper, model of TsAGI" [66, 48-45].

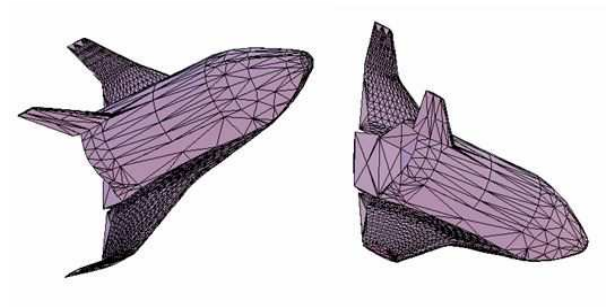


Figure 2.9 Geometrical view of aerospace vehicle "Clipper"

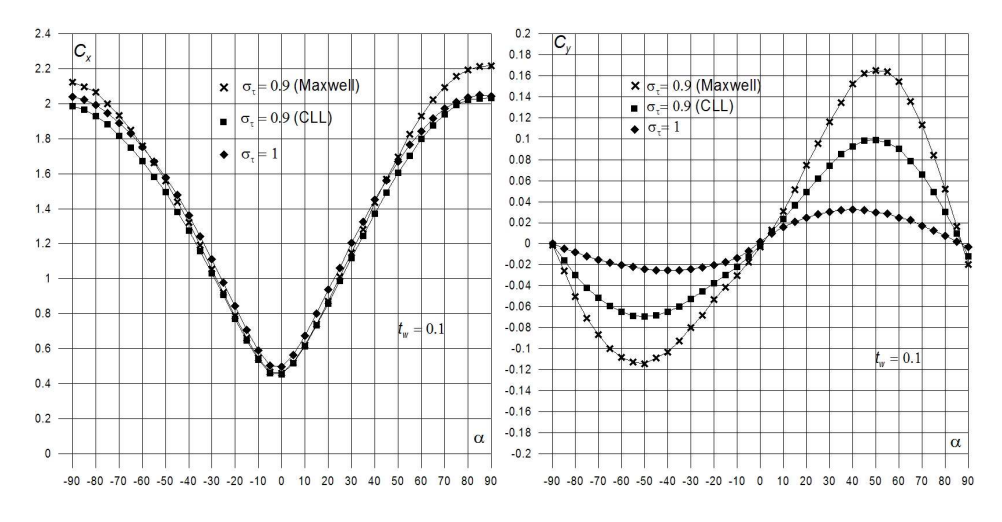


Figure 2.10 Dependencies of $C_x(\alpha)$ and $C_y(\alpha)$ for aerospace vehicle "Clipper"

From these results, we can explain, the drag and lift coefficient results of CLL model less than the Maxwell model as expected. The Maxwell model and CLL model predict the same lift, drag when the accommodation coefficients are equal to zero or one. In fact, for $\alpha_{\tau} = 1$ in Maxwell model and $\alpha_{\tau} = \alpha_n = 1$ in the CLL model, the two models give precisely the same. For accommodation coefficients not equal to zero or one, the CLL model gives higher aerodynamic forces than the Maxwell model for the same value of their respective accommodation coefficients.

In figure 2.11 shows the dependence of $C_x(\alpha)$ and heat transfer coefficient C_h with the use of various gas-surface interaction models (Maxwell, Cercignani-Lampic-Lord (CLL), Lennard-Jones (LJ)). In this reason, the accommodation coefficient σ_{τ} is 1. Coefficient C_x increases with the rise of the angle of attack. From the graphs, it is clear that the coefficients are sensitively different at models of the gas-surface interaction models with surfaces.

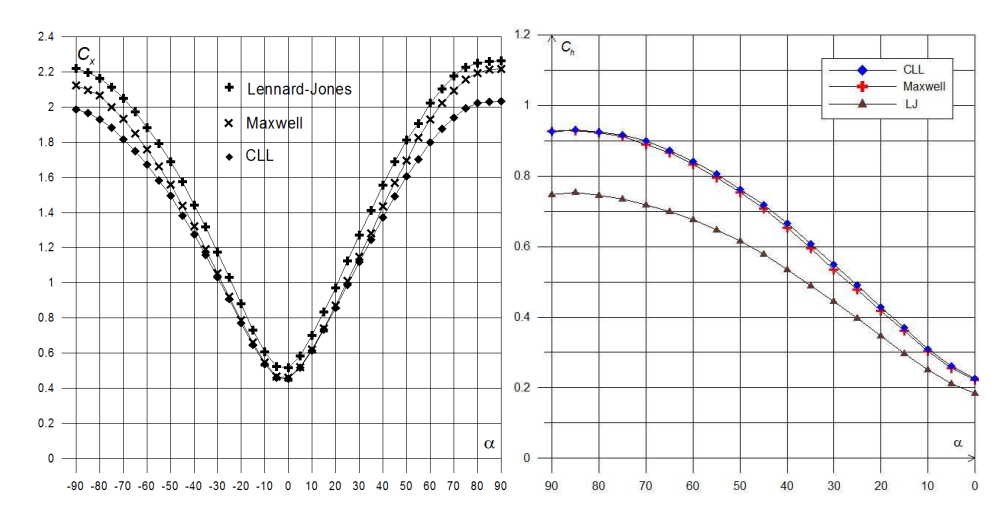


Figure 2.11 Dependencies of $C_x(\alpha)$ and $C_h(\alpha)$ for aerospace vehicle with various gas-surface interaction models

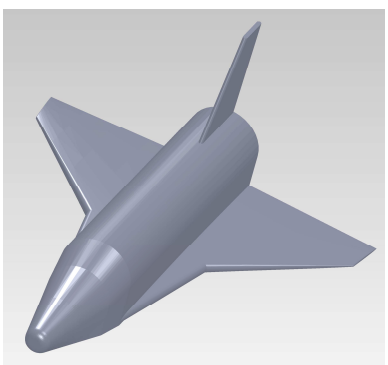


Figure 2.12 Geometry view of aerospace vehicle

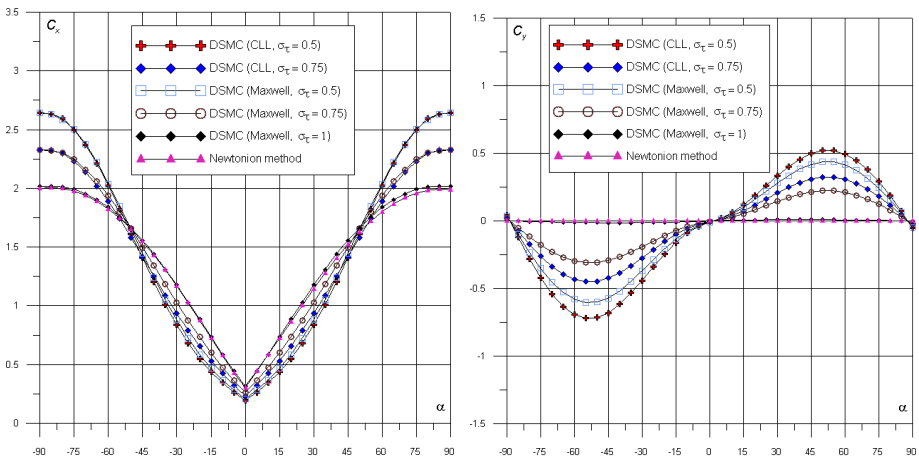


Figure 2.13 Dependencies of $C_x(\alpha)$ and $C_v(\alpha)$ for aerospace vehicles

In figure 2.13 show the calculation results of the coefficients of drag force C_x , lift force C_y with value of angle of attack α from -90 to +90 deg for aerospace vehicle (fig. 2.12) are presented. The calculation has been carried out through the methods described in the previous section. The parameters of the problem are the following: ratio of heat capacities $\gamma = 1.4$; temperature factor $T_w/T_0 = 0.001$, $T_w/T_\infty = 0.1$; velocity ratio s = 15; accommodation coefficients $\sigma_\tau = 0.5$, 0.75, 1.

The Maxwell model and the Cercignani-Lampis-Lord model turned out to have principal differences, but in most cases they gave close values of aerodynamic forces and moments [48, 49].

In order to simulate the partial surface accommodation, the CLL model was implemented into this DSMC calculation. The CLL model is derived assuming momentum components. The two adjustable parameters appearing in the CLL model are the normal component of translational energy α_n and the tangential component of momentum σ_{τ} . However, in the implementation of the CLL model in the DSMC method, Bird has shown that it is equivalent to specify the normal α_n and tangential α_{τ} components of translational energy, since $\sigma_{\tau} = \sigma_{\tau}$ (2– σ_{τ}), assuming that σ_{τ} lies between 0 and 1.

For molecular velocity distributions, the Maxwell and CLL models gave similar ξ_x distributions, but distinct ξ_y distributions, at partial levels of gassurface accommodation. Moreover, while the Maxwell scattering distributions experienced abrupt changes with increasing accommodation and position, the CLL distributions varied smoothly. For no significant additional cost, the CLL model gave more realistic scattering distributions.

The Investigation provided better understanding of the effects of gas-surface interaction models in DSMC calculations and ultimately a better understanding of the accommodation coefficients of materials and gases for orbital and aerobreaking conditions. The gas-surface interaction models have fundamental differences, they give similar predictions of aerodynamic forces on various vehicle design. The calculations with normal. tangential aerospace accommodation coefficients provided are more sensitivity the aerothermodynamics quantities of aerospace technologies.

CHAPTER 3 METHODS FOR DETERMINING AEROTHERMODYNAMIC CHACTERISTICS OF HIGH-SPEED VEHICLES IN TRANSITIONAL FLOW REGIME

It is well known that for flight in the upper atmosphere, where it is necessary to take into account the molecular structure of a gas, kinematics models are applied, in particular, the Boltzmann equation and corresponding numerical methods of simulation. In the extreme case of free-molecular flow, the integral of collisions in the Boltzmann equation becomes zero, and its general solution is a boundary function of distribution, which remains constant along the paths of particles. While aircraft are moving in a low atmosphere, the problems are reduced to the problems that can be solved in the frame of continuum theory or, to be more precise, by application of the Navier-Stokes equations and Euler equations. It is natural to create engineering methods, justified by cumulative data of experimental, theoretical and numerical results, enabling the prediction of aerodynamic and aerothermodynamic characteristics of complex bodies in the transitional regime [67, 68].

Multi-parametric calculations can be performed only by using an approximation engineering approach. Computer modeling allows to quickly analysis the aerodynamic characteristics of hypersonic vehicles by using theoretical and experimental research in aerodynamic of hypersonic flows. Direct simulation Monte Carlo method (DSMC) is the basic quantitative tool for study of hypersonic rarefied flows. DSMC method is required large amount of computer memory and expensive at the initial stage of spacecraft design and trajectory analysis. The solution for this problem is the approximate engineering methods. The Monte Carlo method remains the most reliable approach, together with the local engineering methods, that provides good results for the global aerodynamic coefficients.

3.1. Local engineering methods

The development of engineering semi-empirical methods based on the accumulated experimental data. We usually using in many engineering practice Newton's method and its modified method as shown in below

$$p = p_0 \cos^2 \theta$$

$$p_0 = p_{\infty} \left[\frac{\left(\gamma + 1\right) M_{\infty}^2}{2} \right]^{\gamma/(\gamma - 1)} \left[\frac{\gamma + 1}{2\gamma M_{\infty}^2 - (\gamma - 1)} \right]^{1/(\gamma - 1)}$$

here, p_0 - pressure at the stagnation point on the body surface. For high Mach number $(M_{\infty} \to \infty)$, p_0 is equal to 0.920 at $\gamma = 1.4$.

When modeling the natural conditions, it is necessary to consider the basic similarity criteria and in high-speed aerodynamics most commonly use parameters are: Mach number M, Knudsen number Kn and Reynolds number Re

$$M_{\infty} = \frac{V_{\infty}}{a_{\infty}}, \quad Kn = \frac{\lambda_{\infty}}{L_{ref}}, \quad Re_{\infty} = \frac{\rho_{\infty}V_{\infty}L_{ref}}{\mu_{\infty}}, \quad Kn \approx \frac{M}{Re}$$

where, λ_{∞} - the mean free path, $L_{\rm ref}$ - reference length of vehicle, μ_{∞} - the viscosity coefficient.

At the present time, it is possible to distinguish for convenience many engineering approaches for the calculation of aerodynamic characteristics using the Reynolds numbers Re. One of these approaches consists of the construction of the approximation function at known extreme values, corresponding to a free-molecular flow C(0) and a flow in the regime of continuum medium $C(\infty)$, which is usually determined through the Newton method

$$F(C, \operatorname{Re}, G, t_{w}, \gamma, \operatorname{M}, \dots) \approx \frac{C(\operatorname{Re}) - C(\infty)}{C(0) - C(\infty)},$$

$$F = \Phi \left[\left(\ln \operatorname{Kn} + a \right) / \sigma \right],$$

$$\Phi(x) = \frac{1}{\sqrt{2\pi}} \int_{-\infty}^{x} e^{-y^{2}/2} dy$$

The function F depends on the gas properties, parameters of the incident flow, surface geometry, etc. The values of a and σ are obtained on the basis of statistical processing of experimental data.

The classical method of locality is applied in the present work, and it is assumed that

$$C_p = \sum_{k=0}^{R} A_k (vn)^k$$
, $C_{\tau} = (v\tau) \sum_{k=1}^{R-1} B_k (vn)^k$,
 $(vn) = v \cos \theta$, $(v\tau) = v \sin \theta$.

In the extreme case of a continuum medium, we obtain through the Newton method:

$$C_{r} = C_{n}n = A_{2}(vn)^{2}n$$

In the other extreme of the free-molecular case we obtain:

$$C_x = C_{p_0}(vn)^2 n + C_{\tau_0}(vn)\tau$$

The other approached is classical method of simulation. As applied to highspeed flow, the Newton model for calculating pressure on the exposed leading part of the body surface is widely used.

$$p = 2\sin^2\theta$$
, $\tau = 0$

In high-speed flow, to define pressure and friction forces which are dependent on the coating materials and other global parameters are as follows [26](Kogan, 1969)

$$p = 2(2 - \sigma_n)\cos^2\theta + \sigma_n \left[\frac{\pi(\gamma - 1)}{\gamma}t_w\right]^{1/2}\cos\theta$$
$$\tau = 2\sigma_x \sin\theta\cos\theta$$

where $t_w = T_w/T_0$, T_w , T_0 are surface temperature and adiabatic stagnation temperature respectively, σ_n – normal accommodation coefficient and σ_{τ} - tangent momentum accommodation coefficient.

$$T_0 = T_{\infty} \left[1 + \frac{\gamma - 1}{\gamma} \mathbf{M}_{\infty}^2 \right]$$

where γ - specific heat ratio and M_{∞} - Mach number. It can assumed that a fraction of particles $(1-\sigma_{\tau})$ is reflected mirror-like from the surface and σ_{τ} is

ejected with Maxwell distribution which is characterized by reflected temperature T_r , then so called mirror-diffusion reflection.

In this work we use the expressions for the elementary pressure forces and friction forces are applied in the form described in [69, 70] (Galkin V.S., Erofeev A.I., & Tolstykh A.I.; Khlopkov Yu.I., Chernyshev S.L., Zay Yar Myo Myint & Khlopkov A.Yu.)

$$p = p_0 \sin^2 \theta + p_1 \sin \theta$$
$$\tau = \tau_0 \sin \theta \cos \theta$$

here, coefficients p_0 , p_1 , τ_0 (coefficients of the flow regime) are dependent on the Reynolds number $\text{Re}_0 = \rho_\infty V_\infty L/\mu_0$, in which the viscosity coefficient μ_0 is calculated at stagnation temperature T_0 . Except Reynolds number the most important parameter is the temperature factor T_w/T_0 .

The dependency of the coefficients of the regime in the high-speed flow must ensure the transition to the free-molecular values at $Re_0\rightarrow 0$, and to the values corresponding to the Newton theory, methods of thin tangent wedges and cones, at $Re_0\rightarrow \infty$. On the basis of the analysis of computational and experimental data, the empirical formulas are proposed

$$p_{0} = p_{\infty} + \left[p_{\infty} (2 - \sigma_{n}) - p_{\infty} \right] p_{1} / z$$

$$p_{1} = z \exp[-(0.125 + 0.078t_{w}) \operatorname{Re}_{0eff}]$$

$$\tau_{0} = 3.7\sqrt{2} \left[R + 6.88 \exp(0.0072R - 0.000016R^{2}) \right]^{-1/2}$$

$$z = \left(\frac{\pi(\gamma - 1)}{\gamma} t_{w} \right)^{1/2}$$

$$R = \operatorname{Re}_{0} \left(\frac{3}{4} t_{w} + \frac{1}{4} \right)^{-0.67}$$

$$\operatorname{Re}_{0eff} = 10^{-m} \operatorname{Re}_{0}, \quad m = 1.8(1 - h)^{3}$$

here h is a relative lateral dimension of the apparatus, which is equal to the ratio of its height to its length.

The technique proposed proved to be good for the calculation of high-speed flow of convex, not very thin, and spatial bodies. The calculation fully reflects a qualitative behavior of drag force coefficient C_x as a function of the medium rarefaction within the whole range of the angles of attack, and provides a quantitative agreement with experiment and calculation through the Boltzmann equation with an accuracy of 5%.

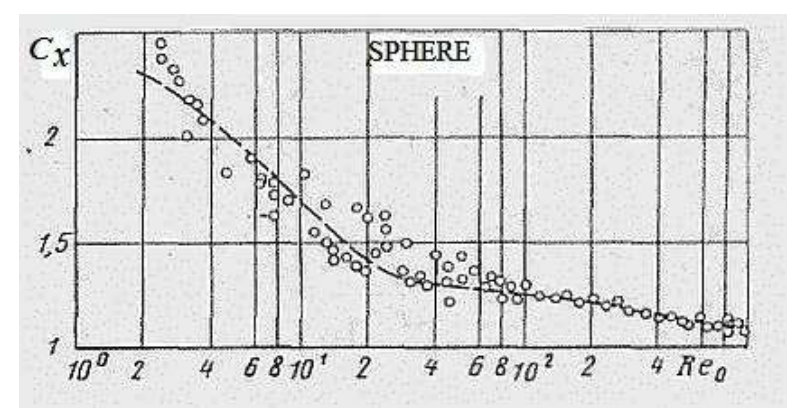


Figure 3.1 Drag coefficient C_x for sphere at various Reynolds number Re₀

On the accuracy of the relation of the locality method can be said that they are applied with the smallest error in the case of the bodies that are close to being spherical, and are not applied in the case of very thin bodies, when the condition is $M_{\infty} \sin \theta >> 1$ [37]. The local-engineering methods of the calculation of aerodynamic characteristics of the bodies in the high-speed flow of rarefied gas in the transitional regime gives a good result for C_x for a wide range of bodies, and a qualitatively right result for lift force coefficient C_y . In this case, it is necessary to involve more complete models that take into account the presence of the boundary layer [37]. In the papers of Khlopkov Yu.I., Zay Yar Myo Myint and Khlopkov A.Yu., described computational results of aerodynamic characteristics for perspective aerospace vehicles by using local-engineering methods.

The calculation results of the coefficients of drag force C_x , lift force C_y , pitching moments m_z and heat transfer C_h with value of angle of attack α from 0 to 90 deg for Russian perspective aerospace vehicle "Clipper, $TsAGI \ model$ " and USA perspective hypersonic technology vehicle "Falcon HTV-2" (fig 3.2) are presented.

The calculation has been carried out through the method described in the previous section within the range of angles of attack α from 0 deg up to 90 deg with a step of 5 deg. The parameters of the problem are the following: ratio of heat capacities $\gamma = 1.4$; temperature factor $T_w/T_0 = 0.01$; velocity ratio s = 15, Reynolds number $Re_0 = 0$, 10, 10^2 , 10^4 .



Figure 3.2 Geometry view of hypersonic technological vehicle "Falcon HTV-2"

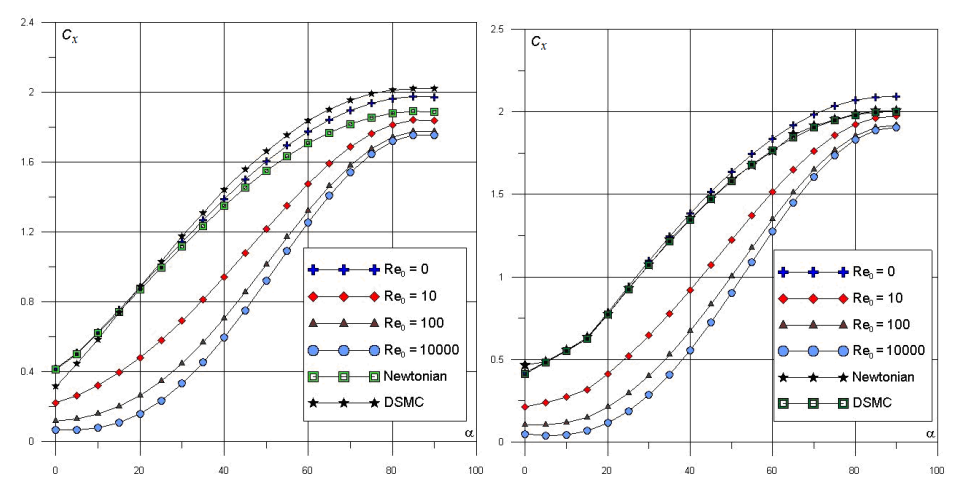


Figure 3.3 Dependencies of $C_x(\alpha)$ for "Clipper" and "Falcon HTV-2"

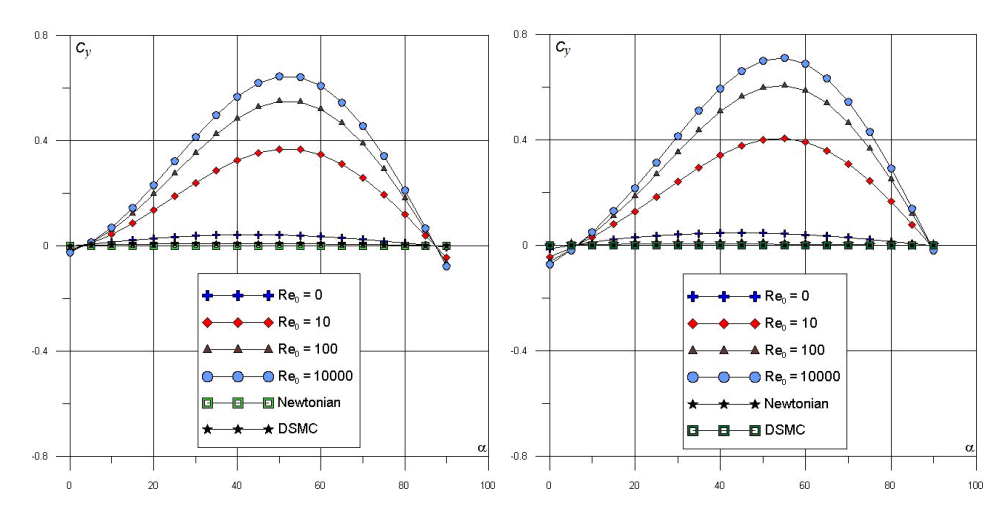


Figure 3.4 Dependencies of $C_{\nu}(\alpha)$ for "Clipper" and "Falcon HTV-2"

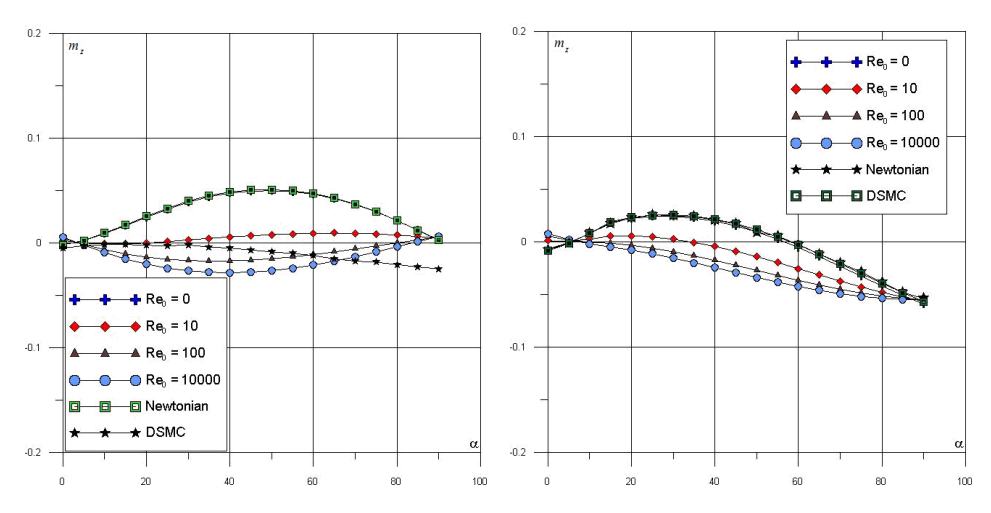


Figure 3.5 Dependencies of $m_z(\alpha)$ for "Clipper" and "Falcon HTV-2"

It can be seen from these results that when the Reynolds number increased, the drag coefficients C_x of vehicle diminished which can be explained by the decrease of normal and tangent stresses. At high Reynolds number $\text{Re}_0 \geq 10^6$, characteristics almost not changed. The dependency $C_y(\alpha)$ is increased at high Reynolds number which can be explained by the decrease of normal and tangent stresses. The values of m_z are quite sensitive to the variation of Re_0 . m_z of Clipper

changes its sign less than zero at $\text{Re}_0 \sim 10^2$. At $\text{Re}_0 \sim 10^4$, the value of $m_z = -0.03$ at the angle of attack is reached at $\alpha \approx 40$ deg. The dependency $C_y(\alpha)$ of Falcon is increased, and the value is reached to 0.54 at $\text{Re}_0 \sim 10^4$. The values of m_z of Falcon are quite sensitive to the variation of Re_0 , changes its sign at $\alpha \sim 5$ deg.

3.2. Local-bridging method to predict aerothermodynamic characteristics of high-speed vehicle in the transitional regime

In this paragraph, we would like to describe engineering method to predict heat transfer coefficient in the transition regime. In the free molecular regime, to determine the heat transfer coefficient equation can write analytically [32]

$$C_{h} = \alpha_{e} \frac{1}{2\sqrt{\pi}} \frac{1}{S_{\infty}^{3}} \left\{ \left(S_{\infty}^{2} + \frac{\gamma}{\gamma - 1} - \frac{1}{2} \frac{\gamma + 1}{\gamma - 1} \frac{T_{w}}{T_{\infty}} \right) \chi \left(S_{\infty, \theta} \right) - \frac{1}{2} e^{-S_{\infty, \theta}^{2}} \right\}$$

$$\chi(x) = e^{-x^{2}} + \sqrt{\pi} x \left(1 + \operatorname{erf}(x) \right), \quad \operatorname{erf}(x) = \frac{2}{\sqrt{\pi}} \int_{0}^{x} e^{-x^{2}} dt$$

Where, α_e – energy accommodation coefficient on surface, $S_{\infty,\theta} = S_{\infty} \cos \theta$ - speed ratio, T_w , T_{∞} - surface temperature and flow temperature respectively. To calculate heat transfer coefficient in continuum regime, equation can described as follow the formula of Lees [71-73]

$$C_{h}(s,\theta) = C_{h0} \cdot \frac{1}{\sqrt{s/r + \frac{1}{s/r + 1}}} \sqrt{1 + \frac{\gamma + 3}{\gamma + 1} \frac{\gamma}{2} M_{\infty}^{2} \cos^{2}\theta / 1 + \frac{\gamma + 3}{\gamma + 1} \frac{\gamma}{2} M_{\infty}^{2}}$$

$$C_{h0} = \frac{2^{k/2}}{2} \Pr^{-2/3} \sqrt{\frac{\gamma + 1}{\gamma - 1} \sqrt{\frac{\gamma - 1}{\gamma}}} \frac{1}{\sqrt{\text{Re}_{\infty,r}}} \left(\frac{\gamma - 1}{2} M^{2}\right)^{\omega/2}$$

here, C_{h0} – heat transfer coefficient on stagnation point, s – distance along the stream line, r – radius of nose of vehicle, Pr – Prandtl number, Re – Reynolds number, ω - exponent in power of viscosity dependence on temperature. k = 1 for spherical stagnation point, k = 0 for cylindrical stagnation point. In the present

work suggested the bridging function to calculate heat transfer coefficient in transitional regime

$$\begin{split} C_{h,ds} &= C_{h,fm,ds} \cdot F_b \left(\text{Re}, \text{M}, \theta, \ldots \right) + C_{h,cont,ds} \cdot \left(1 - F_b \left(\text{Re}, \text{M}, \theta, \ldots \right) \right) \\ F_{b,1} &= \frac{1}{2} \Bigg(1 + \text{erf} \left(\frac{\sqrt{\pi}}{\Delta \text{Kn}_1} \cdot \text{lg} \left(\frac{\text{Kn}_0}{\text{Kn}_m} \right) \right) \Bigg), \quad F_{b,2} &= \frac{1}{2} \Bigg(1 + \text{erf} \left(\frac{\sqrt{\pi}}{\Delta \text{Kn}_2} \cdot \text{lg} \left(\frac{\text{Kn}_0}{\text{Kn}_m} \right) \right) \Bigg). \end{split}$$

Where, $C_{h,fm,ds}$ – heat transfer coefficient in free molecular regime and $C_{h,cont,ds}$ – heat transfer coefficient in continuum regime. If $Kn_0 < Kn_m$, we should use the function $F_{b,1}$ and in opposite reason $F_{b,2}$. The values $Kn_m = 0.3$, $\Delta Kn_1 = 1.3$ and $\Delta Kn_2 = 1.4$ were determined by calculating with the use of DSMC method. Results are compared with the results of Dogra V.K., Wilmoth R.G., Moss J.N. and Vaschenkov P.V. [73-74] in figure 3.6.

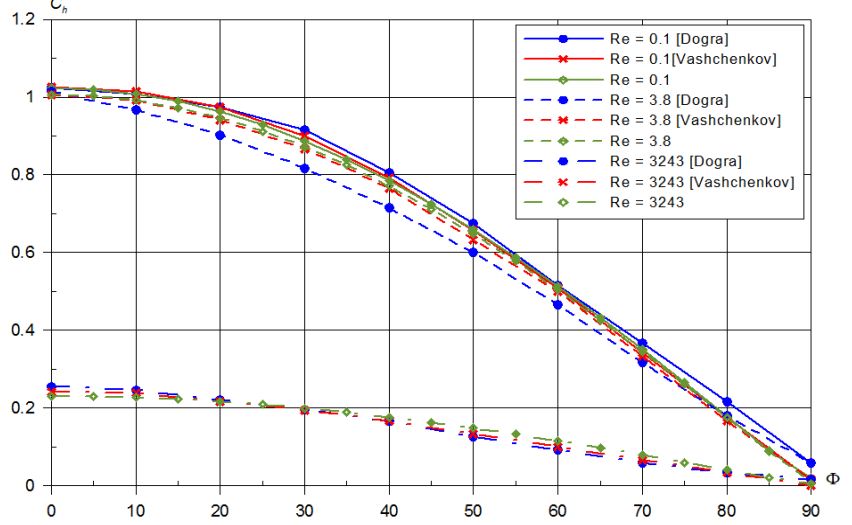


Figure 3.6 Comparison between results of heat transfer coefficient $C_h(\Phi)$ on sphere

The dependencies of $C_h(\alpha)$ for Clipper and Falcon HTV-2 are presented in fig. 3.7 with the use of bridging functions. It can see that the values of Falcon are more than Clipper and reached to 1.02 at Re 0.1 ($40 \le \alpha \le 90$). The values at Re = 0.1 and 10 are not very significant, but when the Re more than 10 the values are significant.

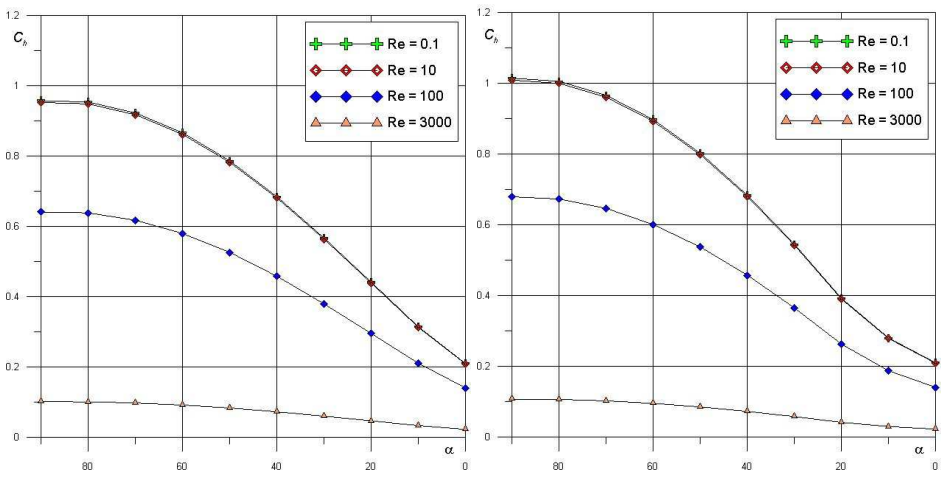


Figure 3.7 Dependencies of $C_h(\alpha)$ for "Clipper" and "Falcon HTV-2"

In this chapter the different methods to calculate aerodynamic and aerothermodynamic characteristics of perspective hypersonic vehicles in rarefied gas flow are carried out. The approximate engineering method to calculate hypersonic aerodynamic in transitional regime are described. The results of calculation of aerodynamic and aerothermodynamic characteristics for hypersonic vehicles by various engineering methods in rarefied gas flow with various Reynolds numbers were presented. Thus, the methods of the calculation of aerodynamic and aerothermodynamic characteristics of the bodies in the hypersonic flow of rarefied gas in the transitional regime give good and qualitatively right results for a wide range of bodies not very thin bodies. The obtained results by engineering methods are compared with the DSMC and Newtonian method. Local bridging methods are more suitable for calculating aerothermodynamics for hypersonic vehicle at the initial stage [75, 70].

3.3. Methods to calculate heat transfer coefficients in boundary layer

The development of high-speed aircraft technology requires continuous improvement of the processes of science research on the heat transfer surface of the body. Creation of high-speed and high-altitude aircrafts, further improving

the spacecraft, creating reusable spacecrafts, improving energy systems for the aviation and aerospace technology, the development of electronics require continuous improvement of the science of processes of heat and mass transfer and heat transfer theory development. Important questions of perfection of modern aviation and aerospace jet engine, thermal protection of high-speed aircraft, the creation and development of energy systems of direct conversion of heat and electricity required further improvement and development of a number of sections of the science of heat transfer [76-84].

The effective length is based on the use of the features of the development of the boundary layer is the fact that in the case of accelerated flows by the flow parameters and boundary layer thickness. In a much lesser extent the heat flow depends on the conditions in which the boundary layer developed from its point of generation to the section under consideration. In accordance with these features, *effective length method* that the calculation of the heat exchange section is replaced with the actual flow over the plate (axisymmetric body - above the cylinder) with the flow parameters. The length of the plate or cylinder x_{eff} chosen from the condition of growth on her thermal boundary layer thickness equal to the thickness of the layer in the calculated cross section of the body [83, 84].

At high speeds, in order to allow for heat dissipation of the kinetic energy at Pr = 1, the formula for calculating the heat transfer must be written in the form $q_w = \alpha (T_{01} - T_w)$

where, α - heat flux, T_w - wall temperature, T_{01} - stagnation temperature outside the boundary layer, characterized by a total heat flux. However, as follows from the consideration of the temperature distribution on the surface of the thermally insulated at $\Pr \neq 1$, on the wall to heat only a portion is converted kinetic energy. Wherein the maximum allowable temperature $T_e = T_1 + ru_1^2/2c_p$ may be used as a value characterizing the thermal energy flow to the outer heat transfer calculation. Here, r - radius of surface of body, c_p - heat capacity, u_1 -

the speed of the external flow can be calculate speed and temperature in boundary layer. an expression for calculating the heat transfer can be written in the form

$$q_w = \alpha (T_e - T_w)$$

This formula has the advantage that in case of a thermally insulated wall, when $T_w = T_e$, for every α the value $q_w = 0$. When Pr = 1, the formulas coincide. Should indicate that the value of the formula T_e is a temperature effective, numerically coincident with the surface temperature of the heat-insulated. Inside the boundary layer on the cooling surface temperature at all points less than T_e .

Formulas for calculating heat transfer in laminar boundary layer

Heat flux is given by Newton

$$q_{w} = \alpha (T_{e} - T_{w})$$

$$T_{e} = T_{1} \left(1 + \frac{\gamma - 1}{2} r M_{1}^{2} \right)$$

For air in the laminar boundary layer r = 0.84. Criterion equation for determining the heat transfer coefficient in the flow over the plate

$$Nu_w = 0.332 \,\mathrm{Re}_w^{0.5} \,\mathrm{Pr}_w^{1/3} .K$$

The *K* factor takes into account the effect of compressibility. Using this equation and the method for calculating the effective length of the heat transfer for an arbitrary distribution of the flow along the body image, we have Nusselt number

$$Nu_{weff} = 0.332 \,\mathrm{Re}_{weff}^{0.5} \,\mathrm{Pr}_{w}^{1/3} \,K \,K_{1}$$

where K_1 - amendment for the effect of pressure gradient

$$Nu_{weff} = \frac{\alpha x_{eff}}{\lambda_{...}}$$
, $Re_{weff} = \frac{\rho_w u_1 x_{eff}}{\mu_{...}}$

In the particular case of T_w = const, an approximate expression for the effective length of the form

$$x_{eff} = \frac{\int_{0}^{x} R^{2}(x) \rho_{w} u_{1} dx}{R^{2}(x) \rho_{w} u_{1}}$$

The integral cost variables R(x), ρ_w , u_1 changing education from the beginning of the boundary layer (critical point) to the section under consideration. Here, R(x), ρ_w , u_1 - radius of rotation, the density and the speed respectively. Given the constant wall temperature T_w , gas density ρ_w can be determined from the relationship

$$\frac{\rho_w}{\rho_{w0}} = \frac{p_1}{p_{01}}$$

where ρ_{w0} and p_{01} air parameters at the critical point. Correction for compressibility is calculated according to the formula

$$K = \left(\frac{\mu^* \rho^*}{\mu_w \rho_w}\right)^{1/3} \left(\frac{\mu_1 \rho_1}{\mu^* \rho^*}\right)^{1/15 T_w / T_e}$$

where μ_w and ρ_w determined by T_w , μ_1 , ρ_1 by T_1 , and $\mu * \rho *$ maximum temperature $T_{max} = T^*$ in the boundary layer.

$$\frac{\gamma - 1}{2} M_1^2 > 1 - \frac{T_w}{T_1}$$

 T^* is defined by the formula

$$\frac{T^* - T_w}{T_{01} - T_w} = \frac{1}{4} \left(1 + \frac{1 - \frac{T_w}{T_1}}{\frac{\gamma - 1}{2} M_1^2} \right), \qquad \frac{\gamma - 1}{2} M_1^2 \le 1 - \frac{T_w}{T_1}$$

The maximum temperature in the boundary layer flow of the external temperature is equal to $T^* = T_1$. In this case

$$K = \left(\frac{\mu_1 \rho_1}{\mu_w \rho_w}\right)^{1/3}$$

Correction for the effect of the velocity gradient

$$K_{1} = \left[1 + 0.16 \left(1 + \frac{T_{w}}{T_{01}}\right) \left(\frac{2m}{m+1}\right)^{1/3}\right]^{1/2}$$

where *m* - the exponent in the expression $u_1 = \beta x^m$,

$$\beta = \frac{c}{R_0} \sqrt{2 \frac{p_{01}}{\rho_{01}}}, \qquad c = \sqrt{1 - \frac{p_{\infty}}{p_{01}}}$$

When the flow in the vicinity of the critical point m = 1 and

$$K_1 = \left[1 + 0.16 \left(1 + \frac{T_w}{T_{01}}\right)\right]^{1/2}$$

In the case of flow around a cone m = 0, $K_1 = 1$. Defining Nu_{weff} and you can find the heat transfer coefficient

$$\alpha = \frac{Nu_{w \text{ eff}} \lambda_{w}}{x_{\text{eff}}}$$

Formulas for calculating heat transfer in turbulent boundary layer

Heat flux is defined by Newton and the effective temperature is of the form

$$T_e = T_1 \left(1 + \frac{\gamma - 1}{2} r M_1^2 \right), \qquad r = 0.89.$$

Criterion equation for determining the heat transfer coefficient by the effective length of the form

$$Nu_{weff} = 0.0296 \, \text{Re}_{weff}^{0.8} \, \text{Pr}_{w}^{0.43} \, K_{T}$$

$$Nu_{weff} = \frac{\alpha x_{eff}}{\lambda_{w}} \, , \, \, \text{Re}_{weff} = \frac{\rho_{w} u_{1} x_{eff}}{\mu_{w}}$$

 K_T - correction for compressibility.

The effective length of the plate in a turbulent flow in the boundary layer and $T_w = const$ is determined from the expression

$$x_{eff} = \frac{\int_{0}^{x} R^{5/4}(x) \rho_{w} u_{1} dx}{R^{5/4}(x) \rho_{w} u_{1}}$$

From the formula obtained on the assumption of constant expressions in x

$$\left[\frac{Nu_{w}}{\operatorname{Re}_{w}^{0.8}}(Te-Tw)\right]^{5/4}$$

In the vicinity of the critical point of change of these values is small and change them with respect to *x* can be neglected. Where the flow rate is low, good results are obtained by correction for compressibility, defined as

$$K_T = \left(\frac{\rho_1}{\rho_w}\right)^{0.6}$$

At high flow rates

$$K_T = \left(\frac{T_w}{T_e}\right)^{0.4} \left(1 + \frac{\gamma - 1}{2}rM_1^2\right)^{0.11}$$

heat transfer coefficient

$$\alpha = \frac{Nu_{weff}\lambda_{w}}{x_{eff}}$$

In some cases, the technical calculations for determining the heat transfer coefficient is more convenient to use the dimensionless equation, which determines the temperature is the temperature of the flow at the outer edge of the boundary layer. For high flow rate, this equation has the form

$$Nu_{f eff} = 0.0296 \operatorname{Re}_{f eff}^{0.8} \operatorname{Pr}_{f}^{0.43} \left(\frac{T_{w}}{T_{e}}\right)^{-0.35} \left(1 + \frac{\gamma - 1}{2} r \mathbf{M}_{1}^{2}\right)^{-0.56}$$

One of the ways to simplify the equations of the boundary layer is the transition from the satisfaction of differential equations for each particle to the satisfaction of these equations in the average thickness of the boundary layer. In

this case, the problem reduces to the solution of ordinary differential equations for the variable x.

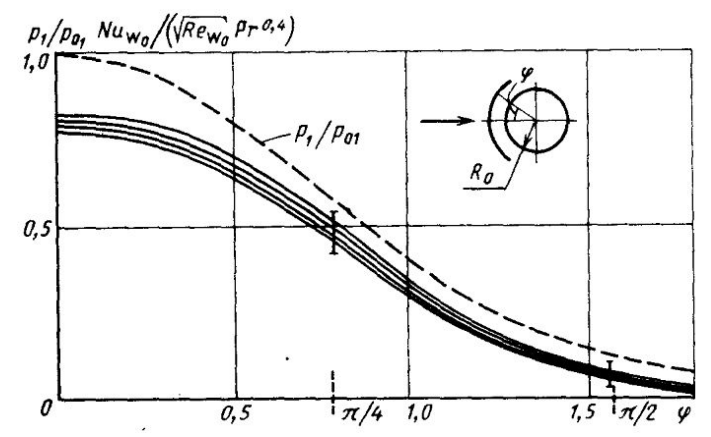


Figure 3.8 Heat transfer coefficients change along a sphere [83]

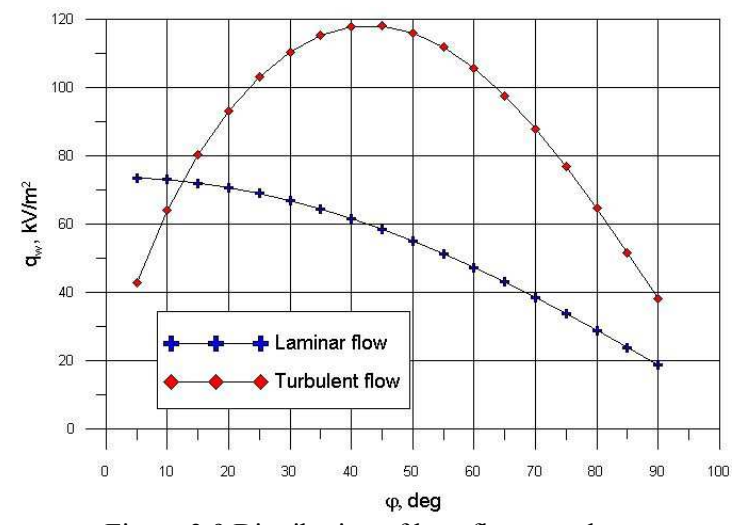


Figure 3.9 Distribution of heat flux on sphere

Such these methods sufficiently give the calculation of heat transfer at the calculation of the characteristics of the boundary layer, particularly in the field of flow with positive pressure gradients. In this case where heat exchange is required to calculate only became possible to obtain even more simple solutions using effective length method or local similarity [85].

CHAPTER 4 APPLICATION OF COGNITIVE TECHNOLOGY IN COMPUTATIONAL AERODYNAMICS

4.1. Development of cognitive technology in modern sciences

The beginning of cognitive science was in 1960. The fundamental concept of cognitive science is that thinking can best be understood in terms of representational structure in the brain, mind and computational procedures that operate on those structures. It examines what cognition is, what it does and how it works. It includes research on intelligence and behavior, especially focusing on how information is represented, processed, and transformed (in faculties such as perception, language, memory, reasoning, and emotion) within nervous systems (humans or other animals) and machines (e.g. computers) [86, 87]. Cognitive science consists of multiple research disciplines such as philosophy, psychology, artificial intelligence, neuroscience, linguistics, and anthropology. [88].

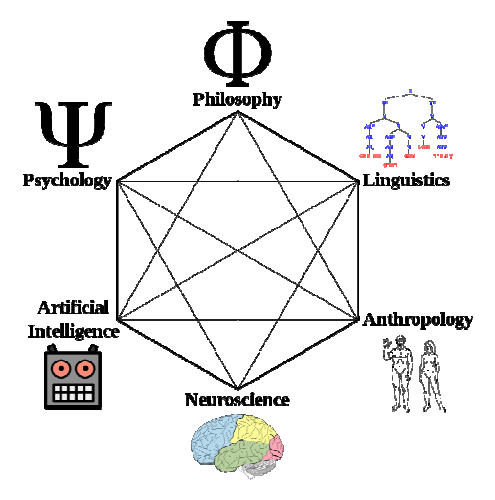


Figure 4.1 Illustrating of cognitive science

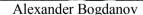
The fundamental concept of cognitive science is that "thinking can best be understood in terms of representational structures in the mind and computational procedures that operate on those structures". The science of studying cognition has undergone major changes as a result of technological developments [89].

Cognitive technologies are technologies that directly or indirectly affect learning, retention, remembering, reasoning and problem solving. The

development of cognitive technologies first became apparent at the 1978 (Practical Aspects of Memory Conference) [90].

Cognitive technologies have invaded many aspects of modern life and because of their rapid growth; a body of knowledge now exits about applications of cognitive theory to the development of these technologies in a variety of fields. Nowadays, we know that the development of cognitive technologies in education, industry, business, the professions and so on. Computers are also widely used as a tool with which to study cognitive phenomena. Computational modeling uses simulations to study how human intelligence may be structured. [91]. Cognitive technology in computer science is combination of methods, algorithms and software for modeling the cognitive abilities of the human brain to solve specific application problems. For example – recognition; identifying patterns in the data; solving computer-aided design of complex systems; decision support systems with fuzzy input; etc.







Norbert Wiener



John Von Neumann

In the last century, the founders of cybernetics Alexander Bogdanov, Norbert Wiener, John Von Neumann formulated the idea of the combining a computer with human abilities. This approach has been practically implemented for the development of nuclear energy for military and peaceful purposes (Los Alamos, Arzamas-16). This was an important achievement in computational technologies.

4.2. Application of Artificial Neural Networks in hypersonic aerospace technology

The development of artificial neural networks began approximately 50 years ago. As modern computers become more powerful and powerful, scientists continue to be challenged to use machines effectively for solving many problems. The interest of artificial neural networks is in many areas for different reasons. For example, electrical engineers find numerous applications in signal processing and control theory; computer engineers are for hardware and robotic systems; computer scientists find for difficult problems in areas such as artificial intelligence and pattern recognition; mathematicians use neural nets for modeling problems for which the explicit form of the relationships among certain variables is not known.

One of characteristic tendencies of development of aerospace technology is continuous extension of requirements to technical characteristics, functionality of aircrafts. In this work investigated possibility use of artificial neural networks in aerospace technology. Questions of the use of artificial neural networks types for the solution of the applied problem, arising at development, optimization and an assessment of parameters of aircraft, processing of results of experiments, identification of dangerous situations are considered. It is shown that application of the methods by using elements of artificial intelligence allows achieving the improvement of quality and speed of the solution for considered problems. The conclusions by the results is laid on expediency of application of such techniques and their further introduction in process of development, modernization of aerospace technology and applied solution of aerospace system.

To reduce project time and the number of expensive full-scale and experiments specialized the computer systems such as Knowledge Based Engineering (KBE), Computer Aided Design (CAD). The mathematical models are based on the "Physics". In aero-hydrodynamics, these models are described

as complex differential and integro-differential equations. Numerical methods have considerable complexity. These reasons are complicated the possibility of preliminary design stage, which is considered a lot of options. Therefore, models based on a cognitive approach become natural. They are built on the basis of scientific and intuitive analysis of data obtained by means of theoretical, experimental, numerical studies. The modeling of high-speed flows stipulates also the compliance with other similarity criteria, which includes first of all the criteria of Mach numbers and Reynolds numbers. For flight in the upper atmosphere, where it is necessary to take into account the molecular structure of a gas, kinematics models are applied, in particular, the Boltzmann equation and corresponding numerical methods of simulation.

Principle of biological neural network

Biological neural networks have inspired the design of artificial neural networks. Your brain is made of approximately 100 billion nerve cells, called neurons. Neurons have the amazing ability to gather and transmit electrochemical signals. Neurons share the same characteristics and have the same makeup as other cells, but the electrochemical aspect lets them transmit signals over long distances (up to several feet or a few meters) and send messages to each other.

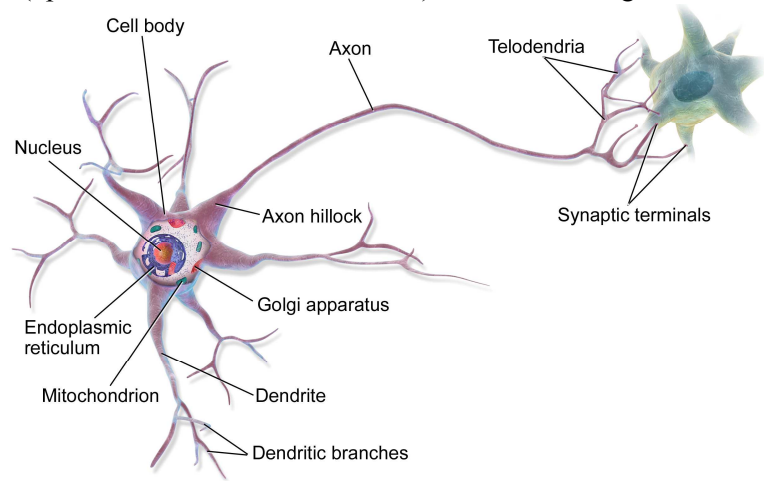


Figure 4.2 Structure of biological neural network

Neurons have three basic parts: Cell body or soma – this main part has all of the necessary components of the cell, such as the nucleus (which contains DNA), endoplasmic reticulum and ribosomes (for building proteins) and mitochondria (for making energy). If the cell body dies, the neuron dies. Axon – this long, cable like projection of the cell carries the electrochemical message (nerve impulse or action potential) along the length of the cell. Depending upon the type of neuron, axons can be covered with a thin layer of myelin sheath, like an insulated electrical wire. Myelin is made of fat and protein, and it helps to speed transmission of a nerve impulse down a long axon. Myelinated neurons are typically found in the peripheral nerves (sensory and motor neurons), while non-myelinated neurons are found in the brain and spinal cord. Dendrites or nerve endings -these small, branchlike projections of the cell make connections to other cells and allow the neuron to talk with other cells or perceive the environment. Dendrites can be located on one or both ends of a cell.

Principle of artificial neural network

An artificial neural network is an information processing system that has performance characteristics with biological (human brain) neural networks.

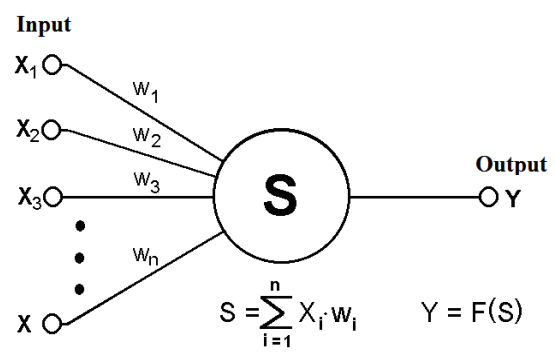


Figure 4.3 Structure of artificial neural network

Artificial neural networks are developed as generalizations of mathematical models of human cognition or neural biology, based on the following characteristics:

- Information processing system occurs at many simple elements called neurons.
- 2. Signals are passed between neurons over connection links.
- 3. Each connection link has an associated weight, which, in a typical neural net, multiplies the signal transmitted.
- 4. Each neuron applies an activation function to its net input to determine its output signal.

$$y = F(\sum_{i=0}^{n} w_i \cdot x_i)$$

where x_1 , ..., x_n - input neurons, w_1 , ..., w_n - weights of synaptic connections of a neuron. In this case $x_0 = -1$, and w_0 - the threshold of the neuron. F(x) - "activation functions" (nonlinear signal converter). As such nonlinear transformer in artificial neural networks are commonly used sigmoidal functions:

the hyperbolic tangent function

$$F(x) = \frac{1}{1 + e^{-x}}$$

and binary functions of the various definitions

$$F(x) = \frac{e^{x} - e^{-x}}{e^{x} + e^{-x}}$$

The artificial neural network consists of three layers: input layer, hidden layer and output layer. The hidden layer enables the network to learn relationships between input-output variables through suitable mappings. Among the many network models, the backpropagation algorithm is the well known and

usually used. In the work [92-96] described the principle of artificial neural networks.

4.3. The training on artificial neural network for aerodynamic characteristics of hypersonic vehicle

To calculate the aerodynamics characteristics of hypersonic vehicle used "ADANAT" (Aerodynamic Analysis to ensure the creation of aerospace engineering) information technology which developed by professor Khlopkov in MIPT. As elements "ADANAT" includes method of solving the kinetic equations of statistical modeling methods (Monte Carlo), solution of the equations of a continuous medium "ARGOLA-2". On the results of the calculation are trained neural network is proposed. The parameters are wide range of Reynolds numbers Re (Altitude varies from zero to 10 000 km), the collision of gas molecules with the surface considered various interaction potentials (combination of specular reflection - the Maxwell model, the Cercignani-Lampis-Lord (CLL) model, Lennard Jones potential), the ranges of angles of attack α from –90° to +90° and various temperature factors.



Figure 4.4 Scheme of algorithm

In fig. 4.5 presented the training result on artificial neural network of the coefficient of drag force C_x depending on the angle of attack α for hypersonic vehicle.

The neural network is constructed with 4 inputs, 1 output, 2 hide layers and over 4000 patterns (2000 for training and 2000 for testing) using the program

Neuro Module21, which is written by colleagues of DAFE MIPT. Parameters for the inputs are given the following: speed ratio of 5 to 30 in steps of 5; angle of attack of α -90 to +90 deg, the temperature factor $T_w/T_\infty = 0.0001$, 0.001, 0.01, 0.1, 1. After training received good results for C_x with an error MSE/SQDEV (relative error of mean squared error and derivative of mean squared error) - 4%. The results of this research show promising application systems with artificial neural network in the interests of the aerospace industry.

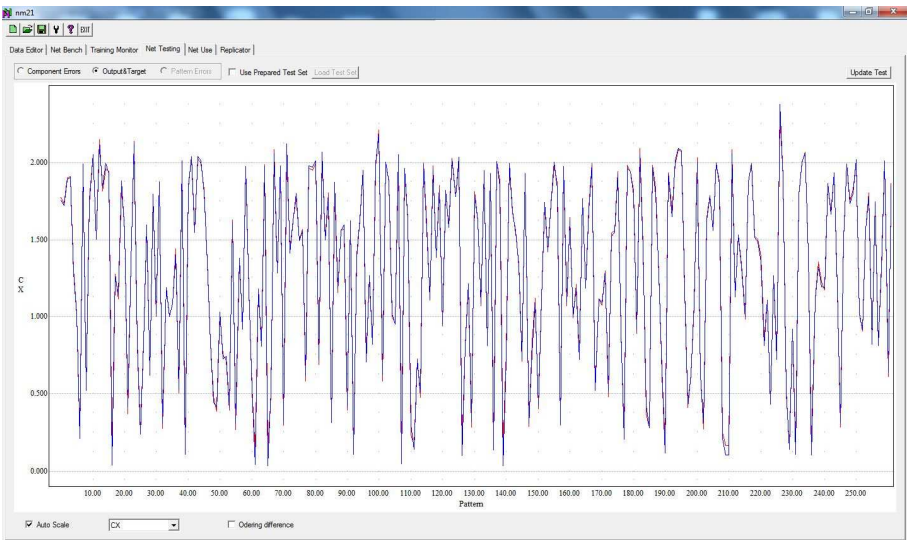


Figure 4.5 Training on artificial neural network for $C_x(\alpha)$

In this paragraph, the development of artificial neural network in hypersonic aerodynamics is discussed. The training on artificial neural network for aerodynamic characteristics of hypersonic vehicles is presented. Application of artificial neural networks in the design of the hypersonic vehicles can significantly improve the accuracy of the evaluation of the characteristics of stability and controllability of the vehicle shape [97, 98].

CHAPTER 5 BASIC CONCEPTS OF PROPULSION SYSTEM FOR HIGH-SPEED AIRCRAFTS

Hypersonic propulsion systems can be categorized as solid-fueled and liquid-fueled rockets, turbojets, ramjets, scramjets, and the dual-combustion ramjet. In the figure shows the specific impulse, i.e., the pounds of thrust generated per pound of fuel flow used, for the various engine cycles as a function of Mach number. Information is presented for a range of engine cycles, with the airbreathing engines using either hydrogen or liquid hydrocarbon as fuel [99, 100].

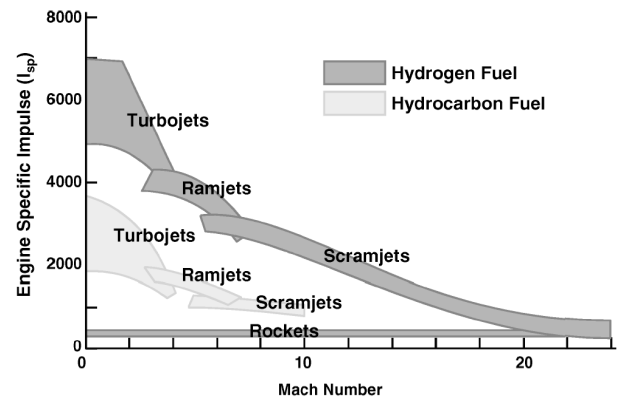


Figure 5.1 Engine specific impulse advantages of airbreathing engines [101]

Airbreathing jet engine (or *ducted jet engine*) is jet engine propelled by jet of hot exhaust gases formed from air that is drawn into the engine via an inlet duct. All practical airbreathing jet engines are internal combustion engines that directly heat the air by burning fuel, with the resultant hot gases used for propulsion via a propulsive nozzle, although other techniques for heating the air have been experimented. Most jet engines are turbofans which have largely replaced turbojets. These engines use a gas turbine with high pressure ratio and high turbine entry temperature which together give a high efficiency. Commercial jet aircraft are powered by turbofans; these have an enlarged air compressor which generates most of the thrust from air which bypasses the combustion chamber.

Thrust is the force which moves any aircraft through the air. Thrust is generated by the propulsion system of the aircraft. Different propulsion systems

develop thrust in different ways, but all thrust is generated through some application of Newton's third law of motion. For every action there is an equal and opposite reaction. In any propulsion system, a working fluid is accelerated by the system and the reaction to this acceleration produces a force on the system. A general derivation of the thrust equation shows that the amount of thrust generated depends on the mass flow through the engine and the exit velocity of the gas [102].

Gas turbine engine (or jet engine) worked much like a rocket engine creating a hot exhaust gas which was passed through a nozzle to produce thrust. But unlike the rocket engine which must carry its oxygen for combustion, the turbine engine gets its oxygen from the surrounding air. A turbine engine does not work in outer space because there is no surrounding air. For a gas turbine engine, the accelerated gas, or working fluid, is the jet exhaust. Most of the mass of the jet exhaust comes from the surrounding atmosphere. Most modern, high speed passenger and military aircraft are powered by gas turbine engines. Because gas turbine engines are so important for modern life, we will be providing a lot of information about turbine engines and their operation. Turbine engines come in a wide variety of shapes and sizes because of the many different aircraft missions. All gas turbine engines have some parts in common [102].

5.1. Rocket engines

There were a number of rocket powered aircraft built to explore high speed flight. In a rocket engine, fuel and a source of oxygen, called an oxidizer, are mixed and exploded in a combustion chamber. The combustion produces hot exhaust which is passed through a nozzle to accelerate the flow and produce thrust. For a rocket, the accelerated gas, or working fluid, is the hot exhaust produced during combustion. This is a different working fluid than you find in a turbine engine or a propeller powered aircraft. Turbine engines and propellers use air from the atmosphere as the working fluid, but rockets use the combustion

exhaust gases. In outer space there is no atmosphere so turbines and propellers can not work there. This explains why a rocket works in space but a turbine engine or a propeller does not work.

There are two main categories of rocket engines - *liquid rockets* and *solid rockets*. In a liquid rocket, the propellants, the fuel and the oxidizer, are stored separately as liquids and are pumped into the combustion chamber of the nozzle where burning occurs. In a solid rocket, the propellants are mixed together and packed into a solid cylinder. Under normal temperature conditions, the propellants do not burn; but they will burn when exposed to a source of heat provided by an igniter. Once the burning starts, it proceeds until all the propellant is exhausted. With a liquid rocket, you can stop the thrust by turning off the flow of propellants; but with a solid rocket, you have to destroy the casing to stop the engine. Liquid rockets tend to be heavier and more complex because of the pumps and storage tanks. The propellants are loaded into the rocket just before launch. A solid rocket is much easier to handle and can sit for years before firing.

Liquid rocket engines are used on the Space Shuttle to place humans in orbit, on many un-manned missiles to place satellites in orbit, and on several high speed research aircraft. In a liquid rocket, stored fuel and stored oxidizer are pumped into a combustion chamber where they are mixed and burned. The combustion produces great amounts of exhaust gas at high temperature and pressure. The hot exhaust is passed through a nozzle which accelerates the flow.

Solid rocket engines are used on air-to-air and air-to-ground missiles, on model rockets, and as boosters for satellite launchers. In a solid rocket, the fuel and oxidizer are mixed together into a solid propellant which is packed into a solid cylinder. A hole through the cylinder serves as a combustion chamber. When the mixture is ignited, combustion takes place on the surface of the propellant. A flame front is generated which burns into the mixture. The combustion produces great amounts of exhaust gas at high temperature and

pressure. The amount of exhaust gas that is produced depends on the area of the flame front and engine designers use a variety of hole shapes to control the change in thrust for a particular engine. The hot exhaust gas is passed through a nozzle which accelerates the flow.

The amount of thrust produced by the rocket depends on the mass flow rate through the engine, the exit velocity of the exhaust, and the pressure at the nozzle exit. All of these variables depend on the design of the nozzle. The smallest cross-sectional area of the nozzle is called the throat of the nozzle. The hot exhaust flow is choked at the throat, which means that the Mach number is equal to 1.0 in the throat and the mass flow rate \dot{m} is determined by the throat area. The area ratio from the throat to the exit A_e sets the exit velocity V_e and the exit pressure p_e . The exit pressure is only equal to free stream pressure at some design condition. We must use the longer version of the generalized thrust equation to describe the thrust of the system. If the free stream pressure is given by p_0 , the thrust F equation becomes:

$$F = \dot{m}V_e + (p_e - p_0)A_e$$

Notice that there is no free stream mass times free stream velocity term in the thrust equation because no external air is brought on board. Since the oxidizer is carried on board the rocket, rockets can generate thrust in a vacuum where there is no other source of oxygen. That's why a rocket will work in space, where there is no surrounding air, and a gas turbine or propeller will not work. Turbine engines and propellers rely on the atmosphere to provide air as the working fluid for propulsion and oxygen in the air as oxidizer for combustion. The thrust equation shown works for both liquid and solid rocket engines. There is also an efficiency parameter called the specific impulse which works for both types of rockets and greatly simplifies the performance analysis for rockets. The details of how to mix and burn the fuel and oxidizer, without blowing out the flame, are very complex [102].

5.2. Turbojet

The **turbojet** is a jet engine, usually used in aircraft. It consists of a gas turbine with a propelling nozzle. The gas turbine has an air inlet, a compressor, a combustion chamber, and a turbine (that drives the compressor). The compressed air from the compressor is heated by the fuel in the combustion chamber and then allowed to expand through the turbine. The turbine exhaust is then expanded in the propelling nozzle where it is accelerated to high speed to provide thrust. Two engineers, Frank Whittle in the United Kingdom and Hans von Ohain in Germany, developed the concept independently into practical engines during the late 1930s. Turbojets have been replaced in slower aircraft by turboprops which use less fuel. The jet engine is only efficient at high vehicle speeds, which limits their usefulness apart from aircraft.

At higher speeds, where the propeller is no longer efficient, they have been replaced by turbofans.

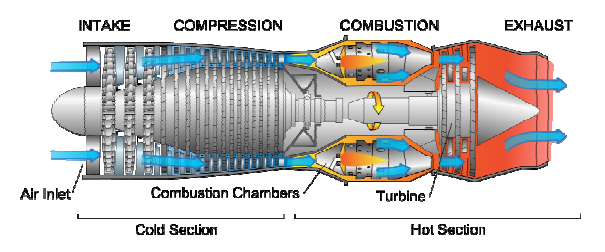


Figure 5.2 Diagram of a typical gas turbine jet engine

The turbofan is quieter and uses less fuel than the turbojet. Turbojets are still common in medium range cruise missiles, due to their high exhaust speed, small frontal area, and relative simplicity [103].

The net thrust F_N of a turbojet is given by:

$$F_N = \left(\dot{m}_{air} + \dot{m}_f\right) V_j - \dot{m}_{air} V$$

where, \dot{m}_{air} - the rate of flow of air through the engine, \dot{m}_f - the rate of flow of fuel entering the engine, V_j - the speed of the jet (the exhaust plume) and is

assumed to be less than sonic velocity, V – the true airspeed of the aircraft, $(\dot{m}_{air} + \dot{m}_f)V_j$ - the nozzle gross thrust, $\dot{m}_{air}V$ - the ram drag of the intake.

If the speed of the jet is equal to sonic velocity the nozzle is said to be choked. If the nozzle is choked the pressure at the nozzle exit plane is greater than atmospheric pressure, and extra terms must be added to the above equation to account for the pressure thrust. The rate of flow of fuel entering the engine is very small compared with the rate of flow of air. If the contribution of fuel to the nozzle gross thrust is ignored, the net thrust is:

$$F_N = \dot{m}_{air} \left(V_j - V \right)$$

The speed of the jet V_j must exceed the true airspeed of the aircraft V if there is to be a net forward thrust on the airframe. The speed V_j can be calculated thermodynamically based on adiabatic expansion [102].

5.3. Turbofan

The **turbofan** or fanjet engine is also a type of air-breathing jet engine that finds wide use in aircraft propulsion [104]. The word "turbofan" is a portmanteau of "turbine" and "fan" – the turbo portion refers to a gas turbine engine which takes mechanical energy from combustion, and the fan, a ducted fan that uses the mechanical energy from the gas turbine to accelerate air rearwards. Thus, whereas all the air taken in by a turbojet passes through the turbine (through the combustion chamber), in a turbofan some of that air bypasses the turbine. A turbofan thus can be thought of as a turbojet being used to drive a ducted fan, with both of those contributing to the thrust. The ratio of the mass-flow of air bypassing the engine core compared to the mass-flow of air passing through the core is referred to as the bypass ratio. The engine produces thrust through a combination of these two portions working in concert; engines that use more jet thrust relative to fan thrust are known as low bypass turbofans, conversely those that have considerably more fan thrust than jet thrust are known as high bypass.

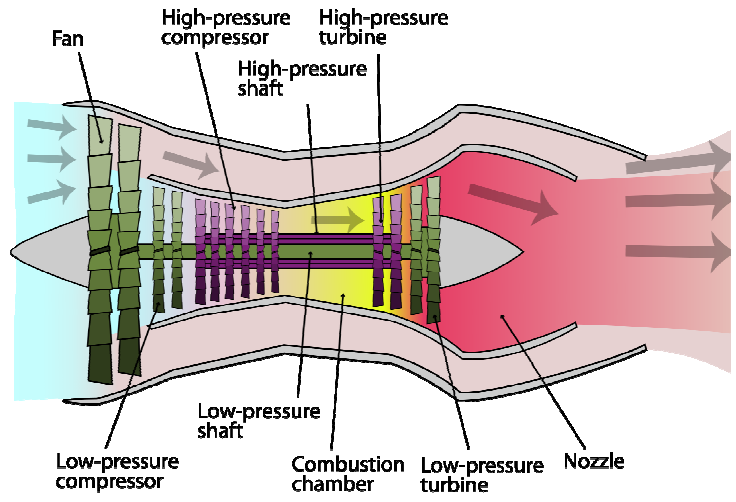


Figure 5.3 Schematic diagram of a high-bypass turbofan engine

Most commercial aviation jet engines in use today are of the high-bypass type, and most modern military fighter engines are low-bypass. Afterburners are not used on high-bypass turbofan engines but may be used on either low-bypass turbofan or turbojet engines. Most of the air flow through a high-bypass turbofan is low-velocity bypass flow: even when combined with the much higher velocity engine exhaust, the net average exhaust velocity is considerably lower than in a pure turbojet.

Engine noise is largely a function of exhaust velocity; therefore turbofan engines are significantly quieter than a pure-jet of the same thrust. Other factors include turbine blade and exhaust outlet geometries, such as noise-reducing "chevrons" seen on the Rolls-Royce Trent 1000 and General Electric GEnx engines used on the Boeing 787 [105, 106]. Turbofans are thus the most efficient engines in the range of speeds from about 500 to 1 000 km/h (310 to 620 mph), the speed at which most commercial aircraft operate. Turbofans retain an efficiency edge over pure jets at low supersonic speeds up to roughly Mach 1.6, but have also been found to be efficient when used with continuous afterburner at Mach 3 and above.

5.4. Airbreathing propulsion systems for high-speed aircraft vehicles

Airbreathing propulsion systems are attractive for applications such as high-speed and long-distance strike or access to orbit. In the latter case, the primary benefit relative to traditional rockets is that the airbreather does not have to carry its oxidizer on board, providing a potential payload fraction advantage.

Relative to a rocket, however, the hypersonic airbreather will be a much more complex system, considering the external physics of high-speed aerothermodynamics and the complex propulsion flowpath physics. The airbreathing propulsion system will be a combined cycle, since no one currently-known cycle can operate from takeoff to high-speed cruise, or to rocket takeover for final boost to orbit. Two combined cycle systems currently under consideration are the rocket-based combined cycle (RBCC) and the turbine-based combined cycle (TBCC).

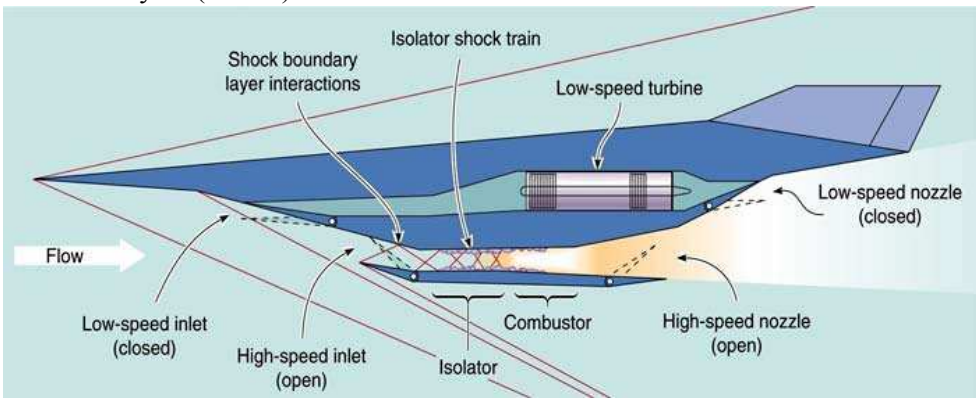


Fig. 5.4. The main components of an "over-and-under" TBCC engine

In the current TBCC design concepts, the turbine flowpath is located parallel to and above the high-speed ramjet/scramjet flowpath and is closed off after ramjet takeover. The process of transitioning from the low-speed turbine flowpath to the high-speed flowpath is the first critical combined cycle mode transition. The acceleration through the ramjet mode to the scramjet mode represents the second critical transition, the dual-mode. The vehicle is operated in

supersonic/hypervelocity modes for the high-speed strike mission, or up to scramjet-to-rocket takeover Mach number for a two-stage-to-orbit (TSTO) vehicle. The flow physics will be much the same for the RBCC or the TBCC. At about Mach 3-4 the transition will occur from the turbine low-speed flowpath to the ramjet/scramjet high-speed flowpath. A diverter door will move to close off the low-speed flowpath as the high-speed engine takes over. The inlets involved in this low-speed transition are indicated on the figure. This low-speed mode transition is very critical since unstart of the low-speed inlet can occur and, during transition, can cause unstart of the high-speed inlet. Such unstart will be controlled by the use of wall bleed, but modeling bleed is currently a difficult research topic.

As the Mach number is increased past about 4, the subsonic ramjet transitions into the dual-mode regime, where the combustor inlet Mach number is increased enough such that a thermal throat is created in the combustor and a precombustion shock train is generated. The isolator is designed to prevent this shock train from reaching the inlet to prevent catastrophic inlet unstart. In this regime the combustor operates in a mixed subsonic/supersonic, or dual-mode. The isolator flowfield contains multiple shock reflections, with complex shock-boundary-layer-interactions (SBLI). As the Mach number is further increased past about 6, the pre-combustion shock train moves out of the isolator and the combustor operates in the supersonic mode. The isolator and combustor involved in the dual-mode transition are labeled in the figure. At Mach numbers higher than about 6, the combustor operates in the supersonic mode. This regime is characterized by intense SBLI and mixing that is diffusion-limited due to the very high free stream velocities [107].

5.5. Ramjet

There are many papers reviewed the history of ramjet engine development and projecting various design approaches to achieving increased flight speed [108].

Meanwhile, the feasibility of supersonic combustion ramjet engine was attracting attention [109]. In the early 1900's some of the original ideas concerning ramjet propulsion were first developed in Europe. In a ramjet, the high pressure is produced by "ramming" external air into the combustor using the forward speed of the vehicle. The external air that is brought into the propulsion system becomes the working fluid, much like a turbojet engine. In a turbojet engine, the high pressure in the combustor is generated by a piece of machinery called a compressor. But there are no compressors in a ramjet.

Therefore, ramjets are lighter and simpler than a turbojet. Ramjets produce thrust only when the vehicle is already moving; ramjets cannot produce thrust when the engine is stationary or static. Since a ramjet cannot produce static thrust, some other propulsion system must be used to accelerate the vehicle to a speed where the ramjet begins to produce thrust. The higher the speed of the vehicle, the better a ramjet works until aerodynamic losses become a dominant factor.

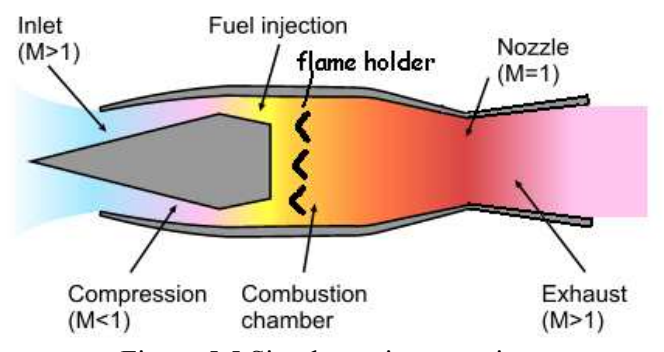


Figure 5.5 Simple ramjet operation

The combustion that produces thrust in the ramjet occurs at a subsonic speed in the combustor. For a vehicle traveling supersonically, the air entering the engine must be slowed to subsonic speeds by the aircraft inlet. Shock waves present in the inlet cause performance losses for the propulsion system. Above Mach 5, ramjet propulsion becomes very inefficient. The new supersonic

combustion ramjet, or scramjet, solves this problem by performing the combustion supersonically in the burner [110].

5.6. Scramjet

In the supersonic combustion ramjet, or scramjet, the losses associated with slowing the flow would be minimized and the engine could produce net thrust for a hypersonic vehicle. Tests were begun to design the supersonic burner and to better integrate the inlet and nozzle with the airframe [111]. Because the scramjet uses external air for combustion, it is a more efficient propulsion system for flight within the atmosphere than a rocket, which must carry all of its oxygen. Scramjets are ideally suited for hypersonic flight within the atmosphere.

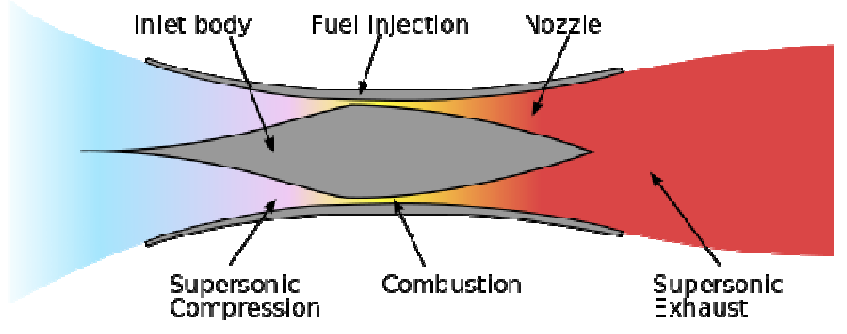


Figure 5.6 Simple scramjet operation

In May 2013 an unmanned X-51A WaveRider reached 4828 km/h (Mach 5.1) during a three-minute flight under scramjet power. The WaveRider was dropped from a B-52 bomber, and then accelerated to Mach 4.8 by a solid rocket booster which then separated before the WaveRider's scramjet engine came into effect. On 9 January 2014 US surveillance satellites observed a supersonic flying object at a speed of Mach 5 up to Mach 10 in around 100 km height. Following Chinese statements the preliminary designation for this object is WU-14. In the first phase this unmanned vehicle was brought to its operating height and speed by a military long-range missile [112].

5.7. Dual Combustion Ramjet and Dual Mode Ramjet

Dual Combustion Ramjet (DCR) is a complex design with two different air inlet systems, which can operate as a "conventional" ramjet with subsonic combustion, or for hypersonic speeds – as a "scramjet". Furthermore, Aerojet's engine runs on conventional liquid hydrocarbon fuel (JP-10), which is much easier to handle than cryogenic fuels (LH2) which have been used on other hypersonic scramjet vehicles so far. Dual Mode Ramjet (DMRJ) is a propulsion system which, dependent on the flight Mach number, operates in two Modes. The flowpath can be fixed geometry and is slightly diverging. Mode 1: As a ramjet with high Mach but subsonic combustion; the "Throat" is provided through thermal choking. An "Isolater" is required for lower Mach operation to provide a combustor entrance pressure higher than the combustion pressure. Mode 2: As a scramjet with supersonic combustion.

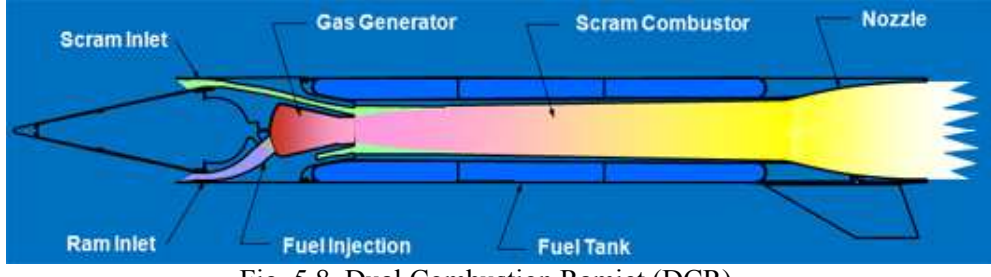


Fig. 5.8. Dual Combustion Ramjet (DCR)

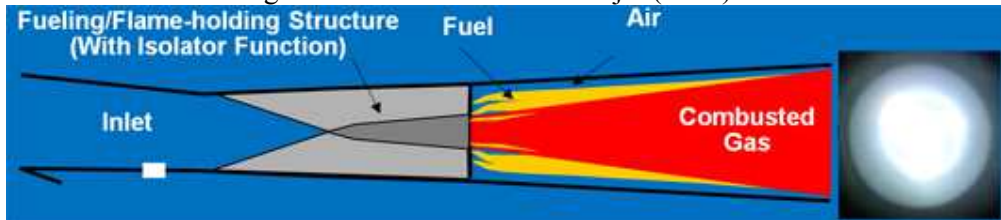


Fig. 5.9. Core-Burning Dual Mode Ramjet

Primary challenges are fuel conditioning, vaporization, mixing, and combustion, and thermal management. DMRJ are suitable for long range missiles and reusable HCVs [113].

CHAPTER 6 A FUTURE SPACE TRANSPORTATION SYSTEM

6.1. Space Elevator

The benefit of developing a space elevator infrastructure is to change our approach to operations in space exploration. Low cost, safe, reliable and flexible delivery of payloads to Geostationary Earth Orbit (GEO) and beyond could create an "off-planet" environment filled with opportunities ranging from commercial space systems to exploration of the solar system.

The key concept of the space elevator appeared in 1895 when Russian scientist Konstantin Tsiolkovsky was inspired by the Eiffel Tower in Paris. He considered a similar tower that reached all the way into space and was built from the ground up to the altitude of 35 790 km, the height of geostationary orbit. He noted that the top of such a tower would be circling Earth as in a geostationary orbit. Objects would attain horizontal velocity as they rode up the tower, and an object released at the tower's top would have enough horizontal velocity to remain there in geostationary orbit. Tsiolkovsky's conceptual tower was a compression structure, while modern concepts call for a tensile structure (or "tether"). The original concept envisioned by Tsiolkovsky was a compression structure, a concept similar to an aerial mast. While such structures might reach space (100 km/62 miles), they are unlikely to reach geostationary orbit. The concept of a Tsiolkovsky tower combined with a classic space elevator cable (reaching above the level of GEO) has been suggested [114, 115]. The concept of a space elevator first came from an inventive Russian, at the dawn of the space age (Artsutanov, 1960) [116].

In 1979, space elevators have been touted by futurists and science-fiction writers, including Arthur C. Clarke in which engineers construct a space elevator. Clarke seemed to predict the carbon nanotubes solution in his 1979 novel The Fountains of Paradise, in which he described a very thin, incredibly strong carbon filament that would one day make the space elevator possible. An Earth-based space elevator would consist of a cable with one end attached to the

surface near the equator and the other end in space beyond geostationary orbit (35 800 km altitude). The competing forces of gravity, which is stronger at the lower end, and the outward/upward centrifugal force, which is stronger at the upper end, would result in the cable being held up, under tension, and stationary over a single position on Earth. Once deployed, the tether would be ascended repeatedly by mechanical means to orbit, and descended to return to the surface from orbit

Since 1959, most ideas for space elevators have focused on purely tensile structures, with the weight of the system held up from above. In the tensile concepts, a space tether reaches from a large mass (the counterweight) beyond geostationary orbit to the ground. This structure is held in tension between Earth and the counterweight like an upside-down plumb bob.

On Earth, with its relatively strong gravity, current technology is not capable of manufacturing tether materials that are sufficiently strong and light to build a space elevator. However, recent concepts for a space elevator are notable for their plans to use materials based on carbon nanotube or boron nitride nanotube as the tensile element in the tether design. The measured strengths of those nanotube molecules are high compared to their linear densities. Carbon nanotubes have the potential to be 100 times stronger than steel and are as flexible as plastic. The strength of carbon nanotubes comes from their unique structure, which resembles soccer balls. Once scientists are able to make fibers from carbon nanotubes, it will be possible to create threads that will form the ribbon for the space elevator. They hold promise as materials to make an Earth-based space elevator possible [117].

The concept is also applicable to other planets and celestial bodies. For locations in the solar system with weaker gravity than Earth's (such as the Moon or Mars), the strength-to-density requirements are not as great for tether

materials. Currently available materials (such as Kevlar) are strong and light enough that they could be used as the tether material for elevators there.

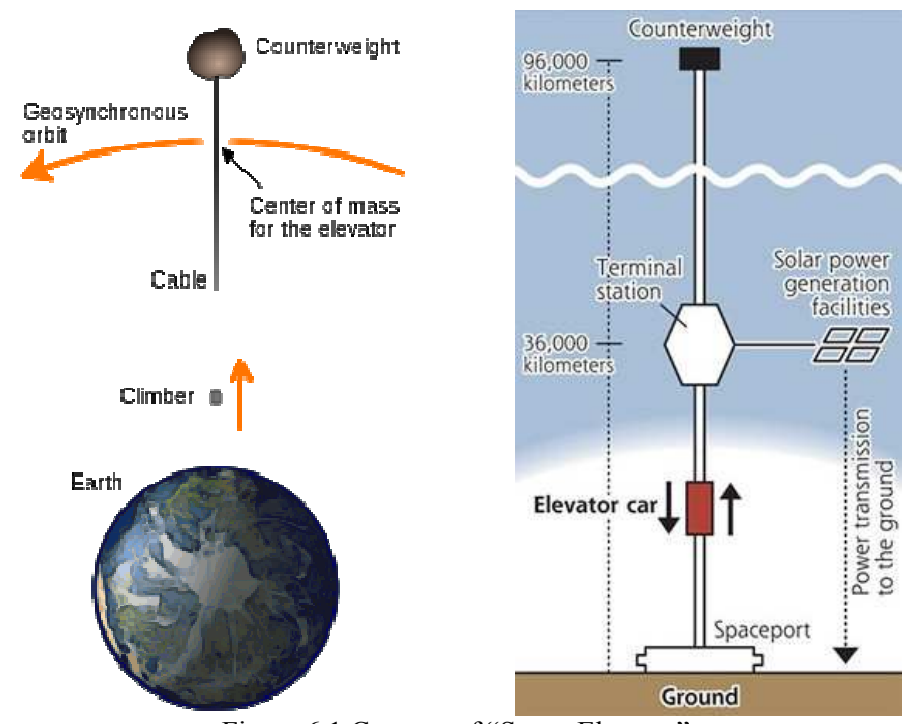


Figure 6.1 Concept of "Space Elevator"

In 2005, the LiftPort Group of space elevator companies announced that it will be building a carbon nanotube manufacturing plant in Millville, New Jersey, to supply various glasses, plastic and metal companies with these strong materials. LiftPort hopes that to eventually use carbon nanotubes in the construction of a 100 000 km (62 000 miles) space elevator. The 100 000 km long space elevator would rise far above the average orbiting height of the space shuttle (115-400 miles/185-643 km). In fact, it would equal nearly a fourth of the distance to the moon, which orbits the Earth at 382 500 km (237 674 miles). LiftPort is already selling novelty "tickets" for an elevator that they claim will be finished by 2031 [118].

In 2012, the Obayashi Corporation announced that in 2050 it could build a space elevator using carbon nanotube technology with a capacity to carry 100 ton climbers. It is composed of a 96 000 km carbon nanotube cable, a 400-m diameter floating Earth Port and a 12 500 ton counter-weight. Other facilities include Martian/Lunar Gravity Centers, Low Earth Orbit Gate (LEO), a GEO station, a Mars Gate and a Solar System Exploration Gate. At 200 km/h, the design's 30 passenger climber would be able to reach the GEO level after a 7.5 day trip. No cost estimates, finance plans, or other specifics were made. This, along with timing and other factors, hinted that the announcement was made largely to provide publicity for the opening of one of the company's other projects in Tokyo [119].



Figure 6.2 Concept drawing of "Space Elevator" [118]

By far the most important is the tether. Projecting current research in carbon nanotubes and similar technologies, the International Academy of Astronautics (IAA) estimates that a pilot project could plausibly deliver packages to an altitude of 1000 km (621 miles) as soon as 2025. With continued research and the help of a successful LEO (anywhere between an altitude of 100 and 1200 miles) elevator, they predict a 100 000 km (62 137 mile) successor will stretch well past GEO just a decade after that.

6.2. Medical and biological aspects in human spaceflight

Theoretical researches in the field of space equipment and designing of aircraft strongly stimulated the development of many sciences, including new branch of knowledge - space biology [120]. The basic problems in space biology and space medicine included: possible noxious effects of cosmic factors on organisms and their prevention and life preservation during space flight, (e.g. air regeneration; selection and training of astronauts). First of all, the choice of the corresponding support system of the astronaut is defined by duration of space flight. Space flights are inevitably connected with number of factors impact on a human body. The factors caused by dynamics of flight (acceleration, vibration, noise, zero gravity). The factors characterizing a space as habitat (high degree of a sparseness of the atmosphere, ultra-violet and infrared beams, radio and the microwave radiations, ionizing radiation, etc.). The factors connected with long stay of the crew in cabins limited on volume of spacecrafts (isolation as a part of small collectives, the artificial gas environment, the changed biological rhythm, etc.).

Without scientific justification of possibility of space flight of the person and ensuring its safety it was impossible to speak seriously about flight of the person in a near-earth space, and furthermore about interplanetary travel [121]. We can only artificially create room of the spacecrafts which gives to the human chance to live and work in space flight. But in attempt to solve this problem it is necessary to answer number of difficult questions. With the development of outer space technologies, the safety of space flights becomes main priority of astronautics [122-124].

Space! How to perceive it? In many research laboratory to test various hypotheses or unfavorable environment of people are developed. Space outside the earth's atmosphere, perhaps, is not hostile, but it requires special training to meet with him. The first human flight proved his ability to be and to conduct

scientific research in space. Thus, carried out in the XX century breakthrough human space marked not only a high level of theoretical and practical achievements of mankind, but it seems that marked a new era in the development of human civilization - a man appeared in a radically new environment. Indeed, flying in outer space manned spacecraft - a tiny island life in the desolate environment. His appearance has been possible only due to the successful solution of not only technical, but also a number of related problems associated with the life and work of a man in an unusual space flight. To deal with the solution of this problem, it is necessary to rely on a solid foundation of knowledge that underlay the problem. At the initial stage of the practical ways of finding space exploration have been associated with the creation and launch of automated vehicles into orbit and to other planets, the first manned flight into space, and a long flight to space stations, of landing a man on the moon. Theoretical studies in the field of space technology and engineering-driven aircrafts dramatically stimulated the development of many sciences, including a new branch of knowledge - space biology [125]. It became apparent that the range of problems associated with long-term space flight includes a plurality of individual problems of biology, physiology, hygiene, psychology, and, if anything, the moral and ethical issues. Specific objectives are part of the complex medical problems that are subject to various purposes (problems of medical examination, selection and training of crews, life support, medical monitoring, prevention, treatment, rehabilitation, and others.). At the junction with adjacent areas of science and engineering problems are born medical support development, ergonomics, engineering psychology, valuation parameters and habitat conditions of activity, forecasting changes in the organism and the environment, management, and many others. Finally, the system approach should provide a common problem, characteristic of space in general, and for all kinds of scientific and practical activities, which it unites safety of manned space flight.

Specified format film (seven pages) does not allow to fully cover the topic, but the fundamental problems can identify.

Practical astronautics both historically and structurally formed and initially developed as a branch of aviation [126]. Most of the first space rocket designers, including Sergei Korolev, came in the space program of the aircraft. The first group of cosmonauts was formed exclusively of military pilots and preparing for space flight in aviation techniques. For this reason, space exploration has many laws governing the development of aviation and the example of aviation can be traced to the laws of space development. Recently deceased, Academician Boris Chertok Yevseyevich (March 1912 - December 2011), an iconic figure in the cohort of the "Fathers of Space", recalled that radio equipment and aircraft, and then in the space program brought him "Aelita". In this regard, it is not to mention the activities of violent fiction romantic framing a new era of human history. This science-fiction writers with their space novels, utopias, such as Alexei Tolstov "Aelita", Ivan Efremov "Andromeda", Ray Bradbury "The Martian Chronicles", Arthur C. Clarke "Fountains of Paradise", Stanislaw Lem "Solaris", the Strugatsky brothers "Hard to Be God". Many of them are fantastic utopia proved prophetic. For example, according to the predictions of Ivan Antonovich Efremov was discovered the largest diamond mine in the world in Yakutia. "Hyperboloid of Engineer Garin" Count Alexei Tolstoy anticipated appearance of lasers, and along with a bunch of Nobel Prizes. And fantastic novel "Fountains of Paradise" by Arthur C. Clarke is currently developed and adopted to implement the project the most economical way to transport people and cargo into space - the project "space elevator". We think that the implementation of the philosophical and moral issues raised in the works of these utopians, is yet to come. Long before the birth of practical astronautics at the turn of the XIX and XX centuries Konstantin Tsiolkovsky laid the foundations of theoretical astronautics, offered a scientific strategy and tactics of human space

exploration, and formulated the basic differences of space from the other sciences [126].





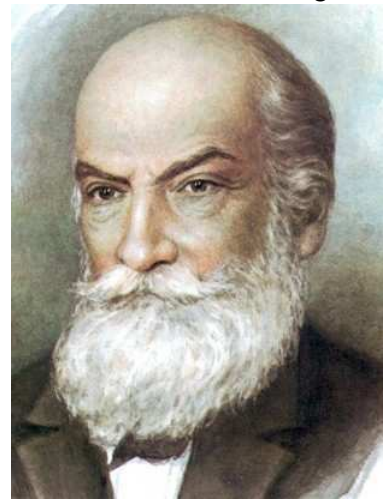
Posters: The Martian Chronicles by Ray Bradbury



Andromeda galaxy - the constellation of the northern hemisphere (left). In the three-star Andromeda 2nd magnitude and spiral galaxy visible to the naked eye already known from the X century (in the center of the star chart with the Atlas 1690). According to Greek mythology, Andromeda was the daughter of the Ethiopian king Cepheus and Queen Cassiopeia, and was given to the father as a sacrifice to the sea monster, ravage the country, but is rescued by Perseus (right). After her death it was set amongst the stars as the constellation.

For example, the representation of the mechanism of long term effects of weightlessness on the human body. It is also necessary to mention the pioneering work on the effects of gravity on living organism Russian biologist Stanislav Fedorovich Stein [127]. The essential difference between the work of Stein from

his predecessors, and many modern scholars, is that Stein did not limit their experimental study, only one species of experimental animals. In accordance with evolutionary ideas, consider the possibility of species characteristics and response of the animals to various environmental factors, Stein conducted research on animals at different stages of evolution.





Zhukovsky N.Y.

Otto Lilienthal

In 1896, Nikolay Yegorovich Zhukovsky theoretically restored the trajectory of the last flight in a glider aeronaut Otto Lilienthal and gave a scientific analysis of the causes of the disaster. These results were published in the article "On the death of balloonist Otto Lilienthal" [128]. Perhaps this is the first publication of safety. If we follow the dynamics of the post-war civil aviation priorities, it will look as follows [122].

- (1950-1970): the safety of the flight, the flight speed, range, performance efficiency, comfort, noise near the airport;
- (1970-1990): flight safety, performance efficiency, noise near the airport, comfort, flight speed, flight range;

- (1990-2015): flight safety, the environment, indicators of efficiency, comfort, flight speed, flight range.

As you can see, with the development of aviation priorities are reversed all but one of which occupies the first position - flight safety. With the advent of manned spaceflight space flight safety is also a top priority of space.

Safety studies as the properties of any aircraft is to determine the area of the limiting values of the parameters and modes of aircraft flight, in which it performs the specified function [126]. In aviation, the Flight Safety Foundation has developed a guide to reduce the risk of accidents in the most difficult flight conditions: the approach and landing. 33th Assembly of ICAO (International Civil Aviation Organization) recognized it as one of the most important elements of the Global Aviation Safety Plan [129, 130].

Mode of entry into the atmosphere, the approach and landing are also the most complex modes of flight of the spacecraft. A notable step in the field of safety was the creation in 1970, the national organization - the National Committee of the USSR on the safety of aircraft and spacecraft, which coordinated the work of all concerned departments of the country. The main objectives of the aircraft and spacecraft were: implementation of relations with international and national foreign organizations, academic institutions and companies directly involved in solving actual problems of safety of aircraft and manned spacecraft. At first, the activity of spacecraft was expressed in a rigorous selection of future cosmonauts on health and psychomotor reactions, in search of such methods cosmonaut training that would enable them to fend off the most likely contingencies and to survive in a possible emergency landing as on land and on the water. Improving the space-rocket systems and ground support equipment, complexity of space activities has led to the fact that under the aircraft and spacecraft, along with sections of the aviation segment was created and space section headed by Georgy Beregovoy.

Referring to the basic problems is ensuring the lives of people in the spacecraft. The first selection of the appropriate life support systems astronaut is determined by the duration spaceflight [131]. Space missions are inevitably associated with the impact on the human body a number of factors, which are conditionally be divided into three main groups [132]. These are the factors due to flight dynamics (acceleration, vibration, noise, weightlessness). Factors are that characterize the space as a habitat (high vacuum atmosphere, ultraviolet and infrared rays, radio and microwave radiation, ionizing radiation, etc.). Factors associated with prolonged stays in limited volume spacecraft cabin (insulation in small groups, artificial gas atmosphere, altering the biological rhythm, etc.). Given the significant risk and complexity of space flight, great importance is attached to animal experiments.

Without scientific substantiation of the possibility of human space flight and its security can not be seriously talking about the flight of man in near-Earth space, and even more so on interplanetary travel. Only artificially created in the living areas of the spacecraft environment gives the person a chance to live and work in space flight. But when you try to solve this problem it is necessary to answer a number of difficult issues. What in particular, this medium should be? With what completeness, it should ensure the diversity of physical and intellectual needs of man? What criteria should be the basis for optimizing the relationship of the organism with an artificial habitat? After a number of criteria in addition to the physiological hygienic, it can be classified as psychological, ergonomic and even philosophical and moral.

Konstantin Tsiolkovsky space exploration called the pursuit of light and space. Of course, the machines give a lot of information, and without them it is difficult to imagine the process of space exploration, but mastered can be considered that part of the space, which, as an infantryman.

6.3. Advances of space medicine and biology research

Strategy of space life sciences at next decade is to continue the fundamental and applied physiological and biological research abroad ISS, space transportation systems and unmanned spacecrafts including research on international basis; to accumulate the new biomedical data related to the extra prolonged orbital manned flights and future flights of crews to the Moon and Mars; to provide the medico-engineering and ergonomic support of new manned space systems development; to improve system for the medical support of human in space. Fundamental and applied research of biology in space are as follow [133]:

- Nature of living in space from molecules to organism in whole. Mechanisms of adaptation and readaptation.
- Specifics of ontogenic and phylogenic development of living system in microgravity.
- Biorythms in space.
- Gravity, radiation and magnetic field are the ambient factors for life on Earth, their role in structure and function of different living systems.
- Combined biological effects of main space flight factors.
- Ways of forming and distribution of life in Universe.
- Potential biological damage inhibited by flights beyond the Earth radiation belts and magnetosphere.
- Experimental modeling of pathology and trauma in space. Means and methods of treatment.
- Biological effects of artificial gravity and prolonged living in low gravity.

- Pharmacodynamics and pharmacokinetics of drugs in Space. Biotechnology Research.
- Biodosimetry methods for radiation safety control in space flights.
- Perspective methods and means of prophylaxis for manned flights beyond the Earth

The main area of fundamental and applied biomedical research are studying the mechanisms of physiological adaptation to the specific factors of space flight and space environment, development and testing of new means and methods for propylaxis of unfavorable changes in organism and protection against adverse effects of space radiation, researching for lowering of potential medical risks in current orbital and future manned flights to the Moon and Mars with the use of contemporary technology and new achievements in general science.

We also need to improve research in ground based simulated experiments. Example, water immersion experiments for study of physiological effects of microgravity, head-down anti-orthostatic hypokinesia experiments for study of physiological effects of micro gravity, short radius centrifuge experiments for stydy of artificial gravity biomedical effects, long-duration experiment in fully hermetical medico-engineering complex to study biomedical effects of some simulated peculiarities of manned mission to Mars and radiation experiment with monkeys.

Space medicine and biology research are important for national activity in space, but it requires continuing the fundamental and applied research in manned and automatic space missions. Certain theoretical and experimental basis for medical support of manned missions to Moon and Mars is developed. New scientific technologies will be used for more active study of biomedical problems of interplanetary manned missions [134, 135].

CONCLUSIONS

Future space launch systems will be designed to reduce costs and improve dependability, safety, and reliability. In the meantime most military and scientific satellites will be launched into orbit by a family of expendable launch vehicles designed for a variety of missions. Every nation has their own launch systems, and there is strong competition in the commercial launch market to develop the next generation of launch systems. Developing a plan to realize a space elevator and reusable hypersonic vehicle system are to change our approach to operations in space exploration. Low cost, safe, reliable and flexible delivery of payloads to GEO.

One of characteristic tendencies of development of aerospace technology is continuous extension of requirements to technical characteristics, functionality of aircraft. Possibility use of cognitive approach to aerospace technology is introduced. Using cognitive technology allows achieving the improvement of quality and speed of the solution of considered problems; arising at development, optimization and an assessment of parameters of aircraft, processing of results of experiments, identification of dangerous situations and in process of development, modernization of aerospace technology and applied solution of aerospace system.

The main strategy of space sciences at next step are: to continue the fundamental and applied physiological and biological research abroad international space station (ISS); space transporation systems and unmanned spacecrafts including research on international basis, to accumulate the new biomedical data related to the extra prolonged orbital manned flights and future flights of crews to the Moon and Mars; to provide the medico-engineering and ergonomic support of new manned space systems development; to improve system for the medical support of human in space. The study was supported by Russian Science Foundation.

REFERENCES

- 1. http://www.aerospace.org/
- 2. T.A. Heppenheimer Facing the heat barrier: A history of hypersonics. The NASA history series, 2007. 336 p.
- 3. http://buran.ru/htm/spiral.htm
- 4. http://en.wikipedia.org/wiki/Boeing X-20 Dyna-Soar
- 5. http://www.astronautix.com
- 6. National Aeronautics and Space Administration. Space Shuttle Workforce Transition Strategy, Initial Report. 2011.
- 7. http://en.wikipedia.org/wiki/Kliper
- 8. http://www.space.com/16658-russia-crew-spacecraft-angara-rocket.html
- 9. http://www.russianspaceweb.com/baikal.html
- 10. http://www.airforce-technology.com/projects/x51-wave-rider/
- 11. www.darpa.mil
- 12. http://www.lockheedmartin.com/us/products/falcon-htv-2.html
- 13. http://www.space.com/24639-united-states-military-space-plane-xs1.html
- 14. http://www.lockheedmartin.com/us/news/features/2013/sr-72.html
- 15. http://www.esa.int/ESA
- 16. http://www.spacefuture.com/archive/space_tourism_for_europe_a_case_study.shtml
- 17. http://en.wikipedia.org/wiki/Hermes (spacecraft)
- 18. http://en.wikipedia.org/wiki/Skylon (spacecraft)
- 19. http://www.globalsecurity.org/space/world/japan/hope.htm
- 20. http://www.chinasignpost.com/2012/05/04/shenlong-divine-dragon-takes-flight-is-china-developing-its-first-spaceplane/

- 21. http://en.wikipedia.org/wiki/Avatar_(spacecraft)
- 22. Hall, "On An Experimental Determination of π ," Messeng. Math, 1873, No. 2, pp. 113–114.
- 23. N. Metropolis and S. Ulam, "The Monte-Carlo Method," J. Amer. Stat. Assoc. 44 (247), 335–341, 1949.
- 24. V. S. Vladimirov and I. M. Sobol', "Calculation of the Minimal Eigenvalue of the Peierls Equation by the Monte Carlo Method," in *Computational Mathematics and Mathematical Physics*, No. 3, pp. 130–137, 1958. (in Russian)
- O.M. Belotserkovskii, Yu.I. Khlopkov Monte Carlo Methods in Mechanics of Fluid and Gas, World Scientific Publishing Co. New Jersey, London, Singapore, Beijing, Hong Kong, 2010.
- 26. J. K. Haviland and M. D. Lavin, "Application of the Monte-Carlo Method to Heat Transfer in Rarefied Gases," Phys. Fluids 5 (1), 279–286, 1962.
- 27. G. A. Bird, "Shock-Wave Structure in Rigid Sphere Gas" in *Rarefied Gas Dynamics*, Academic, New York, Vol. 1, pp. 25–31, 1965.
- 28. S. M. Ermakov, *Monte Carlo Method and Related Topics* Nauka, Moscow, 1985. (in Russian)
- 29. M. Kac, *Probability and Related Topics in Physical Sciences* New York, 1957; Mir, Moscow, 1965. (in Russian)
- 30. G.A. Bird Molecular Gas Dynamics and the Direct Simulation of Gas Flows, Oxford University Press, 1994.
- 31. Lifshitz E.M., Pitaevskii L.P Physical Kinetics, Moscow, Fizmatlit, 2002. (in Russian)
- 32. Kogan N.M. Rarefied Gas Dynamic, New York, Plenum, 1969.
- 33. Axilord B.M., Teller E. Interaction of the van der Waals' type between three atoms // J. Chem. Phys. 1943. No. 11. pp. 299–300.
- 34. *Khlopkov Yu.I., Khlopkov A.Yu., Zay Yar Myo Myint* Processes of triple collisions of molecules // Abstract book of 29th International Symposium on Rarefied Gas Dynamics, Xian, China. 2014 (July 13-18). pp. 222-223.

- 35. Khlopkov Yu.I, Khlopkov A.Yu., Zay Yar Myo Myint Modelling of processes of triple collisions of molecules // International Research and Practical Conference "Science, education and technology: results of 2013", Donetsk, Ukraine, 2013. pp. 49-54.
- 36. *Khlopkov Yu.I., Zay Yar Myo Myint, Khlopkov A.Yu.* The triple collisions of molecules // Physical Chemistry: An Indian journal, India, 2014. Vol. 9, Issue 4, pp. 137-140.
- 37. Khlopkov Yu.I. Statistical modelling in computational aerodynamics. Moscow, MIPT, 2006. 158 p.
- 38. Cercignani, C., and Lampis, M., "Kinetic Models for Gas-Surface Interactions", *Transport Theory and Statistical Physics*, Vol. 1, No. 2, 1971, pp. 101-114.
- 39. Hinchen J.J., Foley W.M. Rarefied gas dynamics, vol. II, p. 505, New York, Academic Press, 1966.
- 40. Lord, R.,G., "Application of the Cercignani-Lampis Scattering Kernel to Direct Simulation Monte Carlo Calculations", *In the proceeding of 17th Int. Symp. on Rarefied Gas Dynamics*, pp: 1427-1433.
- 41. Lord, R., G., "Some Further Extensions of the Cercignani-Lampis Gas-Surface Interaction Model", *Phys. Fluids*, Vol. 7, No. 5, 1995, pp. 1159-1161.
- 42. Padilla, J.,F., "Assessment of Gas-Surface Interaction Models for Computation of Rarefied Hypersonic Flows", Ph.D. Dissertation, University of Michigan, 2008.
- 43. Ketsdever, A., D., and Muntz, E., P., "Gas-Surface Interaction Model Influence on Predicted Performance of Microelectromechanical System Resistojet", *Journal of Thermophysics and Heat Transfer*, Vol. 15, No. 3, 2001, pp. 302-307.
- 44. Utah, S., and Arai, H., "Monte Carlo Simulation of Reentry Flows Based Upon a Three-Temperature Model", *In the proceeding of 23rd Int. Symp. on Space Technology and Science*, Vol. 1, 2002, pp. 1209-1214.
- 45. Santos, W., F., N., "Gas-Surface Interaction Effect on Round Leading Edge Aerothermodynamics", *Brazilian Journal of Physics*, Vol. 37, No. 2, 2007.
- 46. Wadsworth, D., C., Van, Glider, D., B., and Dogra, V., K., "Gas-Surface Interaction Model Evaluation for DSMC Applications", *In the proceeding of 23rd Int. Symp. on Rarefied Gas Dynamics*, 2003, pp. 965-972.

- 47. Kussoy, M., I., Stewart, D., A., and Horstman, C., C., "Hypersonic Rarefied Flow over Sharp Slender Cones", NASA Technical Note, 1972, D-6689.
- 48. Voronich, I., V., and Zay Yar Myo Myint, "Feature Influence of Gas-surface Interaction on the Aerodynamic Characteristics of Aerospace Vehicle", *Electronic magazine of MAI*, Vol. 17, No. 3, 2010, pp. 59-67. (in Russian)
- 49. Zay Yar Myo Myint, Khlopkov, Yu., I., and Khlopkov, A., Yu., "Application of Gas-Surface Interaction Models in Rarefied Hypersonic Flows", *Journal of Physics and Technical Sciences*, Vol. 2, No. 1, 2014, pp. 1-7.
- 50. *Khlopkov Yu.I., Chernyshev S.L., Zay Yar Myo Myint, Khlopkov A.Yu.* Hypersonic aerothermodynamic investigation for aerospace system // Proceeding of 29th congress of the international council of the aeronautical sciences, St. Petersburg, September 7-12, 2014.
- 51. Khlopkov, Yu., I., Khlopkov, A., Yu., and Zay Yar Myo Myint, "Computer Modelling of Aerothermodynamic Characteristics for Hypersonic Vehicles", *In the proceeding of 2014 Spring World Congress on Engineering and Technology*, Journal of Applied Mathematics and Physics, No. 2, 2014, pp. 115-123.
- 52. Zay Yar Myo Myint, and Khlopkov, A., Yu., "Aerodynamic Characteristics of an Aircraft with a Complex Shape Taking into Account the Potential of Molecular Flow Interaction with a Surface", *TsAGI Science Journal*, Vol. 41, No. 5, 2010, pp. 551-566.
- 53. Khlopkov, Yu., I., Zay Yar Myo Myint, Khlopkov, A., Yu., and Tian Van Vyong, "Monte Carlo Methods in Mechanics of Fluid and Gas", *In the abstract book of 29th International Symposium on Rarefied Gas Dynamics*, 2014, pp: 77-78.
- 54. *Khlopkov Yu.I., Khlopkov A.Yu., Zay Yar Myo Myint, Tian Van Vyong* Monte-Carlo methods in applied mathematics and computational aerodynamics // Proceeding of 29th congress of the international council of the aeronautical sciences, St. Petersburg, September 7-12, 2014.
- 55. Khlopkov, Yu., I., Zharov, V., A., Khlopkov, A., Yu., and Zay Yar Myo Myint, "Development of Monte Carlo Methods in Hypersonic Aerodynamics", *Universal Journal of Physics and Application*, Vol. 2, No. 4, 2014, pp. 213-220.
- 56. Shen, C., "Rarefied gas dynamics: Fundamentals, Simulations and Micro Flows", Springer, Berlin Heidelberg, New York, 2005. 421 p.
- 57. Nocilla, S., "Rarefied gas dynamics", New York, Academic Press, 1961, 169 p.

- 58. Nocilla, S., "Rarefied gas dynamics", New York, Academic Press, 1963, 327 p.
- Schaaf, S., A., and Chambre, P., L., "Flow of Rarefied Gases", Princeton University Press, 1961.
- 60. Hurlbut, F., C., and Sherman, F., S., "Application of the Nocilla wall reflection model to free molecular kinetic theory", Physics of Fluids, 1968, Vol. 11, No. 3, pp. 486-496.
- 61. Freedlander, O., G., and Nikiforov, A., P., "Modelling Aerodynamic Atmospheric Effects on the Space Vehicle Surface Based on Test Data", ESA WPP-066, 1993.
- 62. Frank, G., Collins, and Knox, E., C., "Parameters of Nocilla gas-surface interaction model from measured accommodation coefficients", AIAA Journal, Vol. 32, No. 4, 1994, pp. 765-773.
- 63. Musanov, S., V., Nikiforov, A., P., Omelik, A., I., and Freedlander, O., G., "Experimental Determination of Momentum Transfer Coefficients in Hypersonic Free molecular Flow and Distribution Function Recovery of Reflected Molecules", *In the proceeding of 13th International Symposium on Rarefied Gas Dynamics*, New York, Vol. 1, 1982, pp. 669-676.
- 64. Ivanov, M., S., Markelov, G., N., and Gimelshein, S., F., "Statistical simulation of reactive rarefied flows: numerical approach and applications, AIAA Paper 98-2669, 1998.
- 65. Padilla, J., F., and Boyd, I., D., "Assessment of Gas-Surface Interaction Models in DSMC Analysis of Rarefied Hypersonic Flow", AIAA Paper 2007-3891. 2007.
- Vaganov, A.V., Drozdov, S., Kosykh, A.P., Nersesov, G.G., Chelysheva, I.F. and Yumashev, V.L. (2009) Numerical Simulation of Aerodynamics of Winged Reentry Space Vehicle. TsAGI Science Journal, 40, 131-149.
- 67. Alekseev E.V., Barantsev R.G. Local aerodynamic calculation method in a rarefied gas. LSU, 1976. (in Russian)
- 68. Barantsev R.G., Vasiliev L.A. et al. Aerodynamic calculation in a rarefied gas on the basis of the hypothesis of locality. LSU, 1969. (in Russian)
- 69. Galkin, V.S., Erofeev, A.I., & Tolstykh, A.I. Approximate method of calculation of the aerodynamic characteristics of bodies in a hypersonic rarefied gas. *Proc of TsAGI*, (1977). 1833, 6-10. (in Russian)

- Khlopkov Yu., I., Zay Yar Myo Myint, and Khlopkov, A., Yu., "Aerodynamic Investigation for Prospective Aerospace Vehicle in the Transitional Regime", International Journal of Aeronautical and Space Sciences, Vol. 14, No. 3, 2013, pp. 215-221.
- 71. Lees, L. (1956). Laminar heat transfer over blunt nosed bodies at hypersonic speeds, *Jet Propulsion*, 26(4), 259-269.
- 72. Vashchenkov, P.V., Ivanov, M.S., & Krylov, A.N. (2010, July 10-15). Numerical simulations of high-altitude aerothermodynamics of a promising spacecraft model. *Proceeding of 27th International Symposium on Rarefied Gas Dynamics*, Pacific Grove, California, 1337-1342.
- 73. Vaschenkov, P.V. (2012). Numerical analysis of high-altitude spacecraft aerothermodynamics. PhD thesis, Novosibirsk, ITAM SB RAS.
- 74. Dogra, V.K., Wilmoth, R.G., & Moss, J.N. (1992). Aerothermodynamics of a 1.6-meter-diameter sphere in hypersonic rarefied flow. AIAA Journal 30, 1789–1794.
- 75. Luigi, Morsa, Gennaro, Zuppardi, Antonio, Schettino & Raffaele, Votta (2010, July 10-15). Analysis of bridging formulae in transitional regime. *Proceeding of 27th International Symposium on Rarefied Gas Dynamics*, Pacific Grove, California.
- 76. John D. Anderson, "Hypersonic and High Temperature Gas Dynamics," McGraw-Hill, New York, 1989.
- 77. J. J. Bertin, "Hypersonic Aerothermodynamics," AIAA Education Series, Washington D.C., 1994.
- James F. Schmidt, "Turbulent skin-friction and heat-transfer coefficients for an inclined flat plate at high hypersonic speeds in terms of free-stream flow properties," United States. NASA, 1961.
- W. F. N. Santos, "Leading-edge bluntness effects on aerodynamic heating and drag of power law body in low-density hypersonic flow," Journal of the Brazilian Society of Mechanical Sciences and Engineering, Vol. 27, No. 3, 2005.
- 80. S. Saravanan, G. Jagadeesh and K.P.J. Reddy, "Convective heat-transfer rate distributions over a missile shaped body flying at hypersonic speeds," Experimental Thermal and Fluid Science, Vol. 33, No. 4, 2009, pp. 782–790.
- 81. G. K. Mikhailov and V.Z. Parton, "Super- and hypersonic aerodynamics and heat transfer," CRC press, United States, 1993.

- 82. J. O. Reller Jr., "Heat Transfer to Blunt Nose Shapes with Laminar Boundary Layers at High Supersonic Speeds." NACA RM-A57FO3a. 1957.
- 83. V. S. Avduyevskii, "Fundamentals of heat transfer in aviation and rocket and space technology," Moscow, Mechanical Engineering, 1992. (in Russian)
- 84. V. P. Solncev, B. M. Galitseisky, B. M. Glebov, B. M. Kalmyks, I. I. Shkarban and A. E. Pirogov, "Methodological guidelines for settlement and graphic works: heat transfer on the surface of aircraft," Moscow, MAI, 1987. (in Russian)
- 85. Zay Yar Myo Myint and A. Y. Khlopkov, "Calculation method of heat flows in laminar and turbulent boundary layer," Proceedings of the 56th scientific conference of MIPT "Actual problems of fundamental and applied sciences in the modern information society", Zhukovsky, 2013, pp. 28-29. (in Russian)
- 86. Yu.I. Khlopkov, Zay Yar Myo Myint and A.Yu. Khlopkov, Development of cognitive technology in computational aerodynamics, *International Journal of Astronomy, Astrophysics and Space Science*, 1 (2014), 11-15.
- 87. *Khlopkov Yu.I., Zay Yar Myo Myint, Khlopkov A.Yu.* Cognitive approach in computational aerodynamics. Materials of the international conference "Modern science technologies", Israel, International journal of experimental education, 2014 (25 April 2 May). No. 6, pp. 29.
- 88. Thagard, Paul, Cognitive Science, The Stanford Encyclopedia of Philosophy (Fall 2008 Edition), Edward N. Zalta (ed.)
- 89. Marcelo Dascal and Itiel E. Dror The impact of cognitive technologies. Towards a pragmatic approach Pragmatics & Cognition 13:3 (2005), 451–457.
- 90. Walker and Doublas Cognitive Technology: Essays on the Transformation of Thought and Society
- 91. Sun, Ron (ed.) (2008). The Cambridge Handbook of Computational Psychology. Cambridge University Press, New York
- 92. L.P.J. Veelenturf *Analysis and applications of artificial neural networks*, Prentice Hall International (UK) Limited, 1995.
- 93. A.I. Galushkin Neural networks theory, Springer, 2007.
- 94. James A. Freeman and David M. Skapura *Neural networks: algorithms, applications and programming techniques*, Addison-Wesley Pub. Co., 1991.

- 95. Patricia S. Churchland and Terrence J. Sejnowski The computational brain, The MIT press, 1992.
- 96. T. Rajkumar and Jorge Bardina, Prediction of aerodynamic coefficients using neural networks for sparse data, proceeding of: Proceedings of the Fifteenth International Florida Artificial Intelligence Research Society Conference, May 14-16, USA, 2002.
- 97. *Khlopkov Yu.I.*, *Dorofeev E.A*, *Zay Yar Myo Myint*, *Khlopkov A.Yu.*, *Polyakov M.S.*, *Agayeva I.R.* Application of Artificial Neural Networks in Hypersonic Aerospace System. Applied Mathematical Sciences, 2014, Vol. 8, no. 95, pp. 4729 4735.
- 98. Development of neural networks for calculation of aerodynamic characteristics of high-speed aircrafts, Fundamental research, 2013, 11(9). c. 1834-1840. (in Russian)
- 99. David M. Van Wie, Stephen M. D'Alessio, and Michael E. White Hypersonic airbreathing propulsion. Johns Hopkins APL technical digest, vol. 26, No. 4. 2005. pp. 430-437.
- 100.Paul J. Waltrup, Michael E. White, Frederick Zarlingo, Edward S. Gravlin History of ramjet and scramjet propulsion development for U.S. navy missiles // Johns Hopkins APL technical digest, vol. 18, No. 2. 1997. pp. 234-243.
- 101.Ronald S. Fry. The U.S. Navy's Contribution to Airbreathing Missile Propulsion Technology, AIAA Centennial of Naval Aviation Forum "100 Years of Achievement and Progress", 21-22 September 2011, Virginia Beach, VA, 2011-6942, pp. 1-37.
- 102.http://www.nasa.gov/
- 103.http://en.wikipedia.org/wiki/Turbojet
- 104.http://en.wikipedia.org/wiki/Turbofan
- 105.http://www.rolls-royce.com/
- 106.http://www.ge.com/products
- 107.http://hypersonicpropulsioncenter.us/
- 108. Khlopkov Yu.I., Polyakov M.S. Optimization problem of propulsion system choice of high-speed aircrafts at various parameters of flight. International Research and Practical Conference "Science, education and technology: results of 2013", Donetsk, Ukraine, 2013, pp. 45-48.

- 109.Edward T. Curran Scramjet engines: the first forty years. Journal of propulsion and power. Vol 17, No. 6. 2001.
- 110.http://en.wikipedia.org/wiki/Ramjet
- 111.http://www.pw.utc.com/
- 112.http://en.wikipedia.org/wiki/Scramjet
- 113.http://www.rocket.com/scramjets
- 114. The Audacious Space Elevator. NASA Science News. Retrieved, September 27, 2008.
- 115. Tsiolkovski, K. E. *Speculations of Earth and Sky*, and *On Vesta*, (science fiction works, 1895). Moscow, Izd-vo AN SSR, 1959.
- 116.Artsutanov, Y. Into the Cosmos by Electric Rocket, *Komsomolskaya Pravda*, 31 July 1960. (The contents are described in English by Lvov in Science, 158, 946-947, 1967.)
- 117. Edwards, B. C., and Westling, E. A. The Space Elevator: A Revolutionary Earth-to-Space Transportation System, 2003. p. 288.
- 118.Liftport Group. http://lunarelevator.com/
- 119.http://www.obayashi.co.jp/
- 120. Adamovich B.A., Nefedov Yu.G. Bioengineering problems of habitability of spacecraft and planetary stations. NASA TT-11, (1967).
- 121. *Ushakov I.B.*, *Ilyin E.A.* Advances of space medicine and biology research in Russia // Report of the committee on the peaceful uses of outer space, Austria, (2010).
- 122. *Afanasyeva L.A., Khlopkov Yu.I., Chernyshev S.L.* Introduction to the speciality. Aerodynamic aspects of flight safety. Moscow, MIPT. 2011. (in Russian).
- 123. Khlopkov Yu.I., Zay Yar Myo Myint, Khlopkov A.Yu. Features of foundation and development of space biology and medicine, GISAP: Earth and space sciences, London, 2014, no. 4. pp. 25-27.
- 124. Khlopkov Yu.I., Chernyshev S.L., Zay Yar Myo Myint, Khlopkov A.Yu., Kyaw Zin. Space Biology and safety of flight. Proceedings of the international scientific-practical conference "Topical issues and trends in the development of biology,

- chemistry, physics". Novosibirsk, Ed. Siberian Association of Consultants, 2012, pp. 25-31. (in Russian)
- 125. Zay Yar Myo Myint, Khlopkov Yu.I., Chernyshev S.L. Medical and biological aspects of space missions. Materials digest of XXVIII International research and practice conference "Global problems of the state, reproduction and use of natural resources of the planet Earth". London: IASHE, pp. 13-16 (2012).
- 126. *Tsiolkovsky E.K.* Investigation of outer space, the period 1911-1912. Collection 2, Moscow, USSR Academy of Sciences. (in Russian) (1954)
- 127. Stein S.F. Observation of the active and passive rotation of humans and animals. Moscow. (in Russian) (1892).
- 128. *Zhukovsky N.E.* On the death of Otto Lilienthal balloonist. Full. cit. Op. ML, Vol. 9, pp. 356-368. (in Russian) (1937)
- 129. *Novozhilov G.V., Neumark M.S., Tsesarskaya L.G.* Safety of the airplane. Moscow, Machinery. (in Russian) (2003)
- 130.http://www.icao.int/
- 131. *Gazenko O.G., Calvin M.* Fundamentals of space biology and medicine. Moscow, Vol. 1, 2, 3. (in Russian) (1975)
- 132. *Shibanov G.* From the history of aviation safety in Russia: focus manned space flight magazine "Aviapanorama", No. 4, pp. 47-49. (in Russian) (2010)
- 133. *Khlopkov Yu.I., Chernyshev S.L., Zay Yar Myo Myint, Khlopkov A.Yu.* Development of Biological Aspects in Space Flights. Biotechnology: An Indian Journal, 2015.
- 134.http://www.nasa.gov/ames/research/space-biosciences/
- 135.Khlopkov, Yu., I., Chernyshev, S., L., Zay Yar Myo Myint, and Khlopkov, A., Yu., "Introduction to specialty II. High-speed aerial vehicles", Moscow, MIPT, 2013. (in Russian)



Anton Yurievich Khlopkov

M.Sc., Programming Engineer, Moscow Institute of Physics and Technology (State University), Russia.



Alena Anatolevna Sorokina

M.Sc. student, Moscow Institute of Physics and Technology (State University), Russia.

Brief Introduction to the Book

This book presents the historical overview of development of reusable hypersonic aircrafts system. Methods to predict aerothermodynamics characteristics for hypersonic aircrafts and application of cognitive approach in computational aerodynamics are offered. The basic principles of hypersonic propulsion systems: rocket engine, turbojets, ramjets, scramjets, and the dual-combustion ramjet are explained. It highlights that we need to consider medico-bilogical effect and to improve biological and medical system for human in space flight due to future space exploration plans of delivery manned spacecrafts with crews to the Moon and the Mars.



Price: US \$80

To order more copies of this book, please contact: Open Science Publishers Web: www.openscienceonline.com

Email: book@openscienceonline.com